EVALUATION OF GEOTHERMAL POTENTIAL OF THE BASIN AND RANGE PROVINCE OF NEW MEXICO

Principal Investigators:
Gary P. Landis, Ph.D
J.F. Callender, Ph.D
W.E. Elston, Ph.D
G.R. Jiracek, Ph.D
A.M. Kudo, Ph.D
L.A. Woodward, Ph.D
Department of Geology
The University of New Mexico
C.A. Swanberg, Ph.D
Department of Earth Sciences
New Mexico State University

Technical Report

by

Gary P. Landis, Ph.D
J.F. Callender, Ph.D
W.E. Elston, Ph.D
G.R. Jiracek, Ph.D
A.M. Kudo, Ph.D
L.A. Woodward, Ph.D
Department of Geology
The University of New Mexico
C.A. Swanberg, Ph.D
Department of Earth Sciences
New Mexico State University

June, 1976

This project was conducted under the auspices of the NEW MEXICO ENERGY INSTITUTE at New Mexico State University. The research project was supported by the New Mexico Energy and Minerals Department as Project No. ERB 75-117 and by the U. S. Geological Survey as Contract No. 14-08-001-G-255.

NMEI 6

DISCLAIMER

INTRODUCTION

The sixty known thermal anomalies of New Mexico are concentrated in the Rio Grande rift and in the southwestern part of the State (Fig. 1). Of these sites, twenty-one thermal anomalies, not in the Rio Grande rift, are located in the following areas: 1) Animas Valley (Lightning Cock KGRA), 2) Gila Hot Springs, and 3) Mangas Trench. Of these, the Animas Valley lies in the Basin Range Province and the others in the mid-Tertiary Mogollon-Datil volcanic field, a transition zone between the Basin and Range province and the Colorado Plateau. All these areas have the general characteristics of regions of geothermal energy potential, including active extensional tectonics, recently-active volcanism, active seismicity, high heatflow, young hydrothermal mineral deposits, and numerous hot springs and wells. Partially-molten rock may occur at depth beneath the Socorro segment of the Rio Grande rift, (Oliver, Kaufman, 1976; Sanford, and others, 1973).

This continuing research is designed to provide an integrated geological, geophysical, and geochemical study of the geothermal energy potential of promising thermal anomalies in the Rio Grande rift. Basin and Range province, and the Mogollon-Datil volcanic field of New Mexico. Specific objectives undertaken in this study include the following: a) reconnaissance and detailed geologic mapping (Animas Valley, Radium Springs, Alum Mountain, Truth or Consequences, Ojo Caliente, Albuquerque-Belen basin, and San Ysidro); b) geochemical studies including reconnaissance water sampling (Animas Valley, Radium Springs and Alum Mountain); and c) geophysical surveys using deep electric-resistivity, gravity, and magnetic techniques (Radium Springs, Animas Valley and Truth or Consequences).

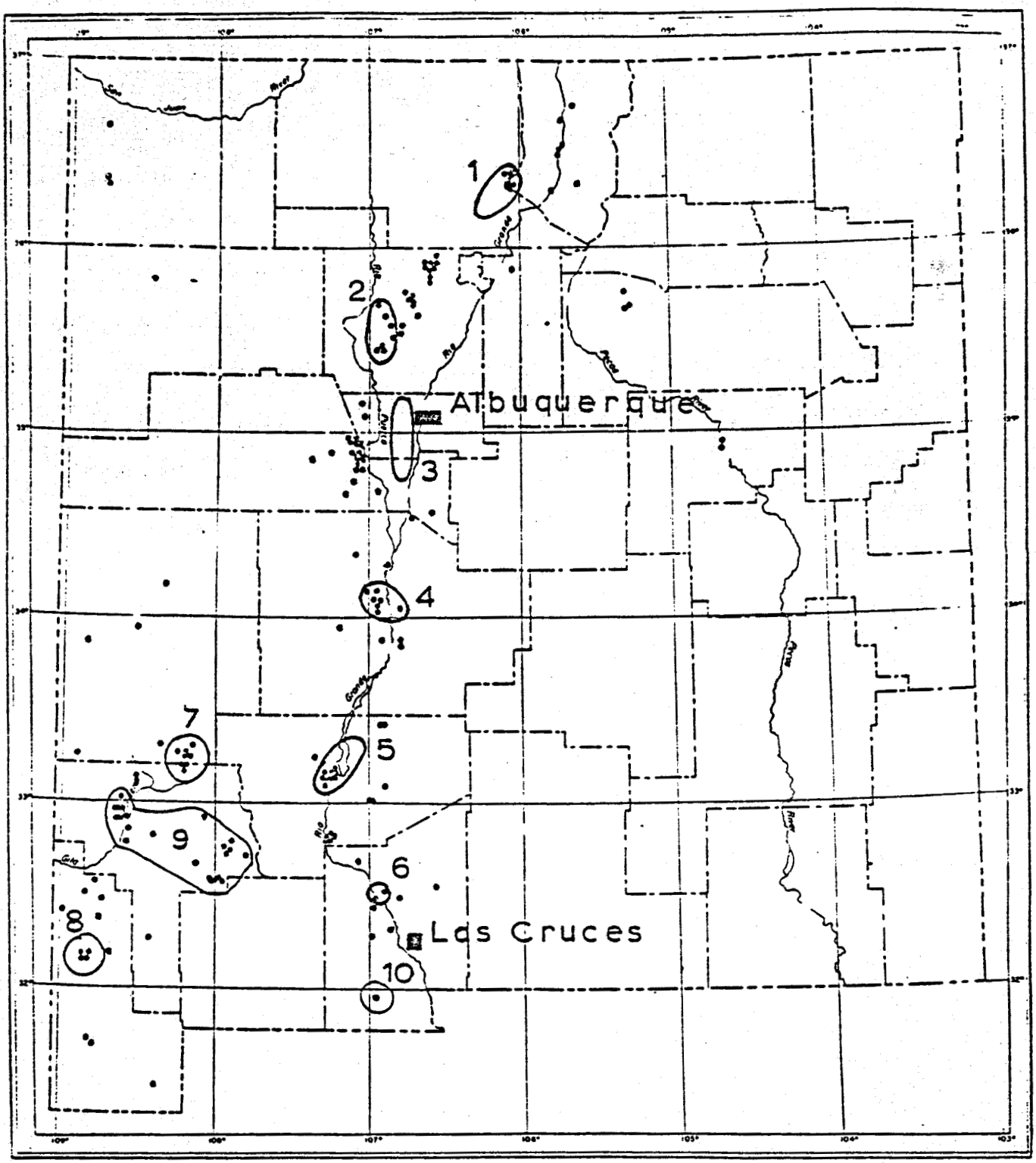

Figure 1. Thermal springs and wells in New Mexico (from Summers, 1965). Circled areas are targets mentioned in this proposal (excluding Socorro): 1 = Ojo Caliente; 2 = San Ysidro; 3 = Albuquerque-Belen; 4 = Socorro; 5 = Truth or Consequences; 6 = Radium Springs; 7 = Alum Mountain; 8 = Lightning Dock; 9 = Mangas Trench region; 10 = Kilbourne Hole.

This report covers the results of one and one-half summer field seasons and approximately two years of analytical work, laboratory research, and development of research equipment and facilities. About one-third of the funding was provided by the U. S. Geological Survey during the reporting period June 27, 1975 to June 27, 1976 on grant number 14-08-0001-G-255, the rest by the State of New Mexico through grants administered by the New Mexico Energy Research and Development Program (NMERDP). The second year of U.S.G.S. funds will be dispersed through grant number 14-08-0001-G-348. A proposal for continued State of New Mexico matching funds was submitted October 14, 1976 for dispersment in January, 1977. Publications, communications, and public service resulting from this first year of U.S.G.S. and State funding are listed in Appendix A.

REGIONAL STUDIES

GEOLOGY

A tectonic map of the Rio Grande rift has been compiled at a scale of 1:500,000, under the N. M. Energy R & D Program. Published, unpublished and original works were compiled for this map and associated text (Woodward, Callender and Zilinski, 1975). A copy of this map is included in Appendix B. Regional overlays of seismic, gravity, aero-magnetic, heatflow, and thermal-spring (including measured and chemical temperatures) were also prepared (50% USGS-funded) and are open-file with the New Mexico Bureau of Mines and Mineral Resources. These data delineate regions in the rift which exhibit the characteristics of geothermal systems, e.g., high heat flow, extensional tectonics, unusual degree of seismic activity, geologically young hydrothermal mineral deposits, recently-active volcanism, and high

calculated chemical reservoir temperatures of thermal springs. Tectonic data are also shown on the recently published "Tectonic map of the Rio Grande region, Colorado-New Mexico border to Presidio, Texas," (Woodward and others, 1975 - NMERDP-funded). The U.S.G.S.plans to compile similar data for southwestern New Mexico with contributions by Elston (U.S.G.S.-funded).

GEOCHEMISTRY

A reconnaissance sampling of more than 200 thermal and non-thermal waters were collected south of Socorro and analyzed (Swanberg, 1975a). Analysis of additional samples collected north of Socorro are in progress. The sampling procedure has been to collect several non-thermal waters from each hot spring area in order to establish background chemistry against which to compare the chemistry of the thermal waters. All samples were analyzed for T (°C), TDS, pH, Na, K, Ca, Mg, CO_3, HCO_3, Cl, SO_4, PO_4, B, F, Fe, and SiO_2. In addition, thermal waters have been analyzed for the following aqueous species: Mo, Co, An, Mn, Sr, Cd, Ba, Ni, Cu, Ag, Pb, Li, As, Se, Sb, Hg, Cr, Br, NO_3, H_2S, NH_4, and Al. A partial list of these data are given in Appendix C. This list includes all elements which may involve adverse environmental or engineering effects of geothermal development in addition to those that are of use in asessing the energy potential of geothermal areas.

The hottest springs in southern New Mexico are located in the Gila National Forest in the southwest part of the state. Many of these springs, including Faywood, Gila, Mimbres, and the hot springs on Turkey Creek have temperatures in excess of 50°C. Despite the high surface temperature of these springs, their chemistry does not suggest the existance of a suitably

high reservoir base temperature for economic development of geothermal electricity. By applying standard geothermometers to chemistry data of these springs, possible reservoir base temperatures below 125°C are generally obtained. Such values fall far short of the 150-180°C minimum values generally quoted for commercial development of geothermal electricity. These springs are also low in such elements as boron, arsenic, and mercury, all of which are frequently found in promising geothermal fields. However, the high quality (low total salts) of the hot springs in the Gila National Forest make these waters ideal for non-electric uses of geothermal energy such as space heating, industrial processes, and agricultural uses.

One area in western New Mexico that does show good geothermal potential is the Lightning Dock KGRA, located in the Animas Valley. Both the silica and Na-K-Ca geothermometers suggest a reservoir base temperature near 170°C for this geothermal area.

The geothermal prospects in southern New Mexico which show the greatest geothermal potential are generally located within the Rio Grande rift, a tectonic province also associated with high regional heat flow. At least seven thermal areas within the rift are likely to be associated with reservoir base temperatures in excess of 200°C. These include the KGRA's at Radium Springs and Kilbourne Hole in addition to the hot springs at Truth or Consequences and Derry Springs, and near San Diego Mountain. Two other very promising areas are the Las Alturas area near Las Cruces, New Mexico, and the Portrillo Maar area on the Mexican border.

A compilation of water chemistry data for thermal and related non-thermal waters has been made from existing published and unpublished data covering Arizona and southwestern New Mexico. Calculation of chemical "reservoir" temperatures were performed, ranked, and plotted as overlays

using computer techniques to provide invaluable regional background information on extent and intensity of geothermal activity. These data, maps, and overlays are available on open file through C. A. Swanberg, New Mexico State University at Las Cruces. Detailed water chemistry and calculated chemical temperatures were determined from well and thermal waters in the Animas Valley. Calculated silica and alkali temperatures clearly define the extent of the lightning Dock KGRA as shown in Figures 2 and 3. Chemical analyses of these waters are reported in Appendix C.

Rubidium-strontium and $^{87}Sr/^{86}Sr$ systematics of young basaltic and related rock types were investigated in order to establish background values for volcanic rocks common in the Rio Grande rift and related geothermal areas of New Mexico. Selected samples from the following three areas were studied before attempting an in-depth investigation of rocks which may have been hydrothermally altered in areas of potential geothermal resources: 1) Mount Taylor volcanic field, 2) San Antonio Mountain volcanic field, and 3) Albuquerque-Belen volcanics. Results of these analyses are given in Table 1.

All of the samples are very young such that an age correction need not be applied to the normalized $^{87}Sr/^{86}Sr$ ratios. Whole rock chemistry for the samples have been completed using combined gravimetric, fluorimetric, and atomic absorption techniques (M.S. thesis studies of L. Crumpler, D. Eppler, and J. Kasten). Sr isotope analyses are precise to $\pm$ 0.1 percent (one sigma); twelve runs of Eimer and Amend standard $SrCO_3$ yielded 0.7080 $\pm$ 0.0002 during the course of this work.

Data are too few from the San Antonio Mountain volcanic area to state other than considerable spread in $^{87}Sr/^{86}Sr$, beyond analytical uncertainty, is noted. The results of leaching experiments performed on two samples from the Albuquerque-Belen basin clearly show that Sr with a high 87/86 ratio, probably due to calcite, is leached from the samples. Sample heterogeneity is suspected as the reason for one sample (TS-7B) not exhibiting a value intermediate between the leachate and insoluble residue

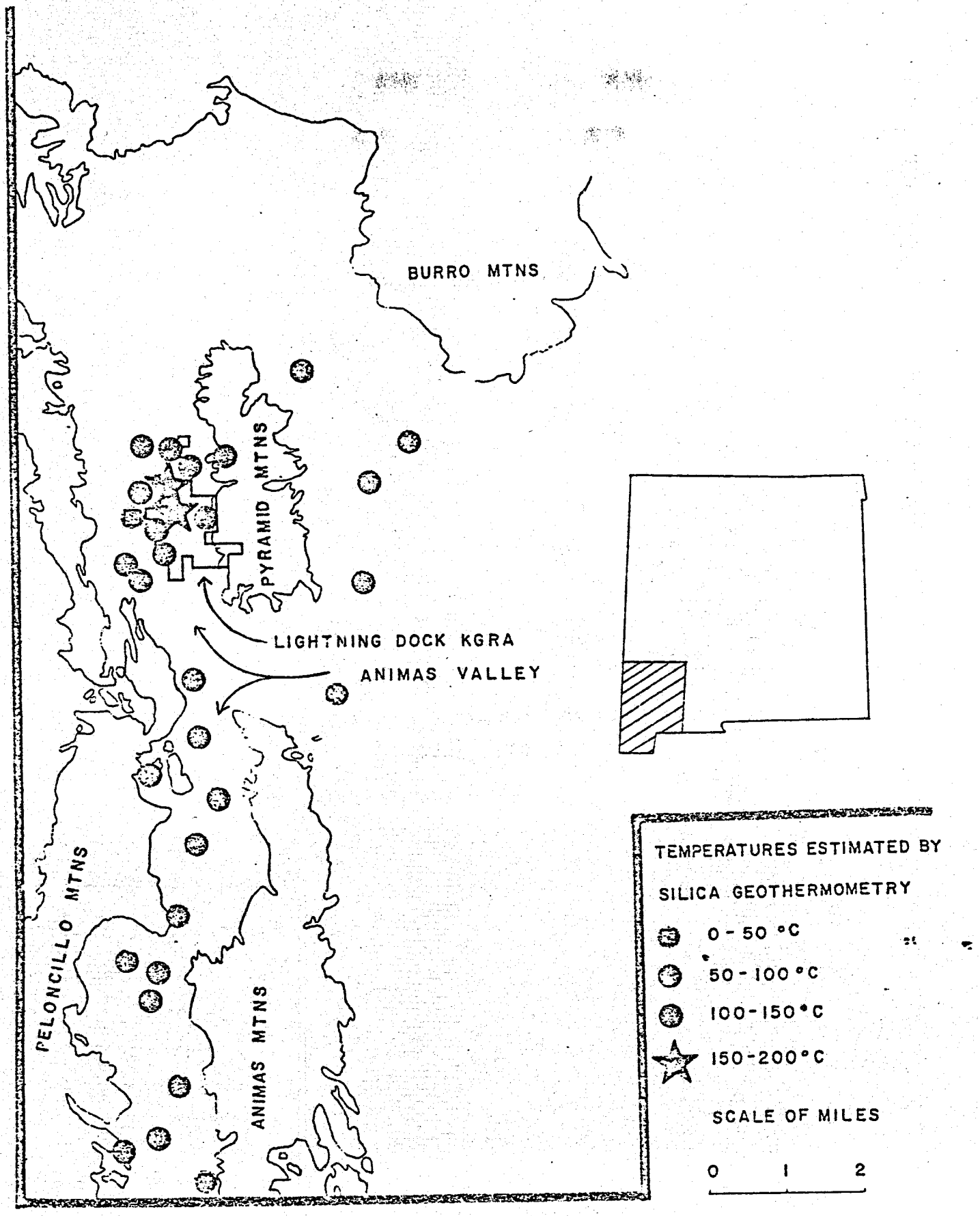
BURRO MTNS
PYRAMID MTNS
LIGHTNING DOCK KGRA
ANIMAS VALLEY
PELONCILLO MTNS
ANIMAS MTNS
TEMPERATURES ESTIMATED BY
SILICA GEOTHERMOMETRY
0 - 50 °C
50 - 100 °C
100 - 150 °C
150 - 200 °C
SCALE OF MILES
0 1 2
ANIMAS VALLEY

Figure 2

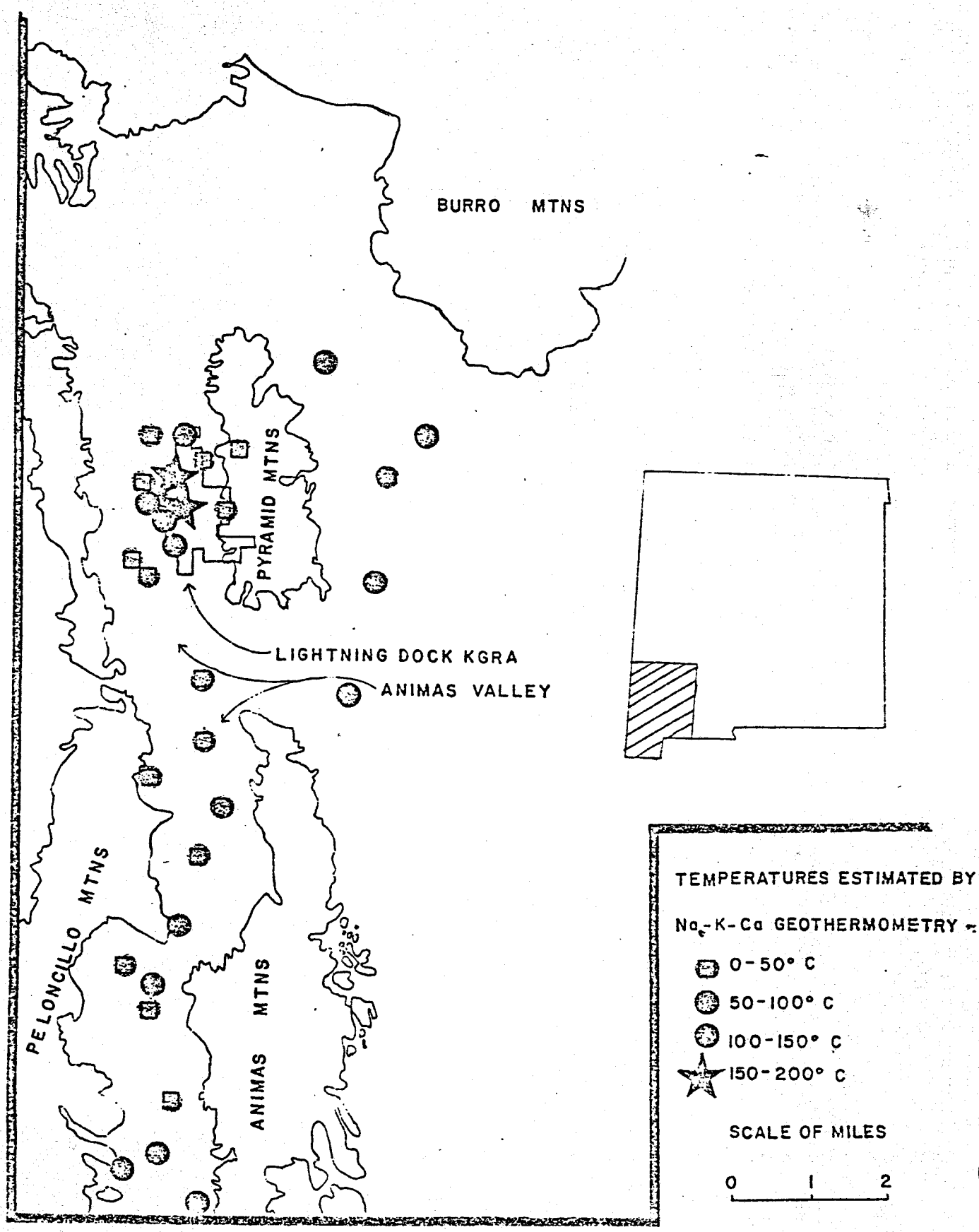
BURRO MTNS
PYRAMID MTNS
LIGHTNING DOCK KGRA
ANIMAS VALLEY
PELONCILLO MTNS
ANIMAS MTNS
TEMPERATURES ESTIMATED BY
Na-K-Ca GEOTHERMOMETRY
0-50° C
50-100° C
100-150° C
150-200° C
SCALE OF MILES
0
1
2

Figure 3

data. Results of these experiments clearly demonstrate the necessity of conducting similar studies on samples from geothermal areas in order to assess possible contamination. The samples from the Mount Taylor volcanic field, with the exception of No. 75-1, yield an average $^{87}Sr/^{86}Sr$ ratio of 0.7050 ± 0.0010 (one sigma). Strontium 87/86 ratio data show no correlation between the 87/86 ratio data and SiO_2/K_2O.

Work in progress includes the collection and preparation of five whole rock samples from the Truth or Consequences area and from the Albuquerque-Belen area for K-Ar age determinations. In addition, whole rock-leachate-insoluble residue $^{87}Sr/^{86}Sr$ experiments are in progress for eighteen samples. Eight calcites possibly related to hydrothermal activity from the Alum Mountain area have been dissolved as well.

Proposed stable isotope studies have been delayed by equipment difficulties and the development of necessary analytical facilities. Carbon, oxygen, and sulfur isotopes are to be analyzed on a U.S.G.S. surplus instrument (1360 RMS) that had not previously performed to modern instrumentation standards. All electronics were obtained through government surplus, purchased (not U.S.G.S. funds), or were fabricated. The extent of necessary electronic and mass spectrometer repairs and modifications had not been accurately anticipated. Considerable time, money, and effort has been invested in bringing the UNM mass spectrometer up to acceptable specifications. This instrument is now in operation and capable of producing top quality data. An outline of instrumentation development and of facilities constructed are given in Appendix D. Performance specifications for the 1360 RMS mass spectrometer are given in Table 2. Hydrogen isotope analysis will be performed on a second mass spectrometer (360 RMS) which is operational.

TABLE I

STRONTIUM ISOTOPE DATA

Sample No.		$^{87}Sr/^{86}Sr$	Rock Description
I. Mount Taylor Volcanic Field			
78-1		0.7056	alkali basalt
109-1		0.7039	trachyte
B23B		0.7053	alkali basalt
66-1		0.7049	trachyte
41a-1		0.7061	hawaiite
FLJ-01		0.7047	trachyte
75-1		0.7142	mugearite
D-11		0.7047	benmorite
134		0.7051	basanite
II. San Antonio Mountain Volcanic Field			
DE-5		0.7070	
DE-19		0.7075	
DE-80-R		0.7036	
DE-327		0.7032	
DE-440		0.7048	
III. Albuquerque-Belen Volcanics			
TS-7A	(whole rock)	0.7080	basaltic andesite
	(leachate)	0.7093	
	(insol. res.)	0.7069	
TS-7B	(whole rock)	0.7057	basaltic andesite
	(leachate)	0.7093	
	(insol. res.)	0.7070	

Construction of the U.S.G.S. funded bromine pentafluoride extraction line is completed. Extensive modifications and added safety features were required when it was determined that BrF_5 was either not available (most standard suppliers) or could be obtained at an extremely high cost and long delivery period. Fluorine gas was obtained as an alternate fluorinating agent, with the provision for using BrF_5 retained. F_2 will have several decided advantages. The fluorination line in its present configuration (see Appendix D) will enable the use of either BrF_5 or F_2 for extraction of oxygen from oxides and silicates, and conversion to CO_2 gas by

TABLE 2

SPECIFICATIONS FOR 1360 RMS

MASS SPECTROMETER CO_2 ($\delta^{18}O$-$\delta^{13}C$)

Radius - Sector Angle	13cm - 60° sector
Total Emmission	1 milliamp
$(I_{trap})/(I_{case})$	1.5
Filament (1% thoriated tungsten)	4.3 amps
Flight Tube Pressure (during analysis)	1×10^{-7} torr
Peak Tail Correction m/e = 45	1.00158
= 46	1.00069
Other Instrumental Corrections:	
Valve cross-mixing: Decade A-B:	
Background: Capillary leak	1.00000
Abundance Sensitivity $(I_m)/(I_{m \pm 1})$	3.8×10^5
Ratio of Peak Widths $(W_{90\%})/(W_{10\%})$	0.429
Effective Collector Slit Width: W_c	0.024"
Actual Slit Width	0.025"
Effective Ion Beam Width at Collector	0.012"
Actual Ion Beam Width at Source Exit Slit	0.010"
Total Beam Focus Aberations	±0.001"
Resolution $R/(W_c + W_i)$	144.35 (97%)
Theoretical Resolution	148.57
Mass 44 + 45 ion current (EA)	2.5×10^{-9} amps (25 volts)
Mass 46 ion current (VRE)	1.5×10^{-11} amps (2.91 volts)
Input Resistor (Ratio Mode)	2×10^{11} ohms
Sensitivity (permil/$\frac{1}{10}$ inch chart division)	0.097 permil
(30 mv in ratio mode)	
Noise Band (30 mv ratio mode)	0.38 permil
Hi Voltage Stability	<0.3 ppm
Magnetic Field Regulation	>1:80,000
(Coil Q factor matched)	

platinum-graphite heating in three interchangeable methods; resistance, RF induction, and photo projection lamps. In addition, SF_6 from sulfides and SiF_4 from silicates can be collected for sulfur and silicon isotope analysis.

Immediate plans are for $\delta^{18}O$ and δD analysis of selected reconnaissance water samples and of water samples collected from Lightning Dock, Radium Springs, Truth or Consequences, and San Ysidro areas. A detailed isotopic study of the Alum Mountain "fossil" geothermal system is in progress. The Alum Mountain study should provide valuable insight into the nature of geothermal plumbing systems, particularly with regards to vapor-dominated systems.

GEOPHYSICS

Resistivity reconnaissance and detailed soundings were initiated at Los Alturas Estates, 2 km southeast of New Mexico State University, Las Cruces. Bipole-dipole mapping from two 2-km long current sources was completed over an area of approximately 25 sq. mi. (64 sq. km.). Two deep Schlumberger soundings were made across the hot, domestic water wells and shallow soundings were completed near the bipole sources. The preliminary interpretation of the data suggests that three intrarift horsts circumscribe a potentially valuable shallow geothermal reservoir.

TARGET AREAS

LIGHTNING DOCK

Geologic and Geohydrologic Setting - In 1948 attention was first drawn to the geothermal anomaly in the Animas Valley now known as Lightning Dock KGRA. Several shallow wells drilled in the area hit steam and boiling

water (101.5°C) at the top of a rhyolitic rock at a depth of 27 m. Other than the Valles caldera, the Lightning Dock area is the only identified hot-water convection system in New Mexico with indicated subsurface temperatures in excess of 150°C (Renner and others, 1975). The area of this anomaly is clearly outlined in winter when the snow melts immediately upon falling within a radius of roughly 0.4 km from the hot wells. There is abundant evidence for numerous extinct hot springs on both sides of the Animas Valley, with a north-south distance of more than 100 km. Hot-spring deposits grade into low-temperature veins of fluorite, psilomelane, calcite (including travertine), and opaline silica.

The Animas Valley with Lightning Dock KGRA is in the Basin and Range province of New Mexico. Field mapping of the Pyramid Mountains, the range on the east side of Animas Valley (four 7-1/2' quadrangles: Pyramid Peak, Swallow fork Peak, Tabletop Mountain, and South Pyramid Peak), suggests that the Pyramid Mountains are a complex of mid-Tertiary volcanics upon which Basin and Range tectonism has been superimposed. At least one and perhaps two rhyolitic calderas, their associated resurgent domes and ring-fracture extrusives, have been mapped. These calderas are only partially preserved in the Pyramid Mountains because the Basin and Range faults transect them, downdropping their western half below the sedimentary cover in the Animas Valley. Thus, this new geologic evidence suggests that the Lightning Dock thermal anomaly may be structurally controlled by the intersection of the margin of a mid-Tertiary caldera with a north-trending Basin and Range fault zone which has been active in Holocene time. A fault noted by Reeder (1957) parallels the mountain front for several km in the valley. It probably represents only the most recent episode of continued Basin and Range faulting.

Several years after the hot wells were drilled, a shallow (1- to 2-m) temperature and temperature gradient survey was conducted in the surrounding area (Kintzinger, 1956). The overall result of Kintzinger's ground temperature mapping was a fan-shaped anomaly over the hot wells, spreading to the north. This shape is by not means surprising given the hydrologic information later published by Reeder (1957). The flow of ground water in the Animas Valley is from south to north, with some local contribution from the flanking mountains. Given a northerly shallow flow of low-temperature ground water, the thermal waters rising at the location of the hot wells would be spread in the pattern that Kintzinger reports. Reeder also published chemical analyses and speculated about the proximity of the recent fault to the hot wells as evidence for structural control for the occurrence of the high-temperature waters. Geochemical temperatures (this study) throughout the Animas Valley are generally low; a base temperature near 170°C is indicated for the hot wells (Swanberg, 1975b).

Evidence suggests that the modern geothermal anomaly (Lightning Dock KGRZ) may be a relic of a much larger hydrothermal system that is now extinct. Widespread fumarolic hydrothermal alteration in the Pyramid Mountains is related to a pre-34 m.y. caldera and not to the modern geothermal anomaly. Rhyolite domes interpreted as younger than Basin and Range faulting by Flege (1959) are Oligocene or older (pre-34 m.y.) and also unrelated to the modern geothermal anomaly. No post-Oligocene felsic volcanism is now known from this part of New Mexico. The time of massive geothermal activity, exhibited by the extensive hot-spring deposits, is now known but is younger than an early Miocene (20.6 $\pm$ 1.5 m.y.) basalt flow in the footwall of one of the manganese oxide veins (Elston and others, 1973). Fluid inclusion and stable isotope studies are in progress in hopes

of clarifying the possible relation between the ancient and modern geothermal systems.

Resistivity Investigations - Reconnaissance roving dipole resistivity measurements were completed during 1975 using more than 200 receiver locations covering an area of more than 125 sq. km. Figure 4 is a total-field apparent resistivity map of the area surrounding the hot wells, indicated in the right center of the figure. The 2-km-long, approximately northwest-oriented bipole transmitter located in the valley to the west of the hot wells was used to generate the map. There are several interesting features on this map:

1. Resistivity generally increases toward the boundaries of the valley to the east and west.
2. Resistivity generally decreases toward the center of the valley, in the vicinity of Valley View Church, and to the north.
3. There is a tight, closed, low-resistivity area associated with the thermal anomaly at the hot wells.
4. There is a high-resistivity ridge trending from about Cotton City northeast through the valley.

Figure 5 is another bipole-dipole total-field apparent resistivity map of the same area. This map was generated using the 2-km-long, essentially E-W bipole transmitter, and shows essentially the same features as Figure 4.

The regions of highest apparent resistivity (60 ohm-m) at the eastern and western margins of the figures are due to the proximity of more resistive basement rock. On the western edge, the Peloncillo Mountains are composed of a thick sequence of Paleozoic marine sediments and granite stocks.

Figure 4. Total-field apparent resistivity map of Lightning Dock project area derived from N-W bipole transmitter.

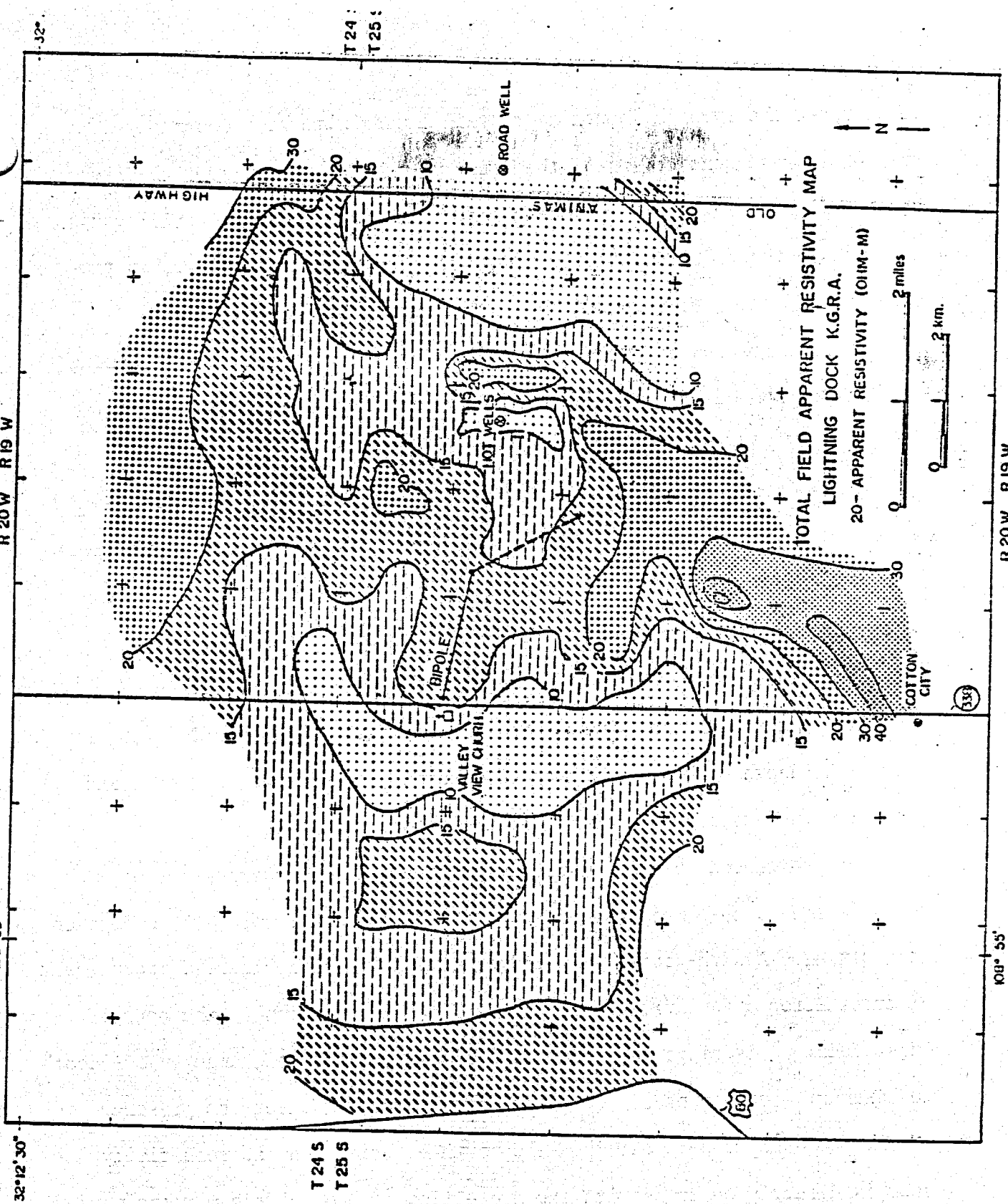

Figure 5. Total-field apparent resistivity map of Lightning Dock project area derived from E-W bipole transmitter.

To the east the Pyramid Mountains contain a monzonite stock possibly related to resurgent doming of the older of the two calderas. Steplike Basin and Range faults are probably responsible for these resistivity highs.

The decrease in resistivity toward the center of the valley, in the vicinity of Valley View Church and to the north, is probably due to increasing thickness of water-saturated sedimentary strata and increasing salinity of the waters. These conclusions are supported by gravity data and by the northerly flow of ground water.

An isolated, closed, low-resistivity contour is associated with the hot wells in both Figures 4 and 5. Such a pattern is expected where there is a near-surface conductive anomaly like the boiling, slightly saline waters encountered by the wells. The geometry and location of these closures relate to the bipole source orientations and in either case indicate that the thermal waters are rising within a constricted zone or conduit at depth. This conduit could possibly be a flexure in Basin and Range faults caused by deflection at the caldera margin.

The pronounced, high-resistivity ridge extending through the hot wells region to the northeast presents further evidence for such deflection in faulting. A high-resistivity ridge, present in both figures, independent of transmitter orientation, reflects structural variation in the near subsurface. This ridge may indicate a simple but abrupt change in the depth to basement produced by a fault. It may, however, reflect the presence of the proposed caldera margin. The northwest ridge on the resistivity maps is directly on trend with the projection of the caldera margins mapped on the surface in the Pyramid Mountains.

Southeast of the hot wells, in both figures, is another low-resistivity region separated from the lows in the center of the valley by the high-

resistivity ridge. This region could be produced by a slight increase to basement in that direction. Such an increase could be accompanied by thickening of fill within the mid-Tertiary caldera.

Figure 6 is a deep dipole-dipole pseudo-section sounding made with 500-m dipoles extending along the line of the E-W bipole transmitter from Valley View Church on the west to Road Well on the east (Figs. 4, 5). The lowest values (<4 ohm-m) are found at the deepest sounding; the highest (>24 ohm-m) are in the center below the hot wells.

The low-resistivity regions near the surface at either end of the sounding are the low-resistivity areas in the valley and to the east, detected by the bipole-dipole surveys. The conductive region intersecting the surface near stations 8, 9, and the hot wells might indicate the conduit for the ascending thermal waters. The high-resistivity regions might be due to the resistive volcanics of the caldera boundary.

This interpretation is certainly not unique; e.g., a similar pattern of highs and lows as in Figure 6 could be generated by a restricted three-dimensional conductive body (thermal waters around the hot wells) in a homogeneous half-space. Numerical modeling of a number of plausible models is in progress.

The low-resistivity region at the bottom of the section is less than 4 ohm-m. It is probably due, at least in part, to the fact that both the transmitter and receiver were located in low-resistivity sediments for that portion of the sounding. However, it could also be due to a relatively low resistivity region at depths on the order of a few km.

A combined asymmetric Schlumberger and bipole-dipole equatorial sounding was conducted on the E-W bipole transmitter, and to the north perpendicular to it, through the thickest section of valley fill (Fig. 7).

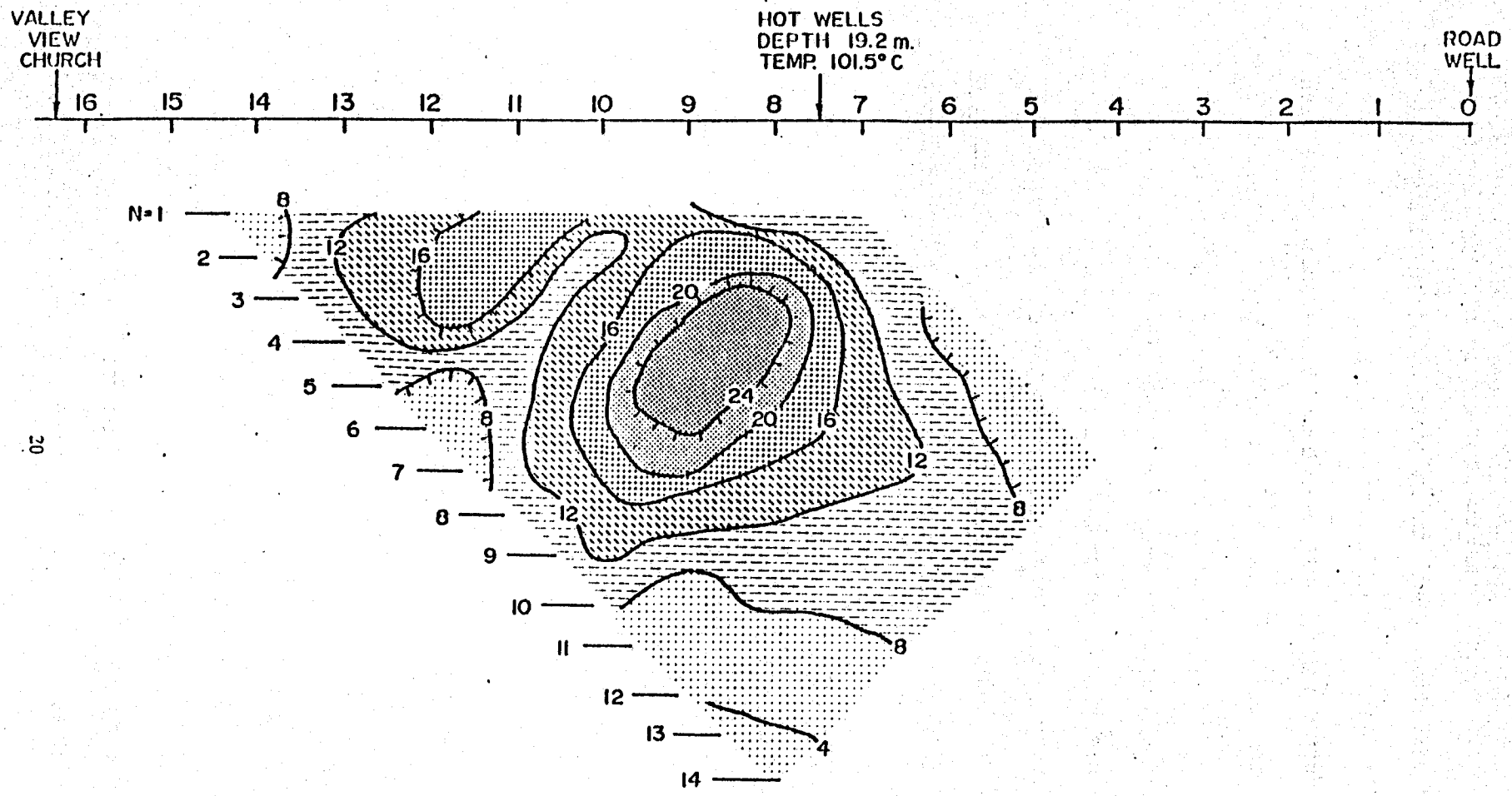

LIGHTNING DOCK K.G.R.A. DIPOLE-DIPOLE PSEUDOSECTION
X=500 m, ρ_a IN OHM-M, C.I.=4 OHM-M

Figure 6. Dipole-dipole pseudo-section sounding through hot wells at Lightning Dock KGRA.

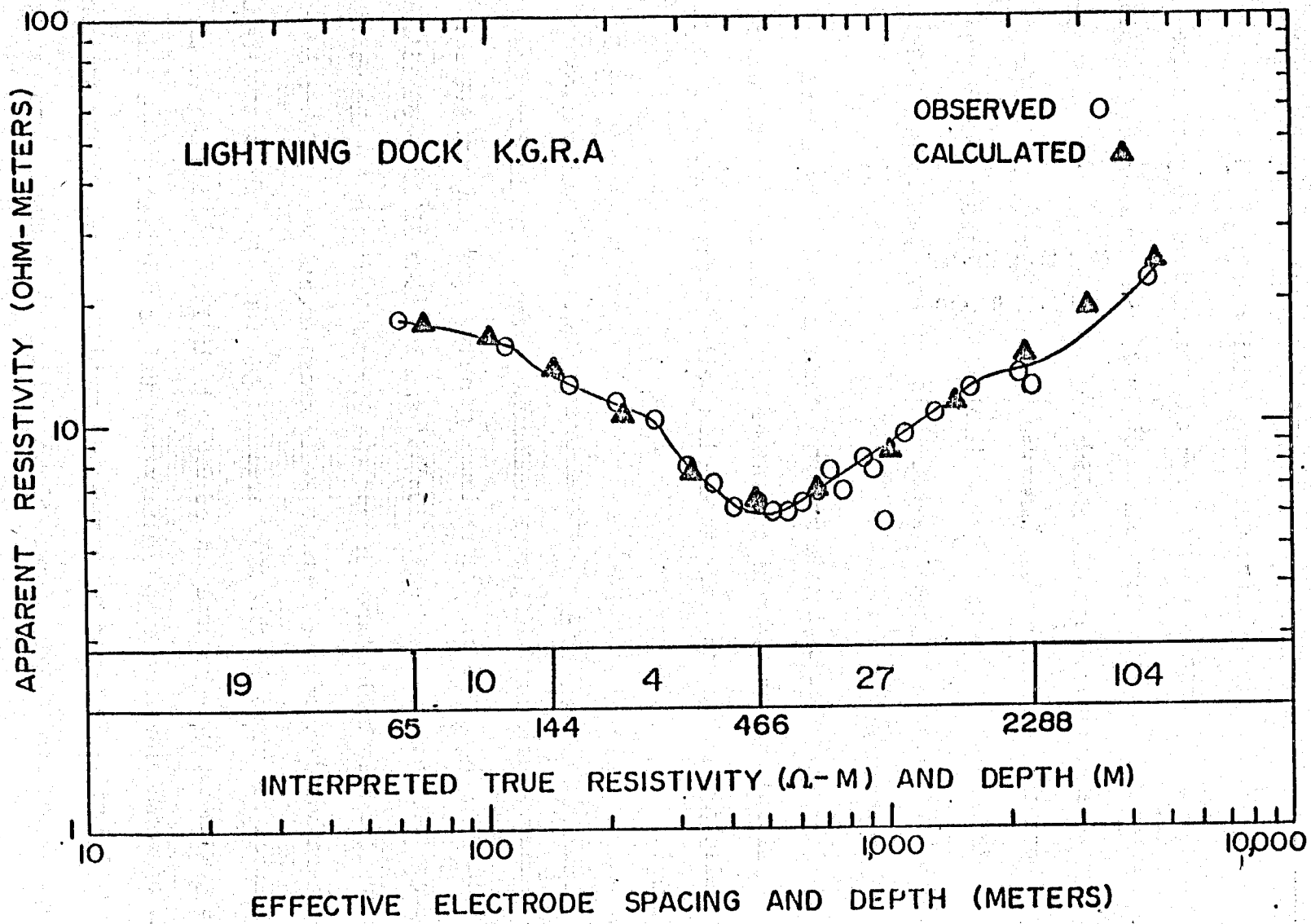

Figure 7. Combined asymmetric Schlumberger and equatorial bipole-dipole sounding at Lightning Dock and five-layer model interpreted by generalized inversions.

The triangles are points calculated by the linear inverse computer routine which generated the model indicated. These results indicate a low-resistivity layer (4-10 ohm-m) between 65 and 466 m in depth. This is probably a layer of decreased water quality in the saturated zone, with less saline water above and decreased permeability below.

Limited self-potential results from the past field season indicate a negative anomaly over the hot wells. In 1976, additional dipole-dipole soundings were continued west of the line from the previous year. Telluric and self-potential profiling was continuously measured from the hot wells to 8 km east along the previous dipole-dipole line. Shallow Schlumberger soundings were completed across the hot wells. Interpretation of these data are in progress.

The newly acquired cryogenic magnetometer was used to make five magnetotelluric soundings across the Animas Valley and to record frequency domain electromagnetic soundings at the hot wells in the range of 1 to 100 sec periods.

Gravity and Magnetic Studies - Regional gravity and selected detailed gravity and magnetic profiling were conducted in the lower Animas Valley near Lordsburg, New Mexico. The regional gravity survey covered 600 sq. km. located at longitude 109°00' - 108°45' and latitude 32°00' - 32°15', excluding the Peloncillo Mountains and the Pyramid Mountains on the western and eastern boundary of the area. Gravity measurements were made at over five hundred locations in the above area using a Lacoste-Romberg temperature stable gravimeter with an accuracy of 0.01 milligals. In addition to all points of known elevation approximately two hundred new points were added using differential leveling techniques to provide adequate gravity station spacing. A computer program (Prof. Shawn Biehler, UCR) was used to reduce gravity data to complete Bouguer anomalies, point plots of field

observations, digitally contoured gravity maps of the free air, Bouguer, regional or residual anomalies, and, a series of tables of the relationships between average gravity anomalies and average surface elevations for a given unit area. Data are on file with C.A. Swanberg (New Mexico State University, Las Cruces).

Several interesting features of the complete Bouguer gravity map include the following:

1. Gravity generally increases toward the boundaries of the valley to the east and west.
2. Gravity generally decreases toward the center of the valley and to the north and south.
3. Gravity generally increases twoard the southeastern boundary.
4. There is an elongated gravity high ridge located just east of the hot wells.

The increasing gravity trends toward the boundaries of the valley to the east and west are expected results and are due to the proximity of higher density basement rock. On the eastern margin of the valley the Pyramid Mountains are composed of andesite and a monzonite stock and on the western margin of the valley the Peloncillo Mountains are composed of a thick sequence of Paleozoic margin sediments and granite stocks. The decrease in gravity towards the center of the valley and to the north and south is due to an increasing thickness of detrital sedimentary fill. The increase in gravity towards the southeast is due to decreasing depth to higher density basement rock. Several small rhyolitic and pyroclastic outcrops occur in this area of the lower Animas Valley.

The elongated gravity high ridge is an interesting feature because of lack of surface expression and close proximity to the hot wells and

north trending fault. This gravity high ridge feature was resolved in more detail by selective detailed gravity and magnetic profiling. Five east-west gravity and magnetic profiles were run across the ridge feature with a station spacing of seven stations per kilometer. East-west profiles were separated in a north-south direction by a distance of .73 kilometers. Elevation at these station locations accurate to $\pm$ .1 meter was obtained by using differential leveling techniques. The residual gravity and magnetic profile results are shown in Appendix E. There are several interesting features shown on these graphs:

1. The maximum residual gravity value is + 5 milligals.
2. The maximum residual magnetic value is + 500 gammas.
3. The general shape of the residual magnetic profile curves suggest that this gravity and magnetic high ridge is a slightly inclined dike dipping to the west.
4. Variations in the general shape and magnitude of the gravity and magnetic profiles suggest variable shape, size, and composition of this dike.

Magnetic profile curves are quite useful in interpreting subsurface geological structures. Diagnostic features of magnetic profile curves over theoretical geologic structures and well documented and aid interpretation of magnetic field data. The residual magnetic profile curves obtained over the gravity and magnetic high ridge in the lower Animas Valley generally show theoretical diagnostic features associated with an inclined dike. However, this interpretation is certainly not unique. The diagnostic features shown by the residual magnetic profile curves are:

1. A slight decrease in magnetic intensity at the eastern edge of the magnetic anomaly.

2. A high magnetic gradient just after the slight decrease in magnetic intensity before the maximum magnetic intensity is encountered.
3. A low magnetic gradient just after the maximum magnetic intensity all magnetic profile curves generally show these features.

All magnetic and gravity profile curves show variations in general shape and magnitude of gravity and magnetic intensity. These variations suggest possible variations in shape, size, composition, and or distortions caused by other structural features in this area. In profile number 4, (Appendix E) the minimum gravity value is associated with the maximum magnetic intensity whereas in profiles numbers 2 and 3, the maximum gravity value is associated with the minimum magnetic intensity. These variations indicate possible variations in composition as might be expected in a composite dike. One other known structural feature in this area that could cause possible distortions of the profile curves is the north trending lower Animas Valley fault. The eastern edge of the gravity and magnetic profiles do cross this fault zone. The steep gravity gradients on the western edge of the gravity profiles could be caused by this fault zone. However, the magnetic profile curves do not appear to be affected by this fault zone.

All geophysical and geologic information indicate that this ridge is not associated with the current geothermal activity except for possible subsurface control of the flow of geothermal fluids. This dike was delineated by the resistivity survey as a resistivity high. Most geothermal activity is associated with resistivity lows. Kintzinger's shallow (1-2 meter) temperature and temperature gradient survey did not show this dike

feature, as might be expected if this dike was hot enough to produce the current geothermal activity. However, this effect could possibly be marked by near surface fast flowing cool waters directly above this dike feature. In the area directly above this dike no distortion of the near surface temperature contour lines was observed. Geologic information indicates that this intrusion may be related to other known intrusions in the Animas Valley which date from mid to late Tertiary. A small shallow dike of mid to late Tertiary age could not retain its original heat to the present date and therefore could not be associated with any present day geothermal activity. However, close proximity of the dike to the hot wells and fault zone indicates possible subsurface control of the flow of geothermal fluids. Furthermore, close association and parallel alignment of the long axis of the dike with the north trending fault suggest that this dike forcefully intruded into the structurally weakened fault zone. It is also possible that this dike is related to the calderas proposed by Elston. The gravity survey delineated no other gravity anomalies that could be associated with cap rocks, silicification, or buried magma chambers, common features associated with geothermal reservoirs.

RADIUM SPRINGS

Geologic and Geohydrologic Setting - There is little available literature to guide the initial investigation of Radium Springs; the only references were contained in two hydrologic reports, listings of hot springs, and one revealing study of its geothermometry. During the fall of 1975, a geologic map of the area and several pertinent articles were published by Seager (1975a, b). Geologic detail reported by W. R. Seager (and R. E. Clemons) has been field checked and re-examined in the context of this study.

Radium Springs is located at the northern end of the Mesilla basin, one of the southernmost grabens that comprise the Rio Grande rift. The springs emerge at the intersection of features produced by three major stages of tectonism: 1)Laramide uplift, 2) Oligocene rhyolitic volcanism, and 3) late Tertiary block faulting in the Rio Grande rift. The axis of a north-trending Laramide anticline passes approximately 3 km west of Radium Springs and, in the subsurface, it could provide a large, as yet unsuspected, reservoir for the waters that emerge at Radium Springs. This postulated reservoir for geothermal fluids could be governed by many of the confirmed relations found in anticlinal oil and gas traps. These relations have been explored by Smith (M.S. thesis in progress, University of New Mexico).

Two Oligocene volcanic centers have been mapped in the vicinity of Radium Springs. The silicic volcanism of these events gave way about 26 m.y. ago to basaltic-andesitic flows (Seager and others, 1975). The inference from this shift is that this age marks the beginning of active extensional tectonics in the Rio Grande rift.

Evidence for active rifting from early Miocene to Pleistocene time can be found in the area immediately surrounding Radium Springs. The Pliocene appears to represent the culmination of rifting and basaltic activity. Broad intrarift basins were segmented into prominent intrabasic horsts and grabens, and basalt dated at 9 m.y. was erupted (Seager, 1975b). A narrow intrarift horst separating the upper Mesilla Valley from the Jornada del Muerto basin to the northeast formed during this most recent stage of uplift. It is not likely that the fault which bounds the horst is the same fault along which Radium Springs emerge (Seager, personal communication, 1976). The presence of this horst may be inferred from our resistivity studies.

Radium Springs lies on the contact of the intrabasin horst and the flank of a Laramide anticline and emerges along a fault or system of faults which have been active for much of the Cenozoic. They are undoubtedly controlled by these complex structural elements.

Two major ground-water studies have concerned the Radium Springs area in the upper Mesilla Valley, those of Conover (1954) and King and others (1971). The limited thickness of the aquifer in the valley near Radium Springs is governed by the pinching out of the Mesilla Valley where it abuts the uplift to the north. The aquifer thickness and width can be expected to increase southeastward down the valley.

The recorded surface temperature of Radium Springs is 85°C as reported by Summers (1965), who also published a chemical analysis of the waters. A thorough study of the geochemical indicators of subsurface equilibrium temperatures in the region was recently completed by Swanberg (1975a). His data for the Na-K-Ca geothermometer show temperatures in excess of 200°C both at Radium Springs and at a nearby well. Swanberg's work also postulated an intersection with a northern extension of the Valley fault which passes through Las Cruces to the south. Swanberg (1975a) reports no high geothermometry temperatures in the Jornada del Muerto, substantiating an earlier conclusion (King and others, 1971) of a ground-water barrier between it and the Mesilla Valley.

The search for a heat source for the Radium Springs area must consider the high heat flow (>2 HFU) and a gravity high interpreted by Decker and others (1975) in the Las Cruces area. Their explanation is for either shallow basaltic crustal intrusions or local upwarping of the mantle.

Resistivity Investigations - Several questions to be answered concerning the origin, migration, and accumulation of the thermal fluids include: 1) Is Radium Springs an isolated phenomenon or do similar waters rise all along nearby faults? 2) Is there a structural barrier between the Jornada del Muerto basin, potentially a vast reservoir, and the upper Mesilla Valley? 3) Can any other potential reservoir for the thermal fluids be found? 4) What is the source of heat? To approach these questions, we have thus far conducted a two-phase electrical resistivity exploration program. Two regional surveys demonstrated that the Jornada del Muerto is structurally separated from the upper Mesilla Valley. Secondly, a series of shallow soundings near Radium Springs located the depth to the saline-water horizon, a deeper marine sequence, and the still deeper Precambrian basement. The two most fundamental questions - the location of a large reservoir of the thermal fluids and the source of their heat - were not answered. Both involve deeper probing, perhaps to several km.

We first conducted a bipole-dipole roving reconnaissance survey from a pair of 2-km bipole transmitters, covering an area of approximately 65 sq. km. A water well served as a common electrode for the bipoles. Figures 8 and 9 are the two bipole sources. The upper two-thirds of the figures cover the Jornada del Muerto; the upper Mesilla Valley begins at Radium Springs and extends to the southeast along the Rio Grande.

Figure 8 shows the total-field pattern generated using the east-west bipole transmitter. The broad low to the north is undoubtedly due to the geometry and water-saturated strata coupled with the decreasing water quality also would produce the low-resistivity pattern. The lowest resistivity contour (10 ohm-m) coincides, on either end of the bipole, with Seager's (1975a) postulated Jornada fault.

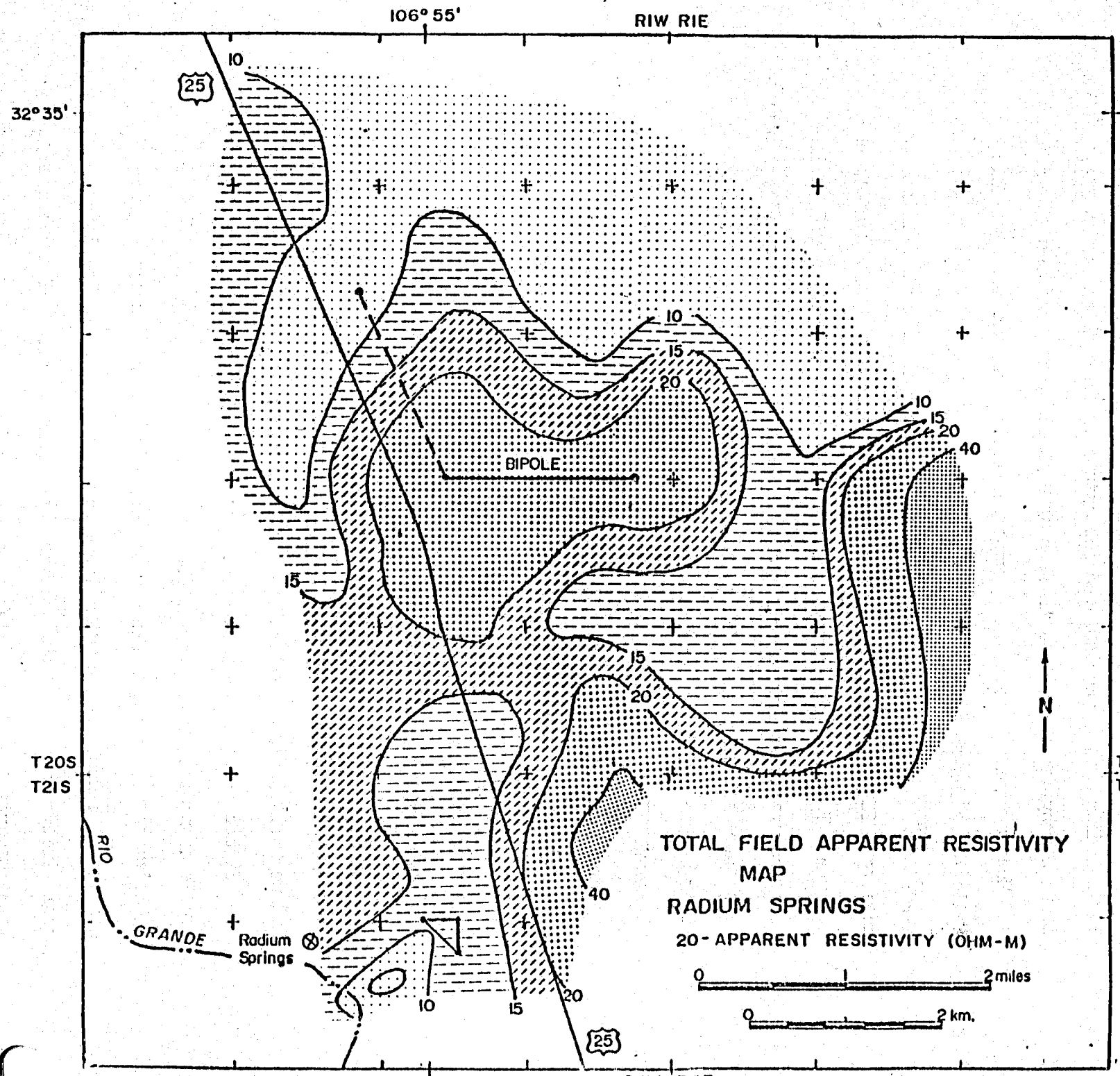

Figure 8. Total-field apparent resistivity map of Radium Springs project area derived from E-W bipole transmitter.

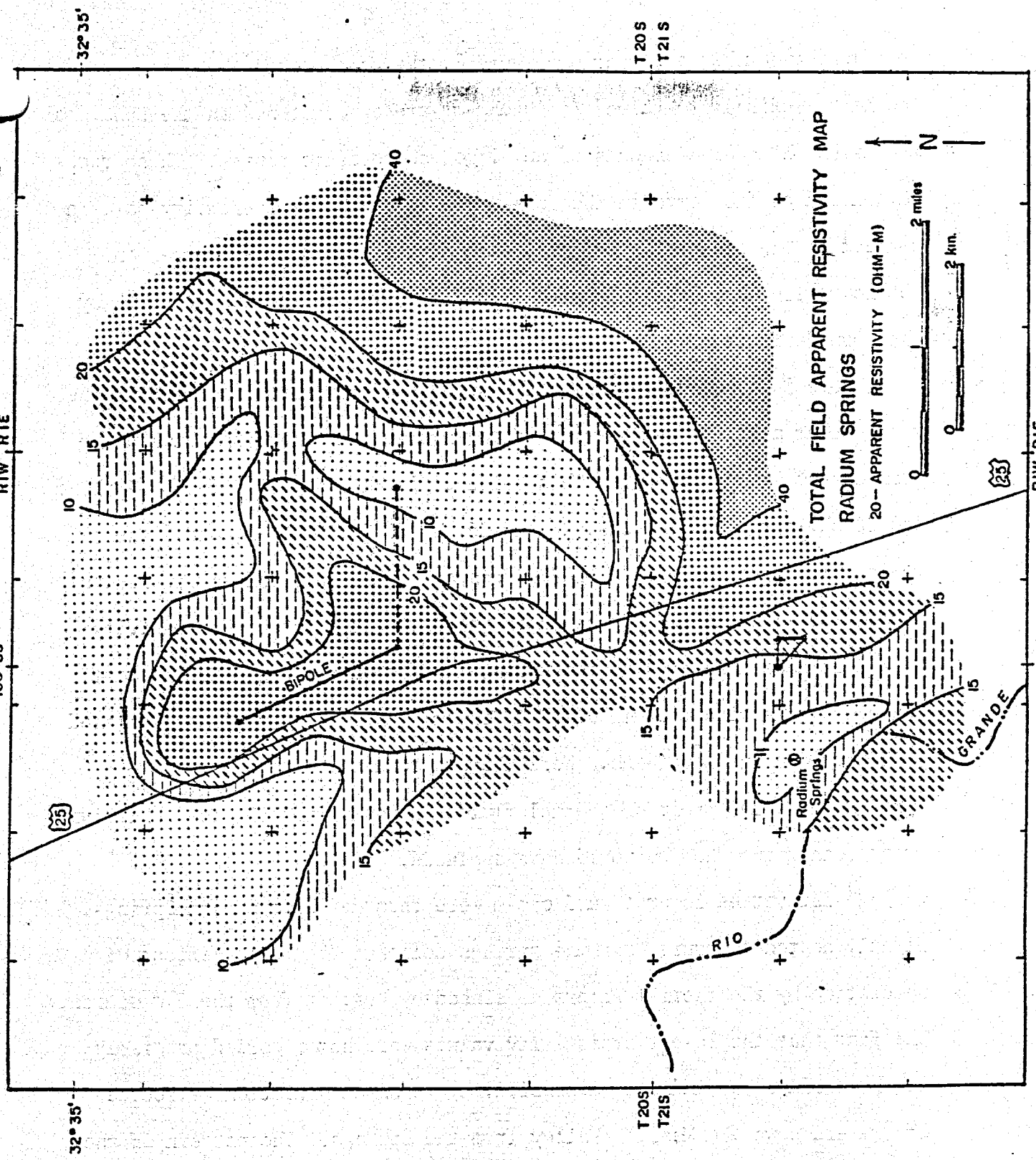

Figure 9. Total-field apparent resistivity map of Radium Springs project area derived from NNW bipole transmitter.

In the southeast corner of Figure 8, the steep contour gradient and the high resistivity values (~ 40 ohm-m) are associated with the Dona Ana Mountains which are remnants of an Oligocene volcanic center. These rocks may extend as far north in the subsurface as our high-resistivity pattern suggests. The steepest gradients, east of the transmitter, correspond to the region where the intrusives would be down-dropped to the north by the Jornada fault.

There is evidence to the southwest of the transmitter suggesting the presence of a structural barrier to any hydraulic connection between the Jornada and Radium Springs. This evidence is the geometry of the 15 ohm-m and 20 ohm-m regions in secs. 35 and 36, T. 20 S., R. 1 W., where the resistivity pattern forms a saddle separating the low-resistivity regions associated with the Jornada basin to the north from the low-resistivity area near Radium Springs to the south. This saddle extends to the east where it links with the higher (> 20 ohm-m) resistivity region associated with the Dona Ana Mountains. Were there a connection between Radium Springs and a reservoir of thermal fluids in the Jornada, a low-resistivity trend connecting the two would have appeared.

Resistivities lower than 5 ohm-m were recorded near Radium Springs. Tightly nested contours near the springs delineate the areal extent of saturation by the thermal waters as sensed by current from the E-W source. The fact that the lowest resistivity values were not recorded precisely at the springs may indicate a sensitivity to an accumulation or source of waters down the Mesilla Valley from the springs. The pattern of the contours could indicate the region of greatest storage of thermal and/or saline waters in the valley fill.

This speculation seems to be substantiated by the closed resistivity lows surrounding Radium Springs generated by data from the other (NNW)

bipole source (Fig. 9). The density of data points is greatest in the area immediately surrounding the springs, resulting in the position of the low-resistivity contours in the Mesilla Valley being as accurate as any from either bipole source.

Comparison of Figure 8 with Figure 9 reveals which of the contours of each figure are products merely of bipole orientation effects and which are governed by subsurface changes in earth resistivity. Figure 9 preserves the essential features noted in Figure 8: 1) the low-resistivity zone centered about the hot springs as discussed above; 2) the saddle between the hot spring low-resistivity zone and 3) much more extensive low-resistivity marking the Jornada del Muerto to the north; and 4) the region of highest resistivity associated with the Dona Ana Mountains. An interesting difference between the figures is found in the extreme north-east corner. Over 5.5 km along the perpendicular bisector to the N. 26° W. transmitter, the most distant data points represent the deepest soundings made in the Jornada. Thus, the higher resistivity values recorded here in Figure 8 may reflect the resistive basement rock of the Jornada basin.

The second phase of our exploration program concentrated on the low-resistivity anomaly surrounding the hot springs and extending south down the Mesilla Valley. Using the 400-m bipole sources located about 1.5 km due east of the hot springs as indicated in the lower portion of Figures 8 and 9, three bipole-dipole equatorial soundings were made. Figure 10 is a plot of one of these soundings, showing the results of data taken along a line perpendicular to the E-W bipole, which traverses due south.

The survey line running due west of the N-S bipole source passed over an outcrop of volcanic tuff and directly through Radium Springs.

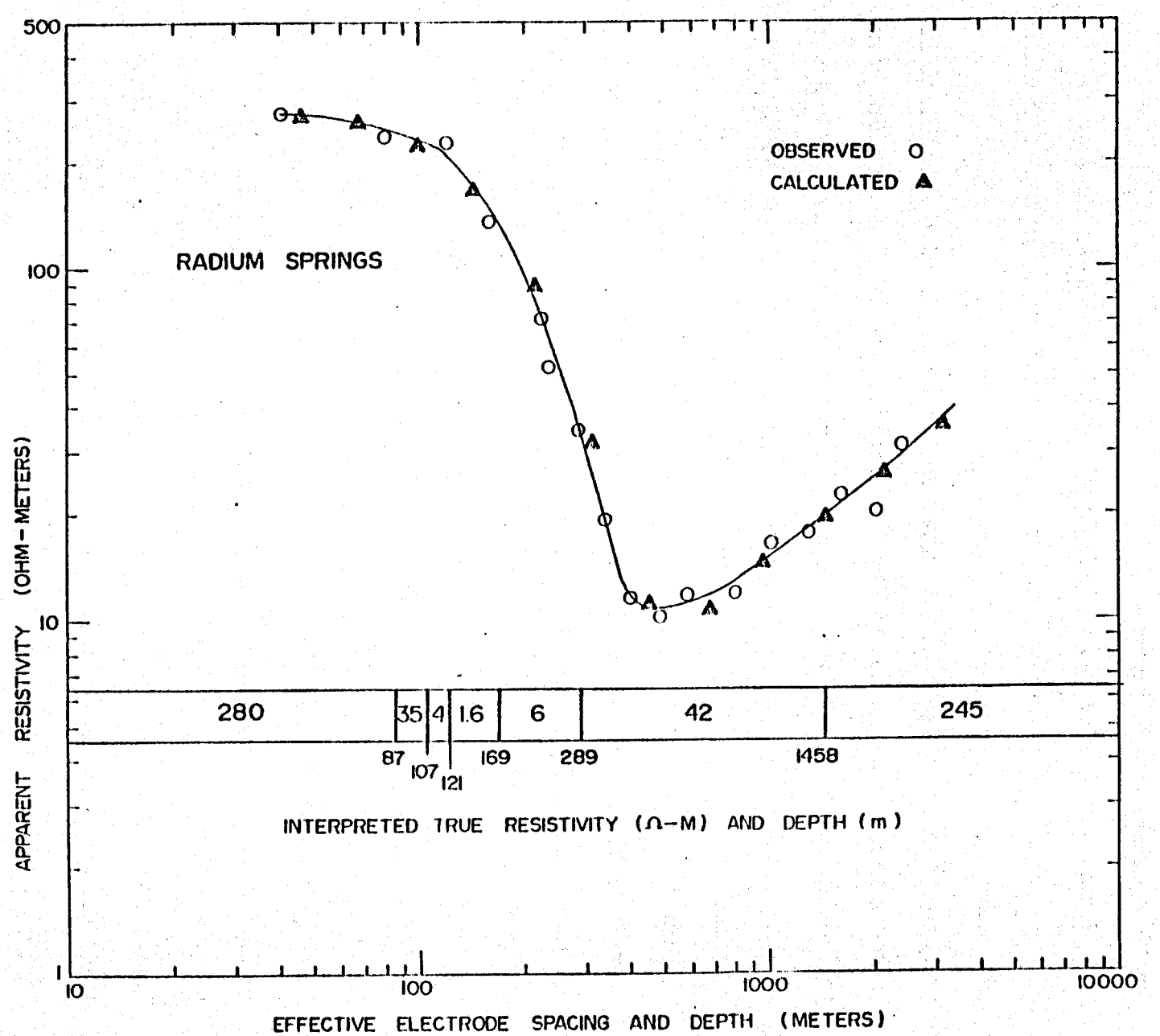

Figure 10. Combined asymmetric Schlumberger and equatorial bipole-dipole sounding at Radium Springs and seven-layer model interpreted by generalized inversion.

The outcrop of highly resistive tuff deformed the sounding curve, making it unsuitable for layered interpretation. However, if the local effect of the resistive dike were smoothed out of the curve, there would be a virtual point-for-point correspondence between the data from the lines passing through Radium Springs and southern traverse. The third sounding ran southwest, bisecting the other two. It produced a very similar resistivity curve with slightly lower values than the other two soundings.

The close agreement among all three sounding curves reveals a pronounced lateral electrical homogeneity in the upper Mesilla Valley. This indicates that there is no hidden shallow structural inhomogeneity within the valley near the hot springs. The obvious exception to this observation is the presence of the highly resistive rhyolitic dike at Radium Springs.

A computer-generated model for the true resistivities of the sediments that nearly duplicated the observed apparent resistivities is shown by the line graph on Figure 10. The upper two layers, with resistivities of 280 and 35 ohm-m, extend to a total depth of 107 m. Of the two, the upper can be expected to reflect the surficial, unsaturated piedmong-slope sediments flanking the valley; the lower represents water-saturated sediments within the valley. This interpretation does not reflect known conditions within the valley where the soil is saturated within a few meters of the surface. It must be remembered that this survey is an equatorial sounding from a source more than 1 km away from the valley center. At shallow depths, therefore, this curve will reflect the more resistive alluvial deposits of the uplands and not the near-surface aquifer and/or water quality variations within the valley fill.

The second set of layers generated by the computer displays remarkably low resistivity values (4, 1.6, 6 ohm-m) extending to a depth of 289 m, with a total thickness of 182 m. The lowest value is sandwiched by a

pair that commonly reflects extensive clay zones. It is, however, so conductive that additional factors must be considered. As these soundings were conducted near Radium Springs it is reasonable to postulate that the 1.6 ohm-m, 48-m-thick layer is the product of admixture of the saline fluids that appear at the hot springs and the clays suggested by the other low values. Whether the low-resistivity value indicates the presence of hot saline waters cannot be determined from our data. The final two layers of progressively greater resistivities in Figure 10 may represent the Paleozoic sequence and the electrical basement, presumably Precambrian rock.

Continued resistivity studies of the Radium Springs KGRA are planned to define the geothermal control imposed by the Valley Fault. Additional bipole-dipole reconnaissance is contemplated to the south, as well as a combined electrical, electromagnetic and self-potential profile perpendicular to the fault trace.

Geochemical Investigations - Nearly 200 NMERDP financed chemical analyses have been completed on waters collected from Dona Ana County, which includes Radium Springs. The majority of samples were collected from non-thermal groundwater wells, although a few thermal wells, and thermal and non-thermal springs, are also represented. The results have been published by Swanberg (1975a).

The water samples collected from Dona Ana County yield a wide range of Na-K-Ca estimated temperatures (Fig. 11). The majority of samples give temperatures of less than 50°C, whereas a few samples give temperatures in excess of 200°C. There is a striking correlation between high Na-K-Ca estimated temperatures and mapped and postulated faults (Fig. 11). Five of the seven samples giving estimated temperatures in excess of 200°C are located on a north-northwest geochemical trend which extends for over

80 km from just west of the Franklin Mountains to San Diego Mountain. This geochemical trend is congruent with the Valley fault inferred for the southern two-thirds of the total distance on the basis of gravity. This geochemical trend also intersects nearly all known occurrences of thermal water in Dona Ana County including Radium Springs, the hot wells at Las Alturas Estates, and the Quaternary travertine deposits near San Diego Mountain (Fig. 11). The coincidence among the Valley fault, the geochemical trend, and the areas of known thermal water indicate that this fault is acting as a conduit for ascending geothermal fluids. This conclusion is also supported by the rapid and systematic decrease in estimated temperatures away from the fault where presumably, the thermal waters mix with the non-thermal groundwaters. Indications are that the entire geochemical trend has essentially the same geothermal potential as the Radium Springs KGRA.

A second approach to assessing the geothermal potential of Dona Ana County is the application of the silica geothermometer (Fournier and Rowe, 1966). The temperatures estimated by the silica geothermometer are shown in Fig. 12. The same trends are apparent in the silica data (Fig. 11) that were observed for the Na-K-Ca geothermometer. The generally lower temperatures estimated from the silica geothermometer are consistent with several explanations (Swanberg, 1975a). Water diffusion studies along the Valley fault are currently in progress where hot and cold waters have probably mixed in the subsurface (Truesdell and Fournier, 1975). Total concentrations of fluoride and boron have been examined to determine their potential use as geothermal indicators. It has been reported that hot springs in New Mexico are routinely high in fluoride (W. K. Summers, personal communication) and relatively high boron concentrations have also been linked with high groundwater temperatures

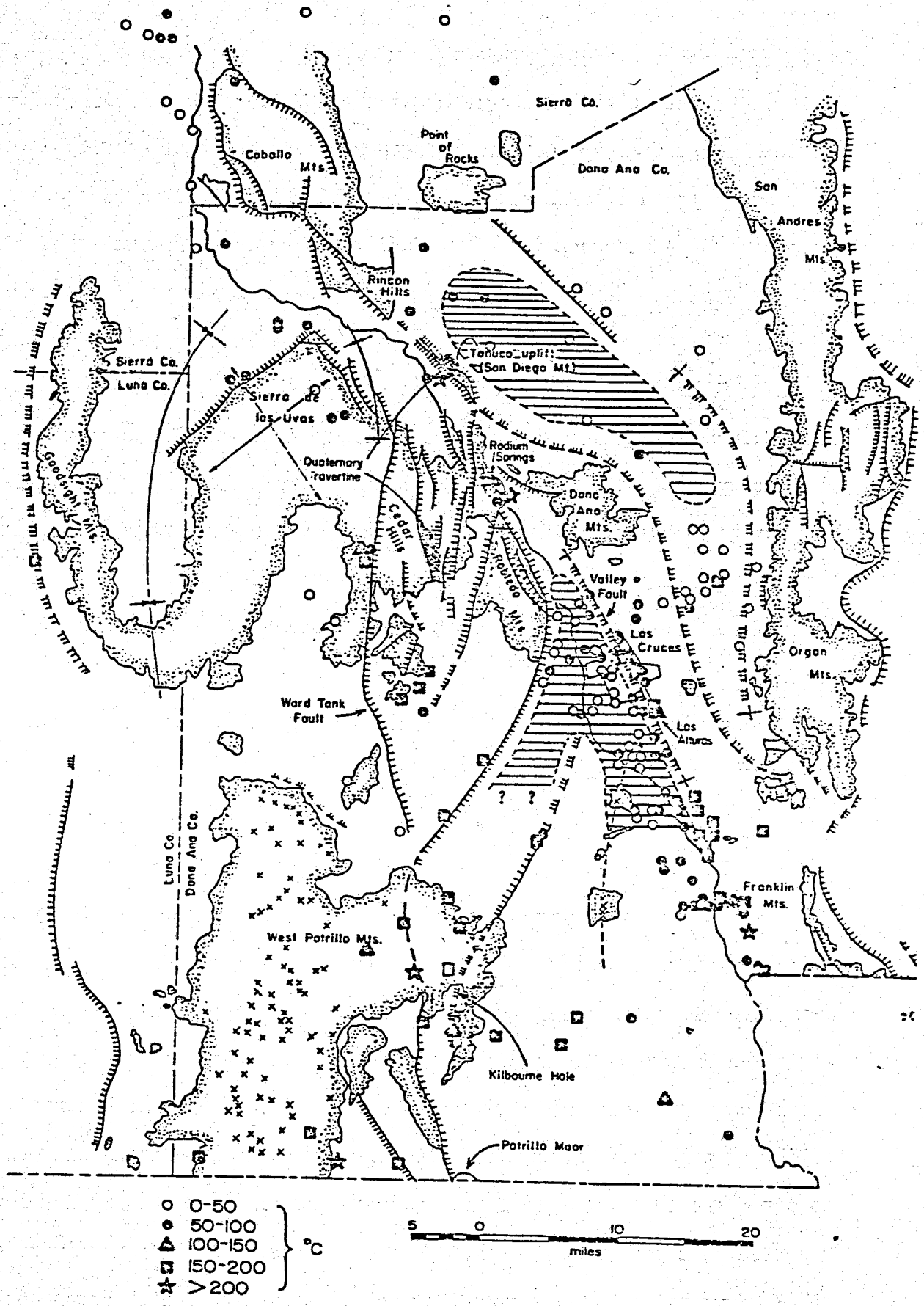

Figure 11. *Temperature estimated by Na-K-Ca geothermometry. For explanation of structural symbols see Figure 1* of Seager, (1975). From Swanberg, 1975a.

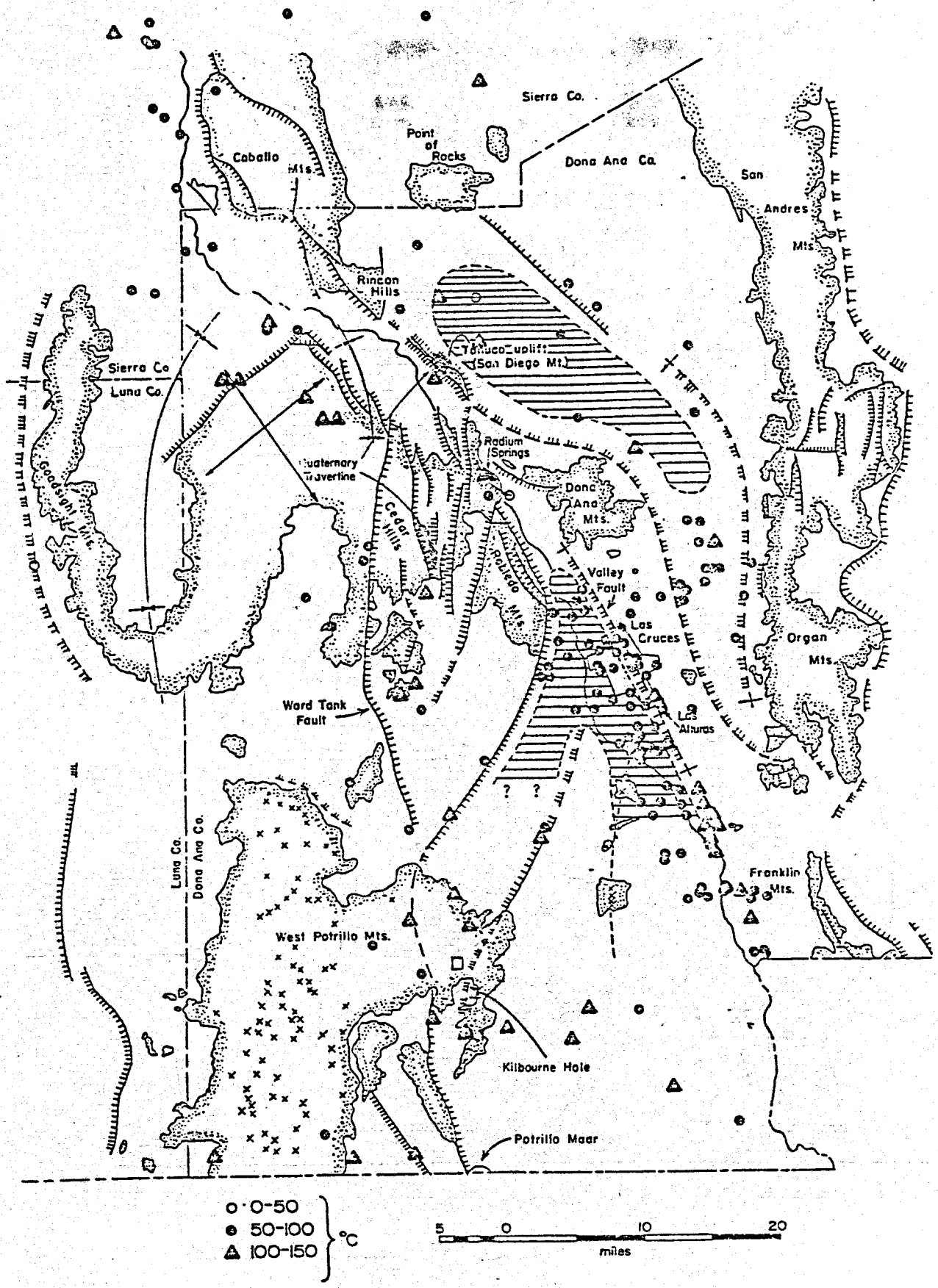

Figure 12. *Temperature estimated by silica geothermometry.* From Swanberg (1975a).

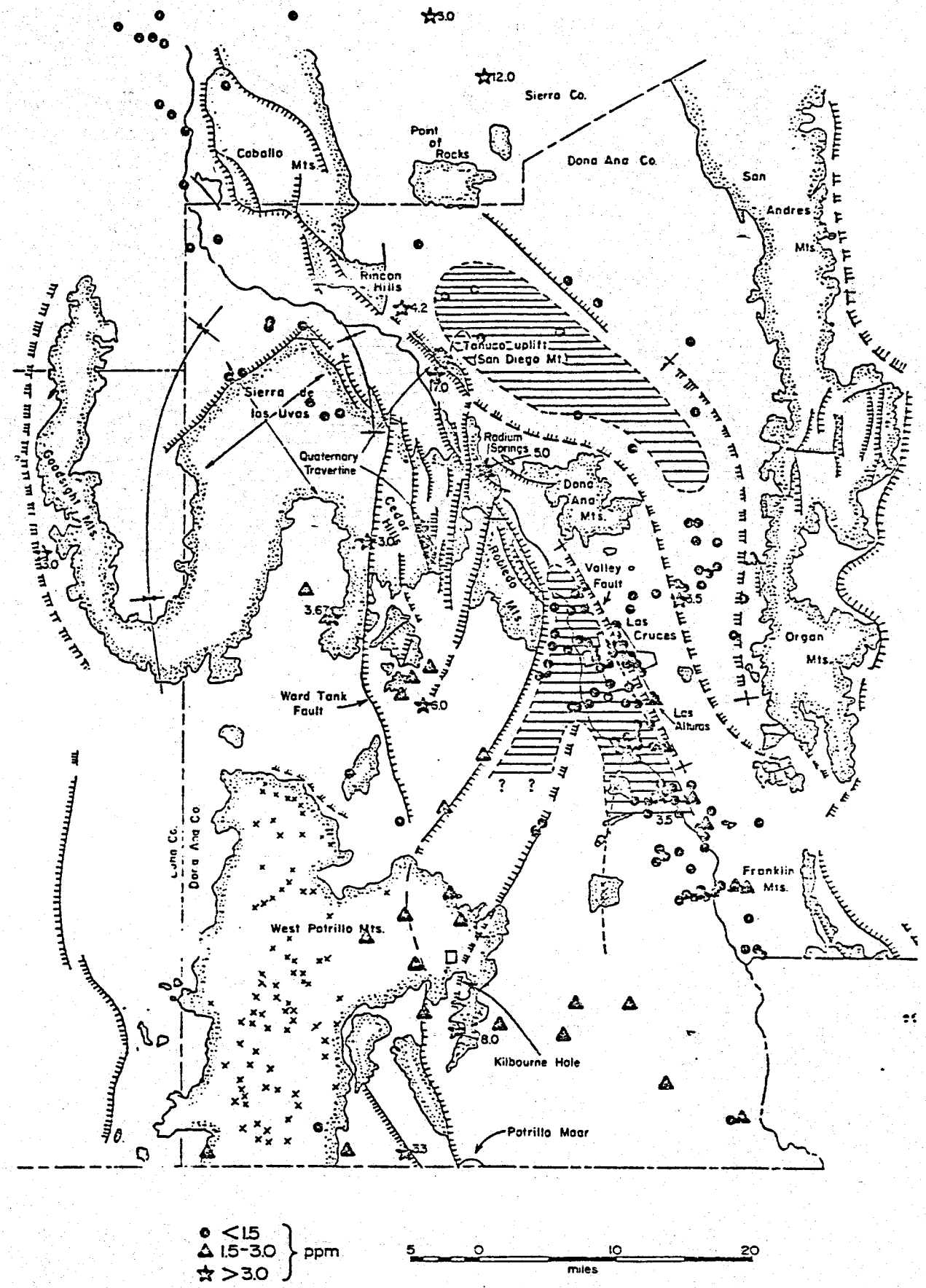

Figure 13. *Concentration of fluoride in groundwater of Dona Ana County.* From Swanberg (1975a).

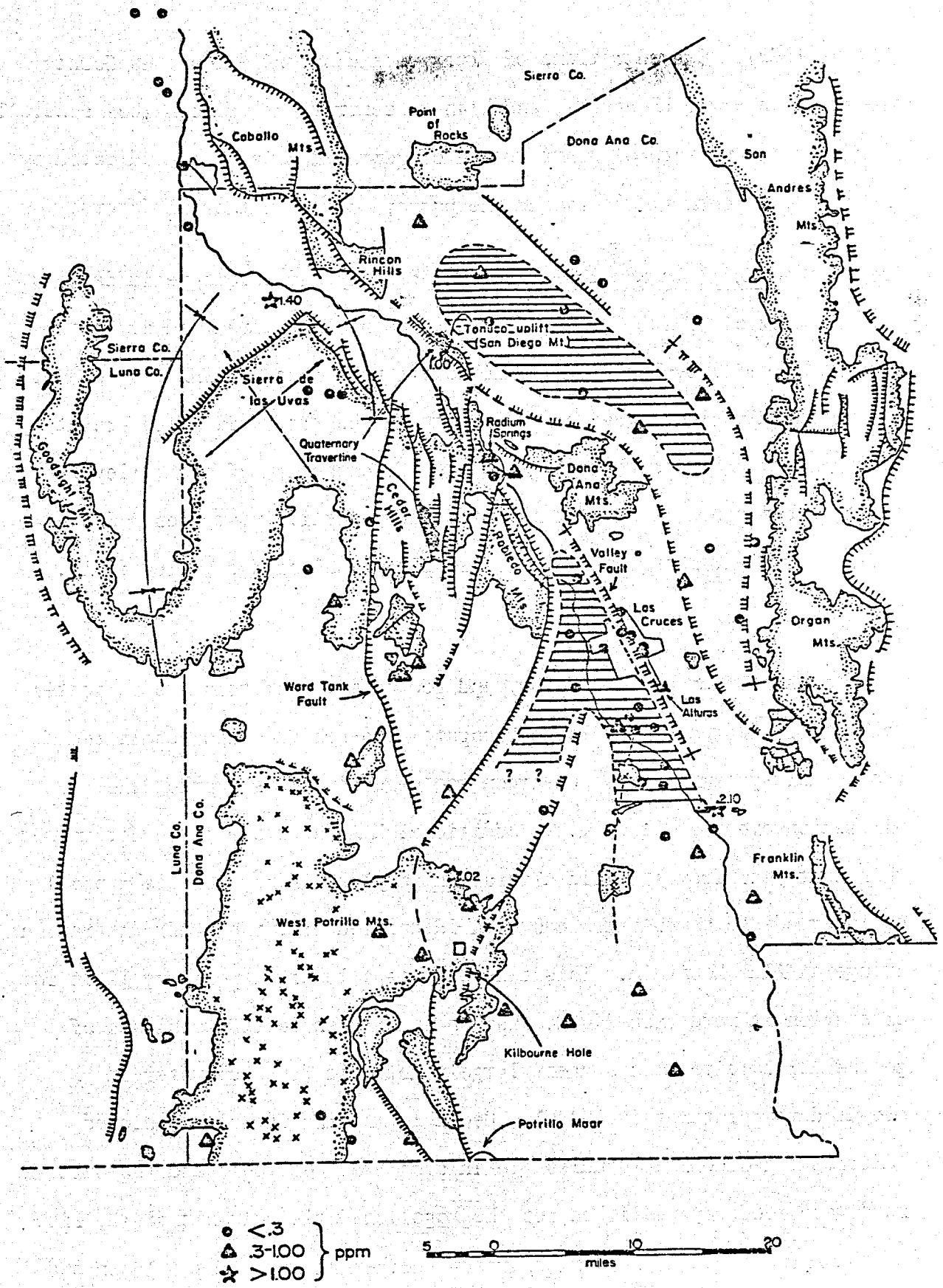

Figure 14. *Concentration of boron in groundwater of Dona Ana County.* From Swanberg (1975a)

(Mahon, 1970). Concentrations of fluoride and boron in Dona Ana County are shown in Figs. 13 and 14, and high concentrations of both ions generally reinforce the pattern of distribution of geothermal water as indicated by the chemical geothermometers and the pattern of known thermal waters.

Gravity and Magnetic Studies - Regional gravity and aeromagnetic data in the vicinity of Radium Springs KGRA have been accumulated and are being compiled from several sources. Microearthquake data obtained by Swanberg has revealed a high degree of seismicity in the area. Detailed gravity measurements near Radium Springs, along the extension of the Valley fault, are planned to augment the proposed resistivity studies. Shallow thermal gradient measurements are also planned along the Valley fault.

ALUM MOUNTAIN

Investigation of the geology and geochemistry of this are indicates the former existence of a large elongate acid-sulfate vapor-dominated geothermal system. Potassium-argon age determinations bracket the alteration event at 22-29 m.y. Additional K-Ar ages are to be determined this next year from specific alteration samples. A new zeolite mineral of intermediate composition has been identified from the outer alteration fringe at Alum Mountain. This mineral sets a lower temperature limit for alteration at more than 240°C. Carbon and oxygen isotope analysis of geothermal calcite also suggest largely meteoric (ground) water at elevated temperatures (> 200°C). Geologic mapping is half completed. Additional geochemical studies are in progress. Geologic and tectonic maps were recently published for the Mogollon-Datil volcanic field, site of the Alum Mountain and Mangas Trench geothermal anomalies (Elston and others, 1976).

TRUTH OR CONSEQUENCES

Geologic mapping, volcanic petrology, and a gravity survey have been completed for the area south and east of the Elephant Butte Reservoir (Loeber, 1976a, b). A generalized geologic map is shown in Figure 15. At least three periods of volcanism have occurred in the area with Tertiary andesite dike intrusions followed by two periods of Quaternary alkali basalt volcanism. K-Ar ages are pending for samples of each period of volcanism. Evidence from ultramafic inclusions contained in basaltic rocks of the region is providing insight into the nature of the upper mantle and its depth. Gravity survey data across the Hot Springs fault has been used successfully to model the fault and adjacent basins and to map its trend. The Hot Springs fault has been active from early Miocene to middle Pleistocene (at least) and has served as a conduit for volcanism and hot spring activity. Present efforts are directed to mapping the north and east end of the reservoir and to tracing the Hot Springs fault northward. Apparently volcanic and hot spring activity along the fault occurred in these areas as well.

Numerous maars and evidence for fossil geothermal activity has been identified. Plane table mapping was completed for the Monticello maar on the northwest side of the reservoir. On the northeast side, mapping of the White Cliffs maar is in progress. These maars acted as centers for hot spring activity which deposited from 25 to 50 feet of opal and diatomaceous material within the maar. Travertine and basalt dikes cut the maars and hot spring deposits.

More detailed hydrologic and geochemical work may be necessary to draw firm conclusions on the geothermal potential of the Truth or Consequences area. Source waters, mixing models, and plumbing systems

must be determined. Research on the kinetics of the Na-K-Ca geothermometer is in progress. Extensive electron microprobe work on the volcanic rocks is planned.

ALBUQUERQUE-BELEN

Mapping and petrologic studies of the Quaternary volcanic features are complete. Results have been accepted for publication by the New Mexico Bureau of Mines and Mineral Resources (Kelley and Kudo, 1976). A guidebook to the Albuquerque Basin is also available (Kelley and others, 1976). Preliminary Sr-isotope data were given earlier in this report. K-Ar ages are reported in a manuscript submitted to Isochron West (Kudo and others, 1976). The youngest volcanic activity in this part of the rift took place in the Cat Hills volcanic field (basaltic) about 140,000 years ago. Most magmatic centers are likely to be deeper than 24 km, which precludes their development for geothermal energy. Andesitic centers at Los Lunas, Torre Hill and Black Butte, however, were generated at shallow crustal levels and may have acted as heat sources. Alignment of volcanic centers parallel to the rift boundaries, and volcanism that has been active for over two million years and continues to be so, suggest the possibility of additional heat sources at shallow depths in the crust. No active hot springs are known, but geothermal waters may be present at depth, in and below the Santa Fe Group. The western border of the basin contains ample evidence of a "fossil" geothermal system less than two million years old. Detailed geologic mapping has established at least four periods of hot- and cold-spring activity, and the geometry of the local geothermal "plumbing" system has been delineated (Callender and Zilinski, 1976; Callender, in preparation). Geochemical sampling has been undertaken and resistivity and gravity surveys are planned in the later stages of the project.

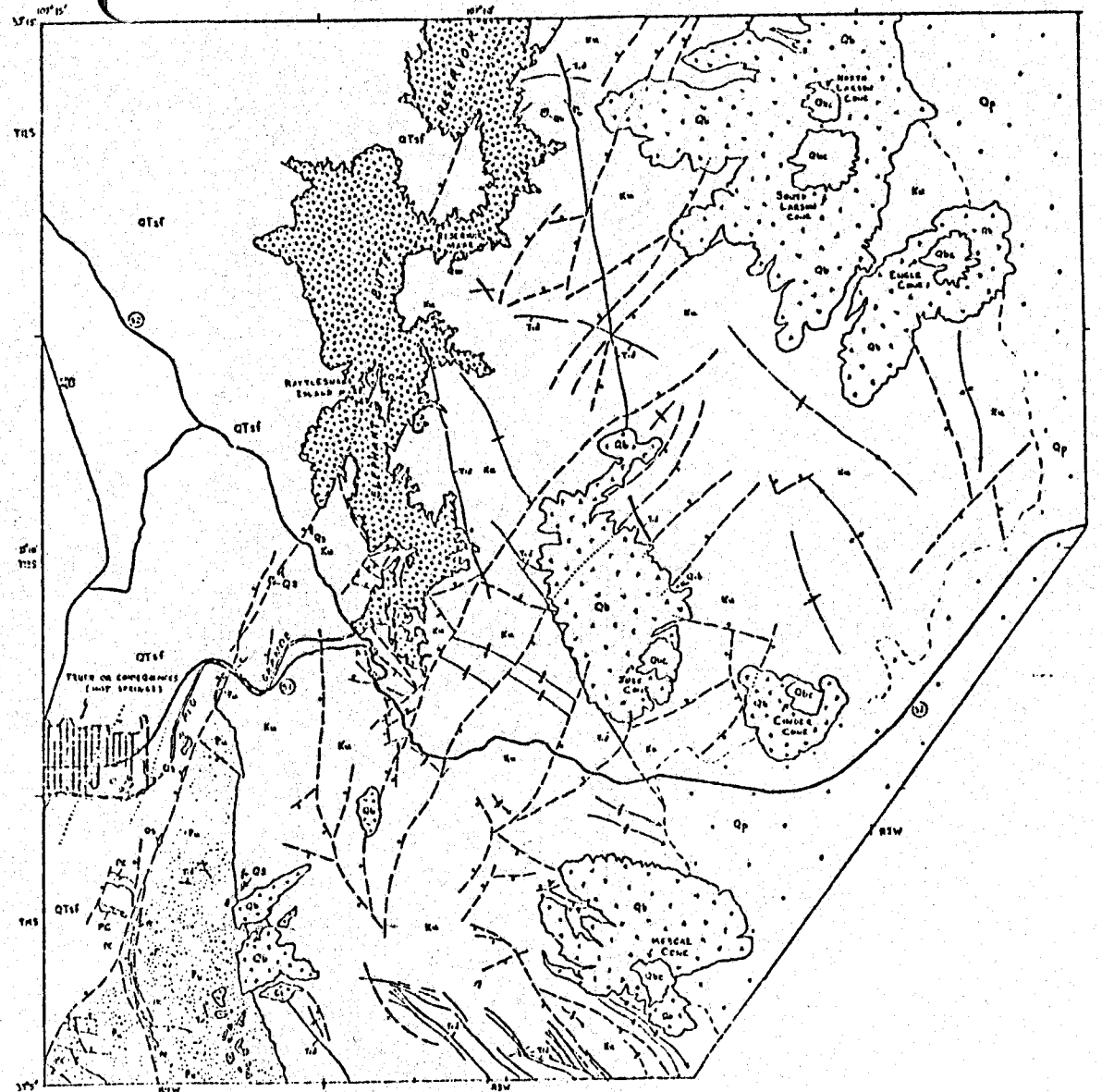

Preliminary Geologic Map of the Truth or Consequences - Engle Area, Sierra County, New Mexico

(overlay to accompany Engle, New Mexico U.S.G.S. 15' Quadrangle)
(compiled from geologic mapping at scale of 1:12000)

Geology and Compilation by
A.M. Kudo and K.N. Loeber
December, 1975

Rock Units

- **Qs** — Hot spring deposits, including travertine, manganese. (Quaternary)
- **Qp** — Pediment gravels. (Quaternary)
- **QTsf** — Santa Fe Group, unconsolidated sediments filling graben. (Quaternary-Tertiary)
- **Ku** — Cretaceous undifferentiated {includes Mesa Fm., Mesaverde Gp., Mancos Shale, Dakota Sandstone.
- **Pu** — Paleozoic undifferentiated {includes Permian through Cambrian sedimentary units.

Igneous Rocks

- **Qm** — Quaternary dissected volcanic maar.
- **Qb** — Quaternary basalt flows.
- **Qbc** — Quaternary basalt cone.
- **Qib** — Quaternary intrusive basalt plug.
- **Tid** — Tertiary trachy-andesitic dikes.
- **Kib** — Cretaceous intrusive breccia (intermediate composition).
- **PC** — Precambrian igneous and metamorphic crystalline rocks.

Symbols

- Contact, dashed where approximately located.
- Fold Axes { anticline, showing direction of plunge. / syncline, showing direction of plunge.
- Fault, dotted where covered. (all faults are high-angle normal faults) Dot on downthrown side.
- Water

Figure 15.

SAN YSIDRO-JEMEZ SPRINGS-ABIQUIU-CANONES-OJO CALIENTE

Detailed geologic mapping and geochemical sampling are almost complete. Ten 7-1/2' quadrangles along the western boundary of the Rio Grande rift from San Ysidro to Ojo Caliente have been partially or completely mapped (Woodward and Ruetschilling, 1976; Woodward, in press; May, in preparation; Broomfield, in preparation; Wilson, in preparation; Callender, in preparation). Extensive travertine deposits, young volcanic rocks and hot springs are located along major faults. The stratigraphy of the Santa Fe Group is now sufficiently well understood so as to give control necessary to map faults, to reconstruct the "plumbing system" for hot thermal water, and to provide physical data for geophysical modeling. Reservoir temperatures for thermal waters are now being calculated. Electrical resistivity, gravity surveys, age-dates of volcanic and sedimentary rocks, and additional geochemical studies are planned. Interest and knowledge of the geology, geophysics and geothermal potential of this region has increased dramatically in recent years as shown by a number of recent publications (Jiracek, 1974; Bridwell, 1976; Baldridge, 1976; among others). Outside contributions to the project have been made by palynologists and geologists of Amoco Production Co., who are attempting to date the Zia Sand Formation and the Abiquiu Tuff using pollen. These efforts are directed at obtaining a more precise time for the beginning of rifting and associated deformation in the northern part of the rift.

CONTINUATION OF RESEARCH

All specified work and time committments for the first year research on this project have been achieved (Table 3). It is important to recognize that this reporting period incorporates the first year of an

TABLE 3

Estimates of Completed Work in Various Target Areas
(by discipline)

Reconnaissance Geochemistry		75% complete
Radium Springs		
	Geology	100%
	Geophysics	80%
	Geochemistry	80%
Lightning Dock (Animas Valley)		
	Geology	70%
	Geophysics	80%
	Geochemistry	60%
Alum Mountain		
	Geology	60%
	Geophysics	Not planned
	Geochemistry	50%
Truth or Consequences		
	Geology	60%
	Geophysics	20%
Reconnaissance	Geochemistry	50%
San Ysidro		
	Geology	100%
	Geophysics	Not planned
Reconnaissance	Geochemistry	60%
Las Alturas		
	Geology	10%
	Geophysics	50%
	Geochemistry	60%
Albuquerque-Belen		
	Geology	80%
	Geophysics	30%
Reconnaissance	Geochemistry	50%
Ojo Caliente		
	Geology	70%
	Geophysics	20%
Reconnaissance	Geochemistry	30%

on-going research effort. Large amounts of reconnaissance work was conducted. Specific target areas that received careful study include the Animas Valley (Lightning Dock KGRA) and Radium Springs. Geologic studies of the other target areas were initiated. However, much of the detailed geological, geochemical and geophysical objectives remain for the second year. The project emphasis will become more geophysical and geochemical in scope as progress is made.

REFERENCES CITED

Baldridge, W.S., 1976, Petrology of an ultramafic xenolity/xenocryst suite from the northern Rio Grande rift (abs.): Geol. Soc. America, Abs. with Prog., v. 8, p. 567-568.

Bridwell, R.J., 1976, Lithospheric thinning and the late Cenozoic thermal and tectonic regime of the northern Rio Grande rift: New Mexico Geol. Soc. Guidebook, 27th Field Conf., p. 283-292.

Callender, J.F., and Zilinski, R.E., 1976, Kinematics of Tertiary and Quaternary deformation along the eastern edge of the lucero uplift, central New Mexico: New Mexico Geol. Soc. Spec. Pub. 6, p. 53-61.

Conover, C.S., 1954 Ground-water conditions in the Rincon and Mesilla Valleys and adjacent areas in New Mexico: U.S. Geol. Survey Water-Supply Paper 1230, 200 p.

Decker, E.R., Cook, F.A., Ramberg, I.B., and Smithson, S.B., 1975, Significance of geothermal and gravity studies in the Las Cruces area: New Mexico Geol. Soc. Guidebook 26th Field Conf., Las Cruces country, p. 251-259.

Elston, W.E., Damon, P.E., Coney, P.J., Rhodes, R.C., Smith, E.I., and Biberman, M., 1973, Tertiary volcanic rocks, Mogollon-Datil province, New Mexico, and surrounding regions: K-Ar dates, patterns of eruption and periods of Mineralization: Geol. Soc. American Bull., v. 84, p. 2259-2273.

Elston, W.E., Rhodes, R.C., Coney, P.J., and Deal, E.G., 1976, Progress report on the Mogollon Plateau volcanic field, southwestern New Mexico, No. 3 - Surface expression of a pluton: New Mexico Geol. Soc. Spec. Pub. 5, p. 3-28.

Flege, R.F., Jr., 1959, Geology of the Lordsburg quadrangle, Hiladago County, New Mexico: New Mexico Bur. Mines and Min. Resources Bull 62, 36 p.

Fournier, R. O. and Rowe, J. J., 1966, Estimation of unerground temperatures from the silica content of water from hot springs and wet-stream wells: Am. Jour. Sci., v. 264, p. 685-697.

Jiracek, G.R., 1974 Geophysical studies in the Jemez Mountains region, New Mexico: New Mexico Geol. Soc. Guidebook, 25th Field Conf., p. 137-144.

Kelley, V.C., and Kudo, A.M., 1976, Geology of the Albuquerque-Belen basin: N.M. Bur. Mines and Min. Resources, in press.

Kelley, V.C., Woodward, L.A., Kudo, A.M., and Callender, J.F., 1976, Guidebook to Albuquerque Basin of the Rio Grande Rift, New Mexico: New Mexico Bur. Mines and Min. Resources, Circular 153, 31 p.

Kudo, A.M., Kelley, V.C., Damon, P.E., and Shafiquallah, M., 1976, K-Ar ages of basalt flows at Canjilon Hill, Isleta volcano, and the Cat Hills Volcanic Field, Albuquerque-Belen Basin, New Mexico: Isochron/West, in press.

King, W.E., Hawley, J.W., Taylor, A.M., and Wilson, R.P., 1971, Geology and ground-water resources of central and western Dona Ana County, New Mexico: New Mexico Bureau Mines & Mineral Resources Hydrol. Rept. 1, 64 p.

Kintzinger, P.R., 1956, Geothermal survey of hot ground near Lordsburg, New Mexico: Science, v. 124, p. 629-630

Loeber, K.N., 1976a, Cenozoic volcanic geology of the Truth or Consequences Engle area, New Mexico (abs.): Geol. Soc. America, Abs. with Prog., v. 8, p. 601-602.

Loeber, K.N., 1976b, Cenozoic volcanic geology of the Truth or Consequences Engle area, New Mexico: Univ. New Mexico, M.S. thesis, in press.

Mahon, W.A.J., 1970, Chemistry in the exploration and exploitation of hydrothermal systems: Geothermics, Spec. Issue 2, v. 2, pt. 2, p. 1310-1322.

Oliver, J., and Kaufman, S., 1976, Profiling the Rio Grande rift: Geotimes, v. 21, p. 20-23.

Reeder, H.O., 1957 Ground water in Animas Valley, Hidalgo County, New Mexico (with a section on geology by Z.E. Spiegel): New Mexico State Engineer Office Tech. Rept. 11, 101 p.

Renner, J.L., White, D.E., and Williams, D.L., 1975, Hydrothermal convection systems: in Assessment of Geothermal Resources of the United States-1975, D.E. White and D.L. Williams, eds., U.S. Geol. Survey, Circular 726, p. 5-57.

Sanford, A.R., Alptekin, O., and Toppozoda, T.R., 1973, Use of reflection phases on micro-earthquake seismograms to map an unusual discontinuity beneath the Rio Grande rift: Bull. Seism. Soc. America, v. 63, p. 2021-2034.

Seager, W.R., 1975a, Geologic map and sections of south half San Diego Mountain quadrangle, New Mexico: New Mexico Bureau Mines & Mineral Resources Geol. Map 35.

Seager, W.R., 1975b, Cenozoic tectonic evolution of the Las Cruces area, New Mexico: New Mexico Geol. Soc. Guidebook 26th Field Conf., Las Cruces county, p. 241-250.

Seager, W.R., Clemons, R.E., and Hawley, J.W., 1975, Geology of the Sierra Alta quadrangle, Dona Ana County, New Mexico: New Mexico Bureau Mines & Mineral Resources Bull. 102, 56 p.

Summers, W.K., 1965, Chemical characterisitcs of New Mexico's thermal waters -- A critique: New Mexico Bureau Mines & Mineral Resources Circ. 83, 27 p.

Swanberg, C.A., 1975a, Detection of geothermal components in groundwaters of Dona Ana County, southern Rio Grande rift, New Mexico: New Mexico Geol. Soc. Guidebook 26th Field Conf., Las Cruces county, p. 175-180.

Swanberg, C.A., 1975b, Geochemical studies of two geothermal areas in New Mexico (abs.): EOS (Am. Geophys. Union Trans.), v. 56, p. 1073.

Truesdell, A.H. and Fournier, R.O., 1975, Calculation of deep reservoir temperatures from chemistry of boiling hot springs of mixed origin (abs.): Proceedings of Second United Nations Symposium on the Development and Use of Geothermal Resources, #III-88.

Woodward, L.A., Callender, J.F., Gries, J., Seager, W.R., Chapin, C.E., Zilinski, R.E., and Shaffer, W.L., 1975 Tectonic map of the Rio Grande region, Colorado-New Mexico border to Presidio, Texas: New Mexico Geol. Soc. Guidebook 26, p. 239 and map.

Woodward, L.A., Callender, J.F., and Zilinski, R.E., 1975, Tectonic map of Rio Grande rift, New Mexico: Geol. Soc. America, Maps and Charts Series, MC-11.

Woodward, L.A. and Reutschilling, R.L., 1976 Geology of San Ysidro quadrangle, New Mexico: New Mexico Bur. Mines & Min. Resources Geol. Map 37.

APPENDIX A

I. Contact with public and private organizations related to Geothermal research program.

II. Geothermal related publications by this group: 1974-76.

APPENDIX A-I

Contact with public or private organizations
related to Geothermal research program

Albuquerque Geological Society

Channel 7 (KOAT-TV)

Los Alamos Scientific Laboratories

U. S. Geological Survey
(Roswell, Menlo Park, Denver, Reston, Albuquerque offices)

Aminoil USA (subsidiary of Burmah Oil)

American Oil Company

Bear Creek Mining Co. (subsidiary of Kennecott Corp.)

University of Arizona

Sandia Laboratories

Bureau of Land Management, Las Cruces, N. M.

Economic Research Associates, Los Angeles

Secretaria de Energia, Republica Argentina

Japan Geothermal Energy Association

Chevron Oil Co., San Francisco

Amax Exploration, Inc., Denver

Exploration Associates, Tulsa

Earth Satellite Corp., Berkeley

Geonomics, Berkeley

Phillips Petroleum Co., Del Mar, Calif.

W. Kelly Summers, Consultant, Socorro, N. M.

Tom McCants, Homeowner, Animas, N. M.

Geothermal Power Corp., San Francisco

Thermal Power Corp., Dallas

Hydro-Search, Inc., Reno, Nevada

Burmah Oil and Gas Co., Santa Rosa, California

Energy Research & Development Agency

Tech. Information Center, Oak Ridge, Tennessee

Systems, Science, and Softward Library, La Jolla, Ca.

Sun Oil Co., Dallas

Lawrence Berkeley Laboratory, Berkeley

APPENDIX A-II

Geothermal related publications by this group during 1974-76

Aubele, J. C., Crumpler, L. A., Loeber, K. N., and Kudo, A. M., 1976, Maare and tuff rings of New Mexico: in Tectonics and mineral resources of Southwestern North America: New Mex. Geol. Soc. Spec. Publ. 6, p. 109-114.

Brookins, D. G., Forbes, R. B., Laughlin, A. W., Naeser, C. W., and Turner, D. L., 1976, Rb-Sr, K-Ar and Fission Track Geochronological studies from LASL Drill Holes GT-1, GT-2, and EE-1, (in press).

Brookins, D. G., and Laughlin, A. W., 1976a, High 87/86 strontium ratios in fracture-filling calcite from GT-2: EOS, Amer. Geophys. Un. Trans., v. 57, p. 352-353.

Brookins, D. G., and Laughlin, A. W., 1976b, Rb-Sr Geochronologic investigation of Precambrian samples from drill holes GT-1, GT-2, and EE-1: Los Alamos Dry Hot Rock Program, Fenton Hill, New Mexico: LASL Rpt. to USERDA, 35 p.

Brookins, D. G., and Laughlin, A. W., 1976c, Rubidium-strontium geochronologic study of GT-1 and GT-2: EOS, Trans. Amer. Geophys. Un., v. 57, p. 352.

Brookins, D. G., and Laughlin, A. W., High $^{87}Sr/^{86}Sr$ ratios in deep seated, fracture-filling calcite from drill hole GT-2, Los Alamos Scientific Laboratory Dry Hot Rock Program (to Jour. Vulcan, and Geoth. Res.), in press.

Broomfield, R., Geology of the Canones area, New Mexico: Univ. N. Mex., M.S. Thesis, in preparation.

Callender, J. F., 1974, Influence of structures in the Precambrian terrain of central New Mexico on late Cenozoic rifting: Geol. Soc. Amer., Penrose Conference on Rio Grande graben and surrounding areas, invited paper.

Callender, J. F., 1975, Overview of the Rio Grande rift: Field trips to central New Mexico, Amer. Assoc. Petroleum Geol., Rocky Mtn. Section, p. 1-4.

Callender, J. F., Woodward, L. A., and Kelley, V. C., 1976, Structural framework of the Rio Grande rift, New Mexico and Colorado (abs.): Geol. Soc. Amer. Abs. with Programs, v. 8, no. 5, p. 573.

Callender, J. F., and Zilinski, R. E., 1976, Kinematics of the Tertiary and Quaternary deformation along the eastern edge of the Lucero uplift, central New Mexico, N. Mex. Geol. Soc. Spec. Publ. 6, p. 53-61.

Carten, R. B., silberman, M. L., Armstrong, A. K., and Elston, W. E., 1974, Geology, trace-metal anomalies, and base-metal mineralizations in the central Peloncillo Mountains, Hidalgo County, New Mexico (abs.): N. Mex. Geol. Soc. Guidebook of Central-Northern New Mexico 25th Field Conf., p. 378.

Elston, W. E., Rhodes, R. C., and Erb, E. E., 1975, Control of mineralization by mid-Tertiary volcanic centers, New Mexico (abs.): N. Mex. Geol. Soc. Guidebook, Las Cruces County, 26th Field Conference, p. 338-339.

Elston, W. E., Seager, W. R., and Clemons, R. E., 1975, Emory cauldron, Black Range, New Mexico: Source of the Kneeling Nun Tuff: N. Mex. Geol. Soc. Guidebook of Las Cruces County, 26th Field Conference, p. 283-292.

Elston, W. E., 1976a, Mid-Tertiary volcanism and plutonism, southwestern New Mexico (abs.): Geol. Soc. Amer. Abs. with Programs, v. 8, p. 585.

Elston, W. E., 1976b, Tectonic-significance of mid-Tertiary volcanism in the Basin and Range province: A critical review with special reference to New Mexico: N. Mex. Geol. Soc. Spec. Publ. 5, 151 p. plus pocket.

Elston, W. E., Rhodes, R. C., Coney, P. J., and Deal, E. G., 1976, Progress report on the Mogollon Plateau volcanic field, southwestern New Mexico, No. 3 - Surface expression of a pluton: N. Mex. Geol. Soc. Spec. Publ. 5, p. 3-28.

Helmick, S. B., and Brookins, D. G., 1975, Trace element studies in GT-2 core, EHR Project: LASL Rpt. to USERDA, 52 p.

Helmick, S. B., Brookins, D. G., Balagna, J. P., and Husler, J. W., 1976, Trace element analyses of granite cores from LASL dry hot rock experiment: EOS, Trans. Amer. Geophys. Un., v. 57, p. 350.

Jiracek, R. G., 1974, Geophysical studies in the Jemez Mountains, New Mexico, in N. Mex. Geol. Soc. Guidebook, 25th Field Conf., p. 137-144.

Jiracek, G. R., 1975a, Deep electrical resistivity investigations coupled with dry geothermal reservoir experiments in New Mexico: NSF Tech. Prof. Rpt., Univ. of New Mexico, Albuquerque, 47 p.

Jiracek, G. R., 1975b, Geophysical potential methods in geothermal prospecting: Position papers on Geothermal Resources, Governor's Energy Task Force publication, New Mexico Energy Resources Board, June 1975.

Jiracek, G. R., 1975c, Deep geothermal exploration in New Mexico using electrical resistivity (abs. III-47): Abstracts, Second United Nations Symp. Devel. and Use of Geothermal Res., San Francisco, May 20-29, 1975.

Jiracek, G. R., 1975d, Geothermal exploration in New Mexico (abs.): New Mex. Acad. Sci. Bull., vol. 15, no. 2, p. 19.

Jiracek, G. R., 1975e, Geothermal resources: Enercon, vol. 1, Issue 1, Energy Resources Board, State of New Mexico, p. 3-4.

Jiracek, G. R., Dorn, G. A., Forsythe, G., Gerety, M. T., Schrandt, B., and Smith C., 1975, Resistivity investigations surrounding "hot dry rock" geothermal drill sites in New Mexico (abs.): EOS, Trans. AGU, 56, (4), p. 235.

Jiracek, G. R., Dorn, G. A., Smith, C., and Gerety, M. T., 1975, Deep resistivity measurements at two known geothermal resource areas (KGRAS) in New Mexico (abs.): EOS, Trans. AGU, 56 (12) p. 1073.

Jiracek, G. R. and Kintzinger, P. R., 1975, Deep electrical resistivity investigations coupled with "dry" geothermal reservoir experiments in New Mexico (abs.): Geophysics, vol. 40, p. 175.

Jiracek, G. R., Smith, C. S., Forsythe, G. T., and Dorn, G. A., 1975, Geothermal resistivity investigations in New Mexico (abs.): Abstracts, Program 24th Ann. Mtg. Rocky Mtn. Sect., AAPG, p. 18.

Jiracek, G. R., and Smith, C., 1976, Deep resistivity investigations of two known geothermal resource areas (KGRAS) in New Mexico: Radium Springs and Lightning Dock: N. Mex. Geol. Soc. Spec. Publ. 6, p. 71-76.

Jiracek, G. R. and Phillips, R. J., 1976a, Deep electrical resistivity investigations coupled with dry geothermal reservoir experiments in New Mexico: preliminary field and numerical results: Proc. Conf. on Explor. Geothermal Reser., Golden, Colo., in press.

Jiracek, G. R. and Phillips, R. J., 1976b, Deep electrical resistivity investigations coupled with dry geothermal reservoir experiments in New Mexico: preliminary field and numerical results: Digest of NSF Geothermal Res., in press.

Jiracek, G. R., Smith, C., and Dorn, G. A., 1976, Deep geothermal exploration in New Mexico using electrical resistivity: Proc. of Second U.N. Symp. Devel. and Use of Geothermal Reserv., in press.

Jiracek, G. R., Smith, C., and Gerety, M. T., 1976, Deep electrical resistivity soundings in the Rio Grande rift (abs.): Abs. with Programs, Annual 1976 Meeting, Geol. Sox. Amer., in press.

Kasten, J. A., Bolivar, S. L., Kudo, A. M., and Brookins, D. G., 1976, Calc-alkaline andesite within the Rio Grande rift (abs.): Trans. Amer. Geophys. Un., v. 55, p. 487.

Kelley, V. C. and Kudo, A. M., 1976, Volcanoes and related basalts of the Albuquerque Basin, New Mexico: N. Mex. Bur. Mines and Min. Resources, Circular, in press.

Kelley, V. C., Woodward, L. A., Kudo, A. M., and Callender, J. F., 1976, Guidebook to Albuquerque Basin of the Rio Grande Rift, New Mexico: N. Mex. Bur. Mines and Min. Resources, Circular 153, 31 p.

Kintzinger, P. R., and Jiracek, G. R., 1976, Geophysical measurements at Fenton Hill (abs.): EOS, Trans. AGU, 57 (8), p. 600.

Kintzinger, P. R., Jiracek, G. R., West, F., and Dorn, G. A., 1976, Electrical measurements at the Los Alamos Scientific Laboratory's geothermal project (abs.): Geophysics, in press.

Kudo, A. M., 1976, Volcanism within the Rio Grande rift (abs.): Geol. Soc. Amer., Abs. with Programs, v. 8, no. 5, p. 597.

Kudo, A. M., Kelley, V. C., Damon, P. E., and Shafiquallah, M., 1976, K-Ar ages of basalt flows at Canjilon Hill, Isleta volcano, and the Cat Hills Volcanic Field, Albuquerque-Belen Basin, New Meixco: Isochron/West, in press.

Loeber, K. N., 1976, Cenozoic volcanic geology of the Truth or Consequences-Engle Area, New Mexico (abs.): Geol. Soc. Amer., Abs. with Programs, v. 8, no. 5, p. 601-602.

May, S. J., Geology of the Ojo Caliente area, New Mexico: Univ. N. Mex. Ph.D. dissertation, in preparation.

Smith, C., Jiracek, G. R., and Ander, M. E., 1976, Deep electrical investigations of geothermal prospects in the Basin and Range province of southern New Mexico (abs.): Geophysics, in press.

Smith, C., Morgan, P., Jiracek, G. R., and Swanberg, C. A., 1976, New Mexico State University annual energy conference -- geothermal energy: Geothermal Energy, vol. 4, no. 7, p. 19-23.

Swanberg, C., 1975, Detection of geothermal components in groundwaters of Dona Ana County, southern Rio Grande rift, New Mexico: N. Mex. Geol. Soc. Guidebook 26, p. 175-180.

Wilson, J., Geology of the Abiquiu area, New Mexico: Univ. N. Mex., M.S. thesis, in preparation.

Woodward, L. A., 1975, Geometry of Sierrita fault and its bearing on tectonic development of the Rio Grande rift: Reply: Geology, v. 3, no. 7, p. 357.

Woodward, L. A., Callender, J. F., Gries, J., Seager, W. R., Chapin, C. E., Shaffer, W. L., and Zilinski, R. E., 1975, Tectonic map of the Rio Grande region; Colorado-New Mexico border to Presidio, Texas: N. Mex. Geol. Soc. 26th Guidebook, Las Cruces County, p. 239.

Woodward, L. A., Callender, J. F., and Zilinski, R., 1975, Tectonic map of the Rio Grande rift, New Mexico: Geological Society of America Map and Chart Series #MC-11.

Woodward, L. A., and DuChene, H. R., 1975, Geometry of Sierrita fault and its bearing on tectonic development of the Rio Grande rift, New Mexico, Geology, v. 3, no. 3, p. 114-116.

Woodward, L. A., and Ruetschilling, R. L., 1976, Geology of San Ysidro quadrangle, New Mexico: N. Mex. Bur. Mines and Min. Resources Geol. Map 37 (with accompanying text).

Woodward, L. A., Geology of the Gilman 7-1/2 quadrangle, New Mexico: N. Mex. Bur. Mines and Min. Resources Geol. Map, in press.

Woodward, L. A., and Callender, J. F., Tectonics and development of northern part of Rio Grande rift, New Mexico and Colorado (abs.): Geol. Soc. Amer., Abs. with Programs, in press.

Zilinski, R. E., and Callender, J. F., 1975, Structure of Lucero Uplift, eastern Valencia County, New Mexico: Amer. Assoc. Petroleum Geol. Bull., v. 59, p. 925-926.

Zilinski, R. E., Potter, J. M., Jiracek, G. R., and Callender, J. F., 1976, Bouguer gravity map of Rio Grande rift: N. Mex. Bur. Mines and Min. Resources, open-file map.

Zilinski, R. E., Potter, J. M., Jiracek, G. R., and Callender, J. F., 1976, Heatflow and thermal waters of Rio Grande rift: N. Mex. Bur. Mines and Min. Resources, open-file map.

Zilinski, R. E., Potter, J. M., Jiracek, G. R., and Callender, J. F., 1976, Magnetic anomaly map of Rio Grande rift: N. Mex. Bur. Mines and Min. Resources, open-file map.

APPENDIX B

TECTONIC MAP OF THE RIO GRANDE RIFT

THE
GEOLOGICAL SOCIETY
OF AMERICA
3300 Penrose Place • Boulder, Colorado 80301

TECTONIC MAP OF THE RIO GRANDE RIFT, NEW MEXICO

COMPILED BY: L. A. WOODWARD, J. F. CALLENDER, R. E. ZILINSKI
Department of Geology, University of New Mexico, Albuquerque, New Mexico 87131

ERTS photograph of central part of Rio Grande rift and Jemez Mountains with Valles caldera (circular structure in center of photograph).

APPENDIX C

PARTIAL LIST OF CHEMICAL ANALYSIS ON THERMAL AND RELATED WATERS

Sample	ppm	pH	Na	K	Ca	Mg	CO_3	HCO_3	Cl	SO_4
						-mg/l-				
W-1	952	7.75	225.5	15.2	28.8	8.6		320.9	88.6	280.5
W-2	1236	8.25	405.8	26.2	46.3	16.4	14.4	439.3	318.7	222.9
W-3	720	8.66	223.0	10.6	10.2	7.2	37.2	334.4	82.2	132.6
W-4	552	8.50	180.7	16.8	8.2	8.3	25.2	335.6	54.2	94.1
W-5	784	8.00	255.4	14.1	9.0	7.5	0	317.3	77.6	263.2
W-6	888	7.93	286.4	14.1	20.0	10.0	0	358.8	83.7	293.9
W-7	604	8.36	238.8	0.4	3.0	5.8	22.8	369.8	41.5	130.6
W-8	840	7.94	238.8	0.8	24.8	13.0	0	454.0	79.1	146.0
W-9	604	9.26	236.1	8.2	21.4	6.3	90.0	263.6	95.7	105.7
W-10	2600	8.60	414.5	22.7	264.1	48.2	7.2	46.4	314.4	1219.9
W-11	1860	7.56	64.6	7.0	345.7	80.6	0	145.2	19.1	1114.3
W-12	1392	7.54	72.4	7.4	322.2	80.0	0	119.6	30.1	1085.5
W-13	1848	7.49	140.2	5.1	240.5	113.3	0	175.7	90.4	1027.9
W-14	1328	7.69	176.5	3.9	123.8	70.6	0	179.4	129.0	624.4
W-15	1224	7.81	164.8	9.4	110.8	50.8	0	120.8	25.2	979.8
W-16	2480	7.15	197.2	9.8	472.7	14.7	0	52.5	22.0	1498.6
W-17	1968	7.94	152.4	9.0	321.4	49.0	0	45.1	20.6	1181.6
W-18	2616	7.59	144.1	11.7	502.8	29.2	0	43.9	20.2	1575.4
W-19	2120	8.87	388.5	22.3	155.7	58.3	27.6	37.8	229.7	1018.2
W-20	372	8.35	32.2	5.5	36.9	17.9	1.2	197.7	20.9	44.2
W-21	548	7.85	65.0	4.7	36.9	30.4	0	328.3	31.5	61.5
W-22	364	7.57	33.8	4.7	43.9	19.8	0	225.8	19.8	48.0

Sample	P	B	F	Fe	SiO_2
	----------	----------	Mg/l	----------	----------
W-1	.02	.99	2.68	.20	69.5
W-2	.02	1.02	1.36	.04	73.8
W-3	.02	.67	2.15	.12	55.6
W-4	.02	.42	2.15	.10	58.8
W-5	.01	.55	2.24	.15	47.1
W-6	.02	.69	2.68	.42	65.2
W-7	.05	.35	3.67	.42	37.9
W-8	.02	.33	2.68	.34	47.1
W-9	.02	.29	2.68	.01	4.3
W-10	.01	.74	1.40	.21	8.3
W-11	.01	.14	.86	1.24	28.4
W-12	.01	.16	.78	.88	26.5
W-13	.01	.25	1.00	2.24	27.4
W-14	.01	.35	1.26	1.94	23.3
W-15	.01	.55	1.11	.30	48.1
W-16	.01	.27	1.07	.90	14.3
W-17	.01	.16	.93	.10	13.3
W-18	.01	.23	1.15	2.96	68.4
W-19	.01	.90	1.50	.62	43.0
W-20	.02	.10	.86	.88	66.3
W-21	.02	.10	1.04	.46	68.4
W-22	.02	.07	.67	.25	65.2

Sample	Latitude	Longitude	Temperature °C	Comment
W23	32° 11.5	107° 6.0	22	well
W24	32° 1.2	107° 4.9	27	well
W25	31° 59.6	107° 1.2	27	well
W26	31° 55.4	106° 57.9	22	well
W27	31° 55.0	106° 50.2	28	well
W28	32° 2.2	106° 57.6	26	well
W29	32° 20.3	106° 37.4	18	well
W30	32° 25.6	106° 35.9	--	well
W31	31° 56.9	106° 45.1	--	well
W32	31° 51.7	106° 42.7	27	well
W33	31° 47.3	107° 1.7	--	well
W34	31° 47.2	107° 6.5	--	well
W35	31° 49.1	107° 8.6	17	well
W36	31° 47.5	107° 17.0	27	well

Sample	(ppm) TDS	pH	mg/l Na	K	Ca	Mg	CO_3	HCO_3	Cl	SO_4
W-23	334	8.21	52.9	0.8	40.3	18.3	0	248.9	23.7	63.4
W-24	616	8.75	265.1	4.3	5.6	1.6	13.2	428.3	50.7	50.0
W-25	348	8.59	120.0	17.6	8.4	4.2	0	299.0	14.2	50.0
W-26	728	9.02	271.0	5.5	2.6	1.1	42.0	454.0	42.9	126.8
W-27	500	8.50	170.6	16.4	8.4	8.0	13.2	333.2	46.4	80.7
W-28	768	8.44	232.0	12.1	24.4	8.6	0	222.7	178.0	178.7
W-29	228	7.48	18.6	1.2	48.9	7.8	0	109.8	3.2	96.1
W-30	1436	7.83	71.0	3.9	270.0	39.8	0	158.6	80.1	739.7
W-31	616	8.95	211.7	5.5	15.8	6.1	21.6	234.3	70.9	186.4
W-32	720	8.53	242.1	7.8	19.2	6.3	0	379.5	67.0	194.0
W-33	720	9.42	233.3	16.8	10.0	2.1	69.6	371.0	29.4	101.8
W-34	604	10.56	190.1	20.3	3.6	2.3	199.2	41.5	23.7	71.1
W-35	556	8.66	196.8	14.1	9.6	5.5	13.2	458.9	22.3	59.6
W-36	2028	8.09	671.3	37.9	84.5	27.5	54.0	445.4	606.9	475.5

Sample	P	B	F	Fe	SiO_2
	----------	----------	mg/l	----------	----------
W-23	.04	.14	.80	<.15	41.9
W-24	.02	.76	2.50	.61	19.5
W-25	.03	.32	2.50	1.43	41.9
W-26	.28	.90	8.00	.29	53.5
W-27	.04	.41	2.25	<.15	63.1
W-28	.02	.47	1.65	1.00	77.0
W-29	.02	.05	1.15	.27	33.6
W-30	.01	.15	2.50	<.15	39.8
W-31	.01	.40	2.65	<.15	39.8
W-32	.10	.55	2.05	<.15	52.4
W-33	.02	.49	3.30	<.15	93.5
W-34	.02	.25	1.85	.15	85.8
W-35	.05	.21	1.40	2.94	39.8
W-36	.01	.73	3.00	.83	48.1

Sample	Latitude	Longitude	Temperature °C	Comment
LD1 SW132	32° 18.9	108° 38.8	25	well
LD2 SW133	32° 13.7	108° 30.7	33	well
LD3 SW134	32° 10.6	108° 33.6	--	well
LD4 SW135	32° 3.9	108° 34.5	--	Lone Hill Well
LD5 SW136	31° 55.8	108° 36.9	--	well
LD6 SW137	31° 57.0	108° 48.5	--	well
LD7 SW138	31° 48.6	108° 46.5	24	well
LD8 SW139	31° 50.0	108° 52.5	21	well
LD9 SW140	31° 40.2	108° 49.9	19	well
LD10 SW141	31° 35.8	108° 52.2	--	well
LD11 SW142	31° 24.2	108° 51.8	18	well
LD12 SW143	31° 23.2	108° 54.9	18	well
LD13 SW144	31° 20.4	108° 47.9	17	Cienega Springs
LD14 SW145	31° 28.0	108° 50.4	25	well
LD15 SW146	31° 34.2	108° 52.4	21	well
LD16 SW147	31° 37.3	108° 54.3	19	well
LD17 SW148	31° 44.8	108° 48.6	22	well
LD18 SW149	31° 52.9	108° 48.0	--	well

Sample	TDS	pH	Ca	Mg	Na	K	CO_3	HCO_3	Cl	SO_4
					mg/l					
132	564	8.09	7.6	1.4	143.2	5.9	0	234.3	27.6	93.7
133	816	7.86	28.0	2.7	216.1	11.7	0	314.8	47.5	223.8
134	740	7.48	117.4	18.7	98.6	10.2	0	218.4	116.6	181.5
135	592	7.94	10.2	1.8	159.3	1.5	0	301.4	33.0	104.2
136	796	7.82	15.6	1.3	234.5	5.5	0	400.3	50.7	154.6
137	208	7.92	22.0	7.3	27.6	2.0	0	147.7	3.5	19.2
138	208	7.82	40.3	4.9	15.2	2.0	0	156.2	2.5	4.3
19	184	7.57	26.0	2.2	21.1	1.2	0	109.8	2.8	4.3
140	176	7.39	21.0	3.2	6.2	4.5	0	65.9	0.7	33.6
141	156	7.31	17.8	3.3	6.9	6.2	0	57.3	1.4	40.3
142	200	7.74	16.6	4.8	36.8	5.1	0	173.3	1.4	3.8
143	136	6.88	15.8	2.9	13.8	3.5	0	37.8	0.7	52.8
144	132	7.00	8.2	1.7	15.2	2.7	0	22.0	1.4	40.3
145	160	8.80	2.4	0.5	54.7	0.4	0	137.9	4.2	16.3
146	212	8.11	27.6	3.2	16.3	3.1	0	124.4	1.0	13.4
147	164	7.94	29.4	1.7	11.5	2.3	0	117.1	0.1	5.7
148	168	8.06	21.2	0.7	12.9	1.5	0	98.8	0.1	9.1
149	320	8.15	16.4	0.6	65.3	1.2	0	173.3	4.2	32.7

Sample	Ca	Mg	Na	K	Total Cations	CO_3	HCO_3	Cl	SO_4	Total Anions
	mg/l									
132	.38	.12	6.23	.15	6.88	0	3.84	.78	1.94	6.57
33	1.40	.22	9.40	.30	11.32	0	5.16	1.34	4.66	11.16
134	5.86	1.54	4.29	.26	11.95	0	3.58	3.29	3.78	10.65
35	.51	.15	6.33	.04	7.63	0	4.94	.93	2.17	8.04
136	.78	.11	10.20	.14	11.23	0	6.56	1.43	3.22	11.21
137	1.10	.60	1.20	.05	2.95	0	2.42	.10	.14	2.66
138	2.01	.40	.66	.05	3.12	0	2.56	.07	.09	2.72
139	1.30	.18	.92	.03	2.43	0	1.80	.08	.09	1.97
140	1.05	.26	.27	.12	1.70	0	1.08	.02	.70	1.80
141	.89	.27	.30	.16	1.62	0	.94	.04	.84	1.82
142	.83	.40	1.60	.13	2.96	0	2.84	.04	.08	2.96
143	.79	.24	.60	.09	1.72	0	.62	.02	1.10	1.74
144	.41	.14	.66	.07	1.28	0	.36	.04	.84	1.24
145	.12	.04	2.38	.01	2.55	0	2.26	.12	.34	2.72
146	1.38	.26	.71	.08	2.43	0	2.04	.03	.28	2.35
147	1.47	.14	.50	.06	2.17	0	1.92	.003	.12	2.04
148	1.06	.06	.56	.04	1.72	0	1.62	.003	.19	1.81
149	.82	.05	2.84	.03	3.74	0	2.84	.12	.68	3.64

Sample	Cd	Co	Cr	ppm Cu	Hg	ppm H_2S	ppm Li	Mn	Mo	NH_4
132	<.02	<.14	<.1		<.0002	<.1	.14	<.05	<.5	<.05
133	<.02	<.14	<.1	<.10	<.0002	<.1	.31	<.05	<.5	<.05
134	<.02	<.14	<.1	<.10	.0002	<.1	.13	<.05	<.5	<.05
135	<.02	<.14	<.1	<.10	<.0002	<.1	.13	<.05	<.5	<.05
136	<.02	<.14	<.1	<.10	<.0002	<.1	.23	<.05	<.5	<.05
137	<.02	<.14	<.1	<.10	.0002	<.1	.03	<.05	<.5	<.05
138	<.02	<.14	<.1	.69	<.0002	<.1	<.02	<.05	<.5	<.05
139	<.02	<.14	<.1	<.10	<.0002	<.1	.02	<.05	<.5	<.05
140	<.02	<.14	<.1	<.10	<.0002	<.1	<.02	<.05	<.5	<.05
141	<.02	<.14	<.1	.11	<.0002	<.1	<.02	<.05	<.5	<.05
142	<.02	<.14	<.1	<.10	<.0002	<.1	.02	<.05	<.5	<.05
143	<.02	<.14	<.1	<.10	<.0002	<.1	<.02	<.05	<.5	<.05
144	<.02	<.14	<.1	<.10	<.0002	.10	<.02	<.05	<.5	<.05
145	<.02	<.14	<.1	<.10	.0004	<.1	<.02	<.05	<.5	<.05
146	<.02	<.14	<.1	<.10	.0006	.13	<.02	<.05	<.5	<.05
147	<.02	<.14	<.1	<.10	.0004	<.1	<.02	<.05	<.5	<.05
148	<.02	<.14	<.1	<.10	.0009	<.1	.02	<.05	<.5	<.05
149	<.02	<.14	<.1	<.10	.0004	<.1	.11	<.05	<.5	<.05

Sample	ppm Zn	ppm St	Se	NO_3
132	<.02	.03	.005	4.48
133	<.02	.15	.009	.19
134	.21	.46	.016	42.65
135	.33	.07	.008	15.30
136	.05	.04	.010	15.02
137	.13	.06	<.002	4.93
138	2.68	.03	<.002	7.12
139	1.22	.02	<.002	22.75
140	<.02	.02	.002	9.77
141	.20	.03	.002	1.47
142	.44	<.02	<.002	2.15
143	.04	.03	<.002	0
144	.03	<.02	<.002	3.70
145	.17	<.02	.003	3.59
146	.73	.03	<.002	4.88
147	.21	.02	<.002	7.97
148	.63	.03	<.002	1.28
149	.17	.03	.002	7.53

Sample	Fe	F	B	P	SiO_2	Ag	Al	As	Ba	Br
132	<.15	3.66	.46	0	33.52	<.06	<1.0	.012	<.20	.53
133	<.15	6.90	.46	.01	39.64	<.06	<1.0	.017	<.20	.67
134	<.15	.44	.32	.01	43.36	<.06	<1.0	.008	<.20	1.52
135	.37	2.67	.50	.01	32.30	<.06	<1.0	.018	<.20	.56
136	<.15	7.11	.64	.01	47.15	<.06	<1.0	.017	<.20	.99
137	.62	.30	.12	.01	38.08	<.06	<1.0	.003	<.20	0
138	4.70	.16	.12	.02	47.62	<.06	<1.0	.003	<.20	.28
139	6.39	1.34	.06	.01	45.23	<.06	<1.0	.005	<.20	.32
140	<.15	.12	.04	.14	47.62	<.06	<1.0	.003	<.20	0
141	.56	.11	.04	.01	39.28	<.06	<1.0	.002	<.20	0
142	5.77	1.12	.12	.01	52.37	<.06	<1.0	.006	<.20	.35
143	<.15	.18	.06	.01	35.68	<.06	<1.0	.003	<.20	.12
144	<.15	.14	.06	.01	39.28	<.06	<1.0	.017	<.20	.16
145	.56	.31	.10	.01	14.23	<.06	<1.0	.004	<.20	.41
146	1.49	.42	.08	.01	47.62	<.06	<1.0	.003	<.20	.23
147	.22	.22	.08	.01	41.65	<.06	<1.0	.003	<.20	.25
148	1.91	.16	.08	0	44.03	<.06	<1.0	.031	<.20	.23
149	.78	2.26	.12	0	42.85	<.06	<1.0	.007	<.20	.41

Sample	Ni	Sb	Pb
132	<.16	<.5	.005
133	<.16	<.5	.009
134	<.16	<.5	.006
135	<.16	<.5	.006
136	<.16	<.5	.008
137	<.16	<.5	.001
138	<.16	<.5	.039
139	<.16	<.5	.006
140	<.16	<.5	.001
141	<.16	<.5	.001
142	<.16	<.5	.004
143	<.16	<.5	.001
144	<.16	<.5	.001
145	<.16	<.5	.002
146	<.16	<.5	.002
147	<.16	<.5	.001
148	<.16	3.19	867.5
149	<.16	<.5	.025

Sample	Latitude	Longitude	Temperature °C	Comment
1P	32° 8.7	108° 47.6	23	Road Well
2P	32° 8.7	108° 49.9	85	Hot Well
3P	32° 8.9	108° 49.9	81	McCants Well
4P	32° 8.7	108° 50.4	71	well
5P	32° 8.1	108° 50.9	22	well
10P	32° 13.6	108° 49.7	23	Hill Well
13P	32° 13.7	108° 52.4	19	well
14P	32° 10.1	108° 52.8	20	well
15P	32° 6.1	108° 50.7	24	well
20P	32° 4.8	108° 54.0	22	well
22P	32° 4.1	108° 52.9	22	well
23P	32° 12.2	108° 48.8	24	Nation Well
24P	32° 10.9	108° 50.7	--	well
25P	32° 9.1	108° 52.8	23	well

Sample	ppm TDS	pH	Ca	Mg	Na	K	CO_3	HCO_3	Cl	SO_4
			mg/l							
1P	484	8.20	28.0	7.3	68.7	1.9	0	183.1	20.5	79.3
2P	1116	7.71	22.0	0.5	333.6	23.5	0	106.8	88.3	497.1
3P	1024	8.16	23.2	0.8	318.6	21.1	0	103.7	87.6	480.0
4P	1608	7.84	67.3	5.3	493.1	27.8	0	118.9	111.3	893.4
5P	1660	8.08	159.3	34.9	231.7	9.0	0	209.3	181.9	956.3
10P	1708	8.18	67.9	17.1	366.2	6.3	0	255.0	133.6	939.0
13P	756	7.90	38.3	2.7	105.5	3.1	0	237.9	16.7	298.7
14P	668	8.00	47.9	4.4	71.0	2.7	0	209.3	23.0	289.6
15P	868	8.07	78.7	12.6	152.2	5.9	0	201.4	80.5	483.7
20P	632	8.02	43.2	4.1	97.0	2.3	0	192.2	21.3	305.0
22P	600	7.90	49.3	4.4	111.3	2.7	0	192.2	38.6	311.7
23P	640	8.08	18.6	2.4	120.2	1.6	0	250.2	29.1	308.3
24P	1348	7.92	38.5	1.8	321.4	18.0	0	275.8	79.1	768.5
25P	604	8.35	38.1	5.7	78.8	3.5	0	183.1	8.9	285.8

Sample	Ca	Mg	Na	K	Total Cations	CO_3	HCO_3	Cl	SO_4	Total Anions
	----------meq/l----------									
1P	1.40	.60	2.99	.05	5.04	0	3.00	.58	1.65	5.23
2P	1.19	.04	14.51	.60	16.34	0	1.75	2.49	10.35	14.59
3P	1.16	.07	13.86	.54	15.63	0	1.70	2.47	10.00	14.17
4P	3.36	.44	21.45	.71	25.96	0	1.95	3.14	18.60	23.69
5P	7.95	2.87	10.08	.23	21.13	0	3.45	5.15	11.35	19.91
10P	3.39	1.41	15.93	.16	20.89	0	4.18	3.77	11.60	19.55
13P	1.91	.22	4.59	.08	6.80	0	3.90	.47	1.85	6.22
14P	2.39	.36	3.09	.07	5.91	0	3.45	.65	1.95	6.05
15P	3.93	1.04	6.62	.15	11.74	0	3.30	2.27	4.50	10.07
20P	2.16	.34	4.22	.06	6.78	0	3.15	.60	2.60	6.35
22P	2.46	.36	4.84	.07	7.73	0	3.15	1.09	2.25	6.49
23P	.95	.20	5.23	.04	6.40	0	4.10	.82	1.50	6.42
24P	1.92	.15	13.98	.46	16.51	0	4.52	2.23	9.25	16.00
25P	1.90	.47	3.43	.09	5.89	0	3.00	.25	2.70	5.95

	mg/l									
Sample	Fe	F	B	P	SiO_2	Ag	Al	As	Ba	Br
1P	1.10	.35	.08	.01	31.3					
2P	.20	12.6	.48	.02	147.5					
3P	.40	12.0	.50	.02	143.0	<.03	<2.5	.019	<.70	.56
4P	.83	7.25	.42	.01	115.6					
5P	<.10	3.55	.25	.01	42.3					
10P	.53	7.25	.51	.01	60.7					
12P	1.31	3.90	.10	.01	74.1					
14P	.16	.85	.06	.01	48.4					
15P	<.10	2.35	.18	.01	34.3					
20P	<.10	2.65	.10	.01	50.4					
22P	<.10	1.20	.06	.01	43.3					
23P	7.66	1.15	.12	.01	29.3					
24P	21.18	9.35	.50	.01	149.7					
25P	.36	3.55	.12	.01	34.3					

Sample	Latitude	Longitude	Temperature °C	Comment
JW1	32° 53.4	108° 21.5	26	Allen Spring
JW2	33° 49.8	108° 47.9	37	Upper Frisco Hot Springs
JW3	33° 14.6	108° 52.7	43	Lower Frisco Hot Springs
JW4	33° 14.9	108° 52.6	40	Lower Frisco Hot Springs
JW5	33° 14.5	108° 52.8	49	Lower Frisco Hot Springs
JW6	33° 1.6	108° 41.5	21	well
JW7	32° 58.5	108° 37.9	25	Warm Spring

Sample	(ppm) TDS	pH	Ca	Mg	Na	K	CO_3	HCO_3	Cl	SO_4
			mg/l							
JW-1	492	8.12	77.8	38.2	8.3	1.6	0	389.3	2.5	48.0
2	156	9.60	1.2	<.1	62.8	.4	49.2	72.0	.4	19.2
3	992	7.89	49.7	6.8	307.1	15.6	0	129.4	445.3	57.6
4	768	7.95	39.3	7.4	215.6	11.3	0	136.7	294.6	44.2
5	1280	7.79	54.3	6.9	406.0	18.8	0	107.4	574.3	90.3
6	160	8.00	16.8	7.3	23.2	2.0	0	131.8	1.1	19.2
7	164	7.89	13.0	6.9	27.4	2.7	0	140.3	1.4	15.4

	Ca	Mg	Na	K	Total Cations	CO_3	HCO_3	Cl	CO_4	Total Anions
					meq/l					
JW-1	3.88	3.14	.36	.04	7.42	0	6.38	.07	1.00	7.45
2	.06	<.01	2.73	.01	2.80	1.64	1.18	.01	.40	3.23
3	2.48	.56	13.36	.40	16.80	0	2.12	12.56	1.20	15.88
4	1.96	.61	9.38	.29	12.24	0	2.24	8.31	.92	11.47
5	2.71	.57	17.66	.48	21.42	0	1.76	16.20	1.88	19.84
6	.84	.60	1.01	.05	2.50	0	2.16	.03	.40	2.59
7	.65	.57	1.19	.07	2.48	0	2.30	.04	.32	2.66

	Fc	F	B	P	SIO_2	Ag	Al	As	Ba	Br
			ppm		mg/l					
JW-1	<.10	1.05	.04	.02	14.50	<.03	<2.5	.001	<.7	.54
2	<.10	.72	.03	.02	45.35	<.03	<2.5	.007	<.7	.31
3	<.10	1.43	.28	.02	75.18	<.03	<2.5	.018	<.7	.56
4	<.10	1.49	.22	.01	64.80	<.03	<2.5	.014	<.7	.43
5	<.10	1.80	.38	.01	90.94	<.03	<2.5	.021	<.7	.56
6	<.10	.51	.02	.02	26.33	<.03	<2.5	.002	<.7	.22
7	<.10	.62	.04	.01	29.31	<.03	<2.5	.002	<.7	.27

	Cd	Co	Cr	Cu	Hg	H_2S	Li	Mn	Mo	NH_4
					(ppm) mg/l					
JW-1	<.01	<.15	<.1	<.10	.0012	<.1	.02	<.07	<.5	.30
2	<.01	<.15	<.1	<.10	.0011	<.1	.01	<.07	<.5	.90
3	<.01	<.15	<.1	<.10	.0012	<.1	.48	<.07	<.5	.13
4	<.01	<.15	<.1	<.10	.0012	<.1	.54	<.07	<.5	1.24
5	<.01	<.15	<.1	<.10	.008	<.1	.65	<.07	<.5	1.35
6	<.01	<.15	<.1	<.10	.0011	<.1	.04	<.07	<.5	1.16
7	<.01	<.15	<.1	<.10	.0006	<.1	.03	<.07	<.5	.69

Sample	$NO_3 + NO_2$	Ni	Pb	Sb	Se	Sr	Zn
JW-1	5.23	<.03	.027	<.5	.003	.12	.17
2	.60	<.03	.006	<.5	<.002	<.04	.14
3	.96	<.03	.021	<.5	.006	.33	.14
4	1.05	<.03	.018	<.5	.005	.28	.15
5	.96	<.03	.042	<.5	.007	.43	.12
6	2.12	<.03	.004	<.5	<.002	.03	.14
7	1.88	<.03	.005	<.5	.020	.04	.12

Sample	Latitude	Longitude	Temperature °C	Comment
1B	32° 28.2	106° 49.2	--	Cleofas Wells
2B	32° 30.1	106° 55.7	53	Radium Springs (well)
3B	32° 29.6	106° 56.0	--	well
4B	32° 38.8	106° 55.8	--	well
5B	32° 47.7	107° 16.6	--	Derry Spring
6B	32° 47.6	107° 16.6	--	Derry Spring
7B	32° 48.7	107° 16.4	--	well
8B	32° 34.1	106° 59.9	--	well
9B	33° 8.1	107° 15.2	45	well (Mineral Bath-Blackstone)
10B	33° 8.2	107° 14.9	41	Well (Mineral Bath-Wierra)
11B	33° 8.0	107° 14.5	41	Warm Spring
12B	33° 16.7	107° 33.8	--	Warm Spring
13B	34° 2.2	106° 56.2	34	Sedillo Spring
14B	34° 2.8	106° 56.2	--	Cook Spring
15B	33° 14.1	107° 21.4	--	well
16B	33° 30.3	107° 40.4	--	well
17B	33° 34.38	107° 36.05	28	Spring
18B	33° 34.37	107° 35.95	21	Spring
19B	33° 8.1	107° 15.2	41	Yucca Springs

Sample	(ppm) TDS	pH	Ca	Mg	Na	K	CO_3	HCO_3	Cl	SO_4
			mg/l							
B1	592	8.18	101.2	27.6	65.1	7.4	12.0	361.2	26.6	147.9
B2	3532	8.16	118.6	15.2	1135.9	167.0	15.2	378.3	1593.6	263.2
B3	872	8.26	87.0	14.1	189.0	14.1	0	203.8	227.3	159.5
B4	2236	7.66	404.2	29.9	214.0	11.7	0	41.5	14.2	1604.2
B5	1240	8.23	47.1	15.8	323.9	18.8	0	366.1	151.0	376.6
B6	1228	8.62	47.1	16.0	340.0	19.2	22.8	311.2	153.2	374.6
B7	252	8.18	39.2	10.5	34.3	4.7	0	185.5	.4	63.4
B8	2784	8.03	153.9	17.9	806.7	10.6	0	289.2	828.5	647.5
B9	2608	7.79	143.9	18.0	817.5	61.4	0	164.7	1285.2	196.0
B10	2688	7.80	143.9	17.9	791.5	63.0	0	162.3	1353.6	169.1
B11	2640	7.88	136.5	17.1	764.6	62.6	0	136.7	1370.3	115.5
B12	1392	7.90	110.4	9.5	387.4	21.5	0	211.1	602.7	138.3
B13	284	8.48	17.2	4.3	56.1	3.1	0	162.3	10.3	50.0
B14	348	8.33	16.4	4.3	68.5	3.1	0	181.8	12.1	69.2
B15	420	8.14	49.5	4.3	78.4	3.9	0	175.7	80.5	67.2
B16	352	7.79	53.3	7.1	25.7	2.7	0	146.4	15.6	76.8
B17	468	8.24	34.9	1.3	125.5	5.1	0	131.8	104.2	96.1
B18	544	7.91	42.3	1.7	143.5	6.6	0	137.9	132.2	107.6
B19	2708	7.98	164.1	18.7	785.6	62.6	0	224.5	1514.2	107.0

Sample	Ca	Mg	Na	K	Total Cations	CO_3	HCO_3	Cl	SO_4	Total Anions
	meq/l									
B1	5.05	2.27	2.83	.19	10.34	.40	5.92	.75	3.08	10.15
B2	5.92	1.25	49.41	4.27	60.85	.44	6.20	44.95	5.48	57.07
B3	4.34	1.16	8.22	.36	14.08	0	3.34	6.41	3.32	13.07
B4	20.17	2.46	9.31	.30	32.24	0	.68	.40	33.40	34.48
B5	2.35	1.30	14.09	.48	18.22	0	6.00	4.26	7.84	18.10
B6	2.35	1.32	14.79	.49	18.95	.76	5.10	4.32	7.80	17.98
B7	1.97	.86	1.49	.12	4.44	0	3.04	.01	1.32	4.37
B8	7.68	1.47	35.09	.27	44.51	0	4.74	23.37	13.48	41.59
B9	7.18	1.48	35.56	1.57	45.79	0	2.70	36.25	4.08	43.03
B10	7.18	1.47	34.43	1.61	44.69	0	2.66	38.18	3.52	44.36
B11	6.81	1.41	33.26	1.60	43.08	0	2.24	38.65	2.40	43.29
B12	5.51	.78	16.85	.55	23.69	0	3.46	17.00	2.88	23.34
B13	.86	.35	2.44	.08	3.73	0	2.66	.29	1.04	3.99
B14	.82	.35	2.98	.08	4.23	0	2.98	.34	1.44	4.76
B15	2.47	.37	3.41	.10	6.35	0	2.88	2.27	1.40	6.55
B16	2.66	.58	1.12	.07	4.43	0	2.40	.44	1.60	4.44
B17	1.74	.11	5.46	.13	7.44	0	2.16	2.94	2.00	7.10
B18	2.11	.14	6.24	.17	8.66	0	2.26	3.73	2.24	8.23
B19	8.19	1.54	34.17	1.60	45.50	0	3.68	37.07	2.24	42.99

Sample	Cd	Co	Cr	Cu	Hg	H_2S	Li	Mn	Mo	NH_4
	mg/l									
B1	<.01	<.15	<.1	<.10	.0002	<.1	.03	<.07	<.5	0
B2	<.01	<.15	<.1	<.10	.0008		1.18	<.07	<.5	0
B5	<.01	<.15	<.1	<.10	.0148	<.1	.36	<.07	<.5	0
B6	<.01	<.15	<.1	<.10	.0011	<.1	.35	<.07	<.5	.08
B9	<.01	<.15	<.1	<.10	.0009	<.1	1.21	<.07	<.5	0
B10	<.01	<.15	<.1	<.10	.0003	<.1	1.23	<.07	<.5	0
B11	<.01	<.15	<.1	<.10	.0004	<.1	1.24	<.07	<.5	2.01
B12	<.01	<.15	<.1	<.10	.0005	<.1	.42	<.07	<.5	1.84
B13	<.01	<.15	<.1	<.10	.0005	<.1	.06	<.07	<.5	.38
B14	<.01	<.15	<.1	<.10	<.0002	<.1	.08	<.07	<.5	.30
B17	<.01	<.15	<.1	<.10	.0003	<.1	.11	<.07	<.5	.30
B18	<.01	<.15	<.1	<.10	.0003	<.1	.13	<.07	<.5	0
B19	<.01	<.15	<.1	<.10	.0005	<.1	1.20	<.07	<.5	0

Sample	NO_3+NO_2	Ni	Pb	Sb	Sc	Sr	Zn
	mg/l						
B1	5.57	<.03	.070	<.5	.005	1.28	.64
B2	.47	<.03	.844	<.5	.038	2.49	.10
B5	.08	<.03	.090	<.5	.006	.86	.09
B6	1.00	<.03	.139	<.5	.009	.83	.06
B9	2.12	<.03	.202	<.5	.018	4.10	.05
B10	1.88	<.03	.200	<.5	.017	4.12	.07
B11	2.01	<.03	.105	<.5	.015	4.19	.09
B12	11.14	<.03	.623	<.5	.009	2.21	.12
B13	1.63	<.03	.025	<.5	.003	.35	.16
B14	1.82	<.03	.033	<.5	.004	.39	3.58
B17	.84	<.03	.008	<.5	.004	.28	.09
B18	.40	<.03	.005	<.5	.004	.38	.09
B19	1.40	<.03	.257	<.5	.029	4.08	.10

	mg/l									
Sample	Fe	F	B	P	SiO_2	Ag	Al	As	Ba	Br
B1	.12	.67	.12	.01	46.2	<.03	<.25	.004	<.7	.65
B2	.49	4.44	.86	.02	69.9	<.03	<.25	.075	<.7	1.54
B3	.49	.57	.22	.01	35.4					
B4	.53	.45	.23	.03	63.9					
B5	<.10	5.90	.34	.01	31.3	<.03	<.25	.012	<.7	.94
B6	<.10	5.90	.37	.02	32.3	<.03	<.25	.011	<.7	.85
B7	<.10	1.48	.08	.02	28.9					
B8	1.25	.64	.69	.03	44.3					
B9	.38	1.49	.38	.01	44.3	<.03	<.25	.020	<.7	.77
B10	<.10	3.10	.35	.01	44.3	<.03	<.25	.019	<.7	.77
B11	<.10	3.10	.35	.01	44.3	<.03	<.25	.018	<.7	.75
B12	<.10	2.46	.20	.05	37.3	<.03	<.25	.013	<.7	.78
B13	<.10	2.02	.09	.02	25.3	<.03	<.25	.041	<.7	.28
B14	<.10	.69	.09	.02	21.3	<.03	<.25	.037	<.7	.37
B15	.12	1.73	.08	.01	32.1					
B16	.36	.27	.07	.06	44.3					
B17	<.10	3.10	.09	.01	35.3	<.03	<.25	.012	<.7	.23
B18	<.10	2.86	.10	.01	34.2	<.03	<.25	.011	<.7	.30
B19	<.10	3.20	.38	.01	31.3	<.03	<.25	.039	<.7	.82

Sample	Latitude	Longitude	Temperature °C	Comment
20B SW19	33° 3.8	107° 0.6	--	well
21B SW20	33° 17.4	106° 56.2	--	well
22B SW21	33° 28.6	106° 53.5	--	Malpais Well
23B SW22	33° 25.1	106° 52.4	18	Chavez Well
24B SW23	33° 23.3	106° 55.6	24	Tucson Spring
25B SW24	33° 34.4	106° 35.6	29	Ojo Caliente
26B SW25	33° 53.1	107° 31.7	4	Spring
27B SW26	33° 54.0	107° 32.2	4	Spring
28B SW27	33° 45.8	107° 21.0	30	well
Gila 1 SW28	32° 28.7	107° 57.5	18	well
Gila 2 SW29	32° 33.3	107° 59.7	54	Faywood Hot Spring
Gila 3 SW30	32° 33.5	107° 58.1	21	well
Gila 4 SW31	32° 44.9	107° 50.1	58	Mimbres Hot Spring
Gila 5 SW32	33° 12.0	108° 12.5	63	Gila Hot Spring
Gila 6 SW33	33° 12.0	108° 12.6	66	Gila Hot Spring
Gila 7 SW34	33° 14.0	108° 14.2	65	Hot Spring
Gila 8 SW35	33° 9.8	108° 12.7	44	Hot Spring
Gila 9 SW36	32° 34.6	108° 00.5	--	well
Gila 10 SW37	32° 35.1	108° 00.0	--	well
Gila 11 SW38	32° 33.8	108° 2.5	--	well

Sample	TDS	pH	Ca	Mg	Na	K	CO_3	HCO_3	Cl	SO_4
					mg/l					
19	744	8.05	47.0	36.0	149.7	9.7	0	154.9	101.8	299.5
20	2652	8.18	65.8	44.1	706.5	10.5	0	181.8	269.4	1372.8
21	5208	7.99	599.2	273.1	363.1	37.8	0	143.9	232.2	3129.6
22	2152	7.90	420.2	97.5	51.5	4.7	0	134.2	27.7	1296.0
23	2500	8.10	441.2	156.6	66.0	7.0	0	184.2	47.5	1478.4
24	516	8.10	44.2	1.7	137.7	5.5	0	124.4	150.1	107.5
25	104	7.90	12.8	2.4	10.5	1.6	0	36.6	0.1	44.2
26	104	7.81	12.8	2.2	10.8	1.6	0	31.7	0.7	40.3
27	192	7.84	23.4	1.7	24.1	.8	0	108.5	1.4	26.4
28	364	8.10	46.8	7.9	17.4	3.9	0	207.4	1.1	21.6
29	492	7.74	35.6	7.6	90.8	8.2	0	283.0	14.2	72.0
30	456	7.63	25.8	9.6	90.8	2.3	0	256.2	20.8	64.2
31	320	8.97	2.4	<.006	91.7	1.2	20.4	67.1	14.5	84.0
32	408	8.19	10.6	0.1	123.0	3.1	0	108.6	99.4	69.6
33	416	8.15	10.4	0.2	129.7	3.1	0	115.9	100.1	67.2
34	548	7.92	15.4	0.1	151.5	3.5	0	131.1	104.3	118.0
35	516	8.08	18.4	0.8	141.9	2.7	0	125.0	115.7	93.6
36	320	8.15	31.6	13.0	28.9	3.5	0	227.5	1.4	24.0
37	344	7.84	32.0	18.1	24.8	4.3	0	213.5	17.0	16.2
38	428	7.82	39.8	13.2	47.1	5.1	0	236.6	8.5	50.4

	mg/l									
Sample	Ca	Mg	Na	K	Total Cations	CO_3	HCO_3	Cl	SO_4	Total Anions
19	2.35	3.00	6.51	.25	12.11	0	2.54	2.87	6.24	11.65
20	3.29	4.51	30.72	.27	38.79	0	2.98	7.59	28.60	39.1
21	29.96	22.76	15.79	.97	69.48	0	2.36	6.54	65.20	74.1
22	21.01	8.13	2.24	.12	31.50	0	2.20	.78	27.00	29.9
23	22.06	13.05	2.87	.18	36.16	0	3.02	1.34	30.80	35.1
24	2.21	.14	5.99	.14	8.48	0	2.04	4.23	2.24	8.5
25	.64	.20	.46	.04	1.34	0	.60	.003	.92	1.5
26	.64	.18	.47	.04	1.33	0	.52	.02	.84	1.3
27	1.17	.14	1.05	.02	2.38	0	1.78	.04	.55	2.3
28	2.34	.66	.76	.10	3.86	0	3.40	.03	.45	3.8
29	1.78	.60	3.95	.21	6.54	0	4.64	.40	1.50	6.5
30	1.29	.80	3.95	.06	6.10	0	4.20	.52	1.35	6.0
31	.12	<.0005	3.99	.03	4.14	.68	1.10	.41	1.75	3.9
32	.53	.01	5.35	.08	5.97	0	1.78	2.80	1.45	6.0
33	.52	.02	5.64	.08	6.25	0	1.90	2.82	1.40	6.1
34	.77	.01	6.59	.09	7.46	0	2.15	2.94	2.25	7.3
35	.92	.07	6.17	.07	7.23	0	2.05	3.26	1.45	7.2
36	1.58	1.08	1.26	.09	4.01	0	3.73	.04	.50	4.2
37	1.60	1.51	1.08	.11	4.30	0	3.50	.48	.35	4.3
38	1.99	1.10	2.05	.13	5.27	0	3.88	.24	1.05	5.1

	ppm				
Sample	Fe	F	B	P	SiO_2
19	.16	2.70	.30	0	26.87
20	.14	4.10	3.22	0	8.99
21	1.28	2.50	1.96	.02	16.04
22	.32	1.10	.18	0	29.07
23	<.10	1.20	.09	0	26.87
24	.22	.25	.02	0	23.58
25	<.10	.11	0	.01	36.80
26	<.10	.11	0	.01	36.80
27	1.15	2.70	0	0	50.12
28	<.10	.53	0	0	42.06
29	.12	6.10	.01	.01	45.16
30	.25	3.10	.02	0	41.03
31	<.10	16.00	0	0	55.56
32	<.10	8.70	.03	0	72.27
33	<.10	8.70	.02	0	73.31
34	.22	9.50	.07	0	85.89
35	1.25	8.70	.11	.01	85.89
36	.29	.61	.01	0	59.73
37	3.11	.66	.01	0	60.78
38	<.11	3.00	.01	0	54.53

Sample	NO_3+NO_2	Ni	Pb	Sb	Sc	Sr	Zn
			ppm				
19							
20							
21							
22							
23							
24							
25							
26							
27							
28							
29	0	<.13	.014	<.6	.004	.10	<.028
30							
31	0	<.13	.051	<.6	.004	<.02	<.028
32	.29	<.13	.024	<.6	.005	.02	.06
33	.19	<.13	.021	<.6	.005	.02	.06
34	.19	<.13	.021	<.6	.006	.03	<.028
35	0	<.13	.021	<.6	.006	.02	.05
36							
37							
38							

Sample	Cd	Co	Cr	Cu	Hg	H_2S	Li	Mn	Mo	NH_4	Ag	Al	As	Bs
						ppm								
19														
20														
21														
22														
23														
24														
25														
26														
27														
28														
29	<.02	<.18	<.10	<.12	.0006		.16	<.063	<.45	<.05	<.07	<1.10	.009	<.20
30														
31	<.02	<.18	<.10	<.12	.0006		.11	<.063	<.45	<.05	<.07	<1.10	.006	<.20
32	<.02	<.18	<.10	<.12	.0033		.26	<.063	<.45	<.05	<.07	<1.10	.007	<.20
33	<.02	<.18	<.10	<.12	.0007		.26	<.063	<.45	<.05	<.07	<1.10	.008	<.20
34	<.02	<.18	<.10	<.12	.0005		.43	<.063	<.45	<.05	<.07	<1.10	.006	<.20
35	<.02	<.18	<.10	<.12	.0006		.31	<.063	<.45	<.05	<.07	3.10	.009	<.20
36														
37														
38														

Sample	Latitude	Longitude	Temperature °C	Comment
Gila 20 SW150	33° 6.5	108° 29.0	74	Spring on Turkey Creek
Gila 21 SW151	33° 6.5	108° 29.0	28	Turkey Creed
Gila 22 SW152	33° 6.5	108° 29.0	70	Spring on Turkey Creek
Gila 23 SW153	33° 1.1	108° 35.8	29	well
Gila 24 SW154	32° 52.6	108° 35.0	31	Spring
Gila 25 SW155	32° 56.1	108° 36.7	--	well
Gila 26 SW156	32° 55.4	108° 35.0	19	well
Gila 27 SW157	32° 57.9	108° 36.4	20	well
Gila 28 SW158	32° 57.9	108° 36.8	22	Artesian Well
Gila 29 SW159	32° 50.5	108° 30.6	27	Mangas Springs
Gila 30 SW160	32° 48.8	108° 35.5	24	Spring
MF61 SW161	33° 17.0	108° 15.8	31	Spring
MF62 SW162	33° 17.4	108° 16.9	37	Spring
MF63 SW163	33° 17.4	108° 16.9	36	Spring
MF64 SW164	33° 16.4	108° 15.0	26	Spring
R1 SW165	32° 32.7	106° 54.8	25	well
R2 SW166	32° 34.8	106° 55.3	23	well

Sample	TDS	pH	Ca	Mg	Na	K	CO_3	HCO_3	Cl	SO_4
			mg/l							
150	236	8.66	6.8	1.6	61.1	1.5	0	94.0	4.2	64.8
151	200	8.33	10.6	3.5	48.7	2.0	0	103.7	3.9	43.7
152	260	9.10	2.8	<0.1	69.2	1.2	20.4	40.3	5.0	75.9
153	292	8.53	10.4	0.6	77.9	1.5	0	75.7	25.9	99.4
154	332	8.13	18.4	1.3	92.4	1.5	0	234.3	6.4	49.0
155	400	8.04	8.2	0.8	1184	2.0	0	244.1	13.1	55.2
156	444	7.64	36.1	6.9	79.3	1.2	0	290.4	10.6	45.1
157	472	8.79	2.4	0.1	146.7	0.8	13.2	175.7	33.0	107.1
158	272	9.36	1.0	<0.1	87.6	0.4	46.8	125.7	2.8	13.4
159	544	8.00	87.0	16.5	34.9	7.8	0	390.5	18.8	35.0
160	672	7.98	10.0	1.3	190.6	2.7	0	386.8	18.8	142.6

Sample	ppm Zn	ppm Sr	Se	NO_3
150	<.02		<.002	.72
151	.03		.003	.15
152	<.02		.003	.06
153	.14		.003	6.72
154	<.02		.003	.17
155	.03		.004	2.00
156	.22		.003	.59
157	.04		.006	0
159	<.02		.003	.89
160	.07	.03	.006	1.47

Sample	Cd	Co	Cu	ppm Cu	Hg	ppm H_2S	ppm Li	Mn	Mo	NH_4
150				<.10	.0004	<.1	.06			<.05
151				<.10	.0003	<.1	.03			<.05
152				<.10	.0004	<.1	.11			<.05
153				<.10	.0006	<.1	.13			<.05
154				<.10	.0006	<.1	.08			<.05
155				<.10	.0006	<.1	.14			<.05
156				<.10	.0006	<.1	.15			<.05
157				<.10	.0006	<.1	.20			<.05
159				<.10	.0006	<.1	.02			<.05
160	<.02	<.14	<.1	<.10	.0006	<.1	.22	.40	<.5	<.05

Sample	Fe	F	B	P	SiO_2	Ag	Al	As	Ba	Br
150	.31	9.45	.12	.01	67.65	<.06	<1.0	.007	<.20	
151	<.15	7.65	.08	.01	50.00	<.06	<1.0	.004	<.20	
152	<.15	11.85	.12	0	68.91	<.06	<1.0	.006	<.20	
153	.25	10.50	.92	0	21.39	<.06	<1.0	.002	<.20	
154	<.15	5.85	.16	0	34.51	<.06	<1.0	.006	<.20	
155	<.15	7.35	.44	0	47.62	<.06	<1.0	.011	<.20	
156	<.15	3.00	.14	.01	49.40	<.06	<1.0	.006	<.20	
157	<.15	19.05	2.56	.01	63.73	<.06	<1.0	.015	<.20	
158	<.15	1.00	.12	.01	52.95					
159	<.15	.49	.14	.23	57.75	<.06	<1.0	.004	<.20	
160	.49	18.45	.42	.06	48.22	<.06	<1.0	.014	<.20	.15

----------mg/l----------

Sample	Ca	Mg	Na	K	Total Cations	CO_3	HCO_3	Cl	SO_4	Total Anions
150	.34	.13	2.66	.04	3.17	0	1.54	.12	1.35	3.01
151	.53	.29	2.12	.05	2.99	0	1.70	.11	.91	2.72
152	.14	.006	3.01	.03	3.18	.68	.66	.14	1.58	3.06
153	.52	.05	3.39	.04	4.00	0	1.24	.73	2.07	4.04
154	.92	.11	4.02	.04	5.09	0	3.84	.18	1.02	5.04
155	.41	.07	5.15	.05	5.68	0	4.00	.37	1.15	5.52
156	1.80	.57	3.43	.03	5.85	0	4.76	.30	.94	6.00
157	.12	.01	6.38	.02	6.53	.44	2.88	.93	2.23	6.48
158	.05	<.006	3.81	.01	3.93	1.56	2.06	.08	.28	3.98
159	4.34	1.36	1.52	.20	7.34	0	6.40	.53	.73	7.66
160	.50	.11	8.29	.07	8.97	0	5.52	.53	2.97	9.02
161	1.02	.21	1.74	.04	3.10	0	2.39	.09	.62	3.10
162	.19	.13	1.82	.02	2.76	0	2.24	.12	.66	3.02
163	.84	.13	1.90	.03	2.90	0	2.29	.11	.59	2.99
164	.74	.12	1.63	.02	2.51	0	2.15	.09	.40	2.64
165	1.92	1.36	4.23	.19	7.70	0	3.82	.48	3.68	7.98
166	4.57	2.25	5.84	.21	12.87	0	2.74	.71	8.27	11.72

Sample	TDS	pH	Ca	Mg	Na	K	Cl	CO_3
			mg/l					
161		8.80	20.4	2.6	40.0	1.6	3.2	0
162		8.07						
163		8.09	16.8	1.6	43.7	1.2	3.9	0
164		8.15	14.8	1.5	37.5	.8	3.2	0
165	340	8.40	38.5	16.5	97.2	7.4	17.0	0
166	784	7.96						

Sample	HCO_3	SO_4	P	B	F	Fe	SiO_2
				mg/l			
161	145.8	29.8	.20	.05	4.86	.37	51.0
162			.16	.02	5.28	.42	56.0
163	139.7	28.3	.09	.07	5.28	<.10	56.5
164	131.2	19.2	.09	0	5.07	<.10	54.0
165	233.1	176.8	.11	.28	.69	.92	72.5
166			.16	.48	1.06	.37	65.0

Sample	Mo	Co	Zn	Mn	Sr	Cd	Bc	Ni	Ca	Ag	Pb	Li
165	<.5	<.15	.26	<.05	.20	<.02	<.4	<.15	<.10	<.06	.004	.05
166	<.5	<.15	2.72	<.05	1.15	<.02	<.4	<.15	<.10	<.06	.006	.08

Sample	As	Se	Sb	Hg	Cr	Br	NO_3	H_2S	NH_4	Al
165	.01	.01	<.5		<.10		7.38	<.1		<1.0
166	.01	.01	<.5		<.10		8.83	<.1		<1.0

Sample	Latitude	Longitude	Temperature °C	Comment
TR4-1	32° 15.3	105° 38.2	--	well
TR4-2	32° 15.4	105° 32.3	--	well
TR4-3	32° 10.3	105° 26.4	--	well
TR4-4	32° 14.9	105° 25.6	--	well
TR4-5	32° 9.6	105° 22.6	21	well
TR4-6	32° 7.8	105° 34.7	19	well
TR4-7	32° 6.5	105° 39.2	17	well
TR4-8	32° 6.6	105° 39.3	18	well
TR4-9	32° 5.3	105° 44.5	13	well
TR4-10	32° 2.3	105° 52.8	--	well
W50 SW238	32° 12.9	107° 9.8	--	well
W51 SW239	32° 14.1	107° 12.0	--	well
W52 SW240	32° 11.6	107° 12.7	--	well
W53 SW241	32° 9.4	107° 14.7	--	well
W54 SW242	32° 7.8	107° 14.8	--	well
W55 SW243	32° 5.3	107° 4.5	23	well
W56 SW244	32° 10.0	107° 7.0	--	well
W57 SW245	32° 9.2	107° 10.1	22	well
W58 SW246	32° 8.5	107° 2.5	--	well
W59 SW247	32° 11.2	107° 0.3	24	well
W60 SW248	32° 11.3	106° 53.4	24	well

Sample	Latitude	Longitude	Temperature °C	Comment
W61 SW249	32° 9.5	106° 49.2	--	well
W62 SW250	31° 48.0	107° 24.5	--	well
W63 SW251	31° 48.3	107° 30.1	--	well
W64 SW252	31° 47.7	107° 34.3	--	well
W65 SW253	31° 58.2	107° 23.2	--	well
W66 SW254	31° 53.2	107° 26.9	--	well
W67 SW255	31° 48.3	107° 30.1	22	well
W68 SW256	31° 47.7	107° 34.3	26	well
W69 SW257	31° 50.5	107° 31.2	30	well
W70 SW258	31° 53.2	107° 26.9	22	well
W71 SW259	31° 56.2	107° 23.1	21	well
W72 SW260	31° 58.2	107° 23.2	22	well
W73 SW261	31° 54.2	107° 35.2	20	well
W74 SW262	32° 1.3	107° 40.1	21	well
W75 SW273	32° 13.3	107° 26.1	22	well
W76 SW274	32° 13.4	107° 28.8	21	well
W77 SW275	32° 11.3	107° 28.9	--	well
W78 SW276	32° 8.0	107° 28.0	21	well

TABLE 1 (continued)

Sample	Latitude	Longitude	Temperature °C	Comment
W66 SW254	31° 53.2	107° 26.9	--	well
W67 SW255	31° 48.3	107° 30.1	22	well
W68 SW256	31° 47.7	107° 34.3	26	well
W69 SW257	31° 50.5	107° 31.2	30	well
W70 SW258	31° 53.2	107° 26.9	22	well
W71 SW259	31° 56.2	107° 23.1	21	well
W72 SW260	31° 58.2	107° 23.2	22	well
W73 SW261	31° 54.2	107° 35.2	20	well
W74 SW262	32° 1.3	107° 40.1	21	well
W75 SW273	32° 13.3	107° 26.1	22	well
W76 SW274	32° 13.4	107° 28.8	21	well
W77 SW275	32° 11.3	107° 28.9	--	well
W78 SW276	32° 8.0	107° 28.0	21	well
W79 SW277	32° 6.7	107° 28.7	21	well
W80 SW278	32° 5.5	107° 23.3	23	well
W81 SW279	32° 2.2	107° 25.0	20	well
W82 SW280	32° 34.6	107° 0.2	19	well
W83 SW281	32° 30.8	107° 2.6	--	well
W84 SW282	32° 31.0	107° 4.8	--	well

Sample	Latitude	Longitude	Temperature °C	Comment
W79 SW277	32° 6.7	107° 28.7	21	well
W80 SW278	32° 5.5	107° 23.3	23	well
W81 SW279	32° 2.2	107° 25.0	20	well
W82 SW280	32° 34.6	107° 0.2	19	well
W83 SW281	32° 30.8	107° 2.6	--	well
W84 SW282	32° 31.0	107° 4.8	--	well
SW283	32° 11.7	108° 52.2	18	well
SW284	32° 12.2	108° 48.8	19	Nation Well
SW285	32° 10.1	108° 52.8	16	well
SW286	32° 9.7	108° 50.7	24	well
SW287	32° 8.1	108° 50.9	19	well
SW288	32° 7.3	108° 51.2	19	well
SW289	32° 6.3	108° 50.8	20	well
SW290	32° 7.7	108° 53.2	--	well
SW291	32° 4.8	108° 52.8	18	well
SW292	32° 3.5	108° 53.5	18	well
SW293	32° 3.1	108° 54.6	19	well
SW294	32° 4.7	108° 54.0	21	well
SW295	32° 3.1	108° 52.7	26	well
SW296	32° 2.7	108° 55.0	20	Bert Windmill
SW297	32° 47.3	108° 51.2	24	well
SW298	32° 3.6	108° 53.3	20	well
SW299	32° 4.8	108° 52.7	22	well
SW300	32° 5.6	108° 52.2	21	well

Sample	Latitude	Longitude	Temperature °C	Comment
SW301	32° 9.1	108° 46.4	--	well
SW302	32° 5.2	108° 53.6	20	well
SW303	32° 7.2	108° 55.3	19	well
SW304	32° 6.3	108° 51.7	19	well
SW305	32° 9.1	108° 52.7	18	well
SW306	33° 16.4	108° 15.0	34	Spring
SW307	33° 16.4	108° 15.0	32	Spring
SW308	33° 16.4	108° 15.0	7	Middle Fork Gila River
SW309	33° 10.6	108° 12.1	--	East Fork Gila River
SW310	33° 10.8	108° 12.3	--	West Fork Gila River

APPENDIX D

STABLE ISOTOPE LABORATORY AND INSTRUMENTATION

LAB 333
UNM STABLE ISOTOPES

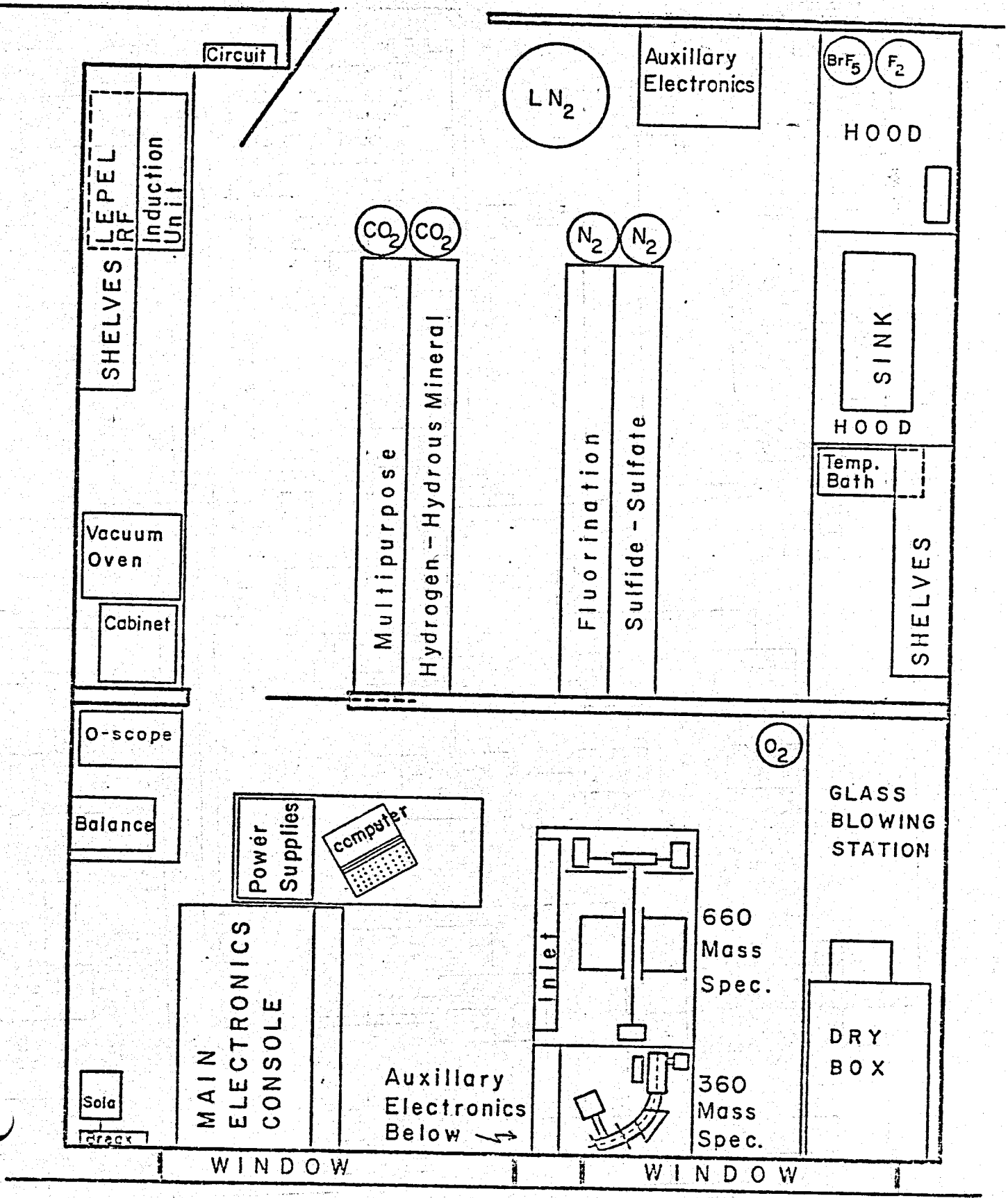

ELECTRONIC BLOCK DIAGRAM

NM-660 & NM-360 MASS SPECTROMETERS

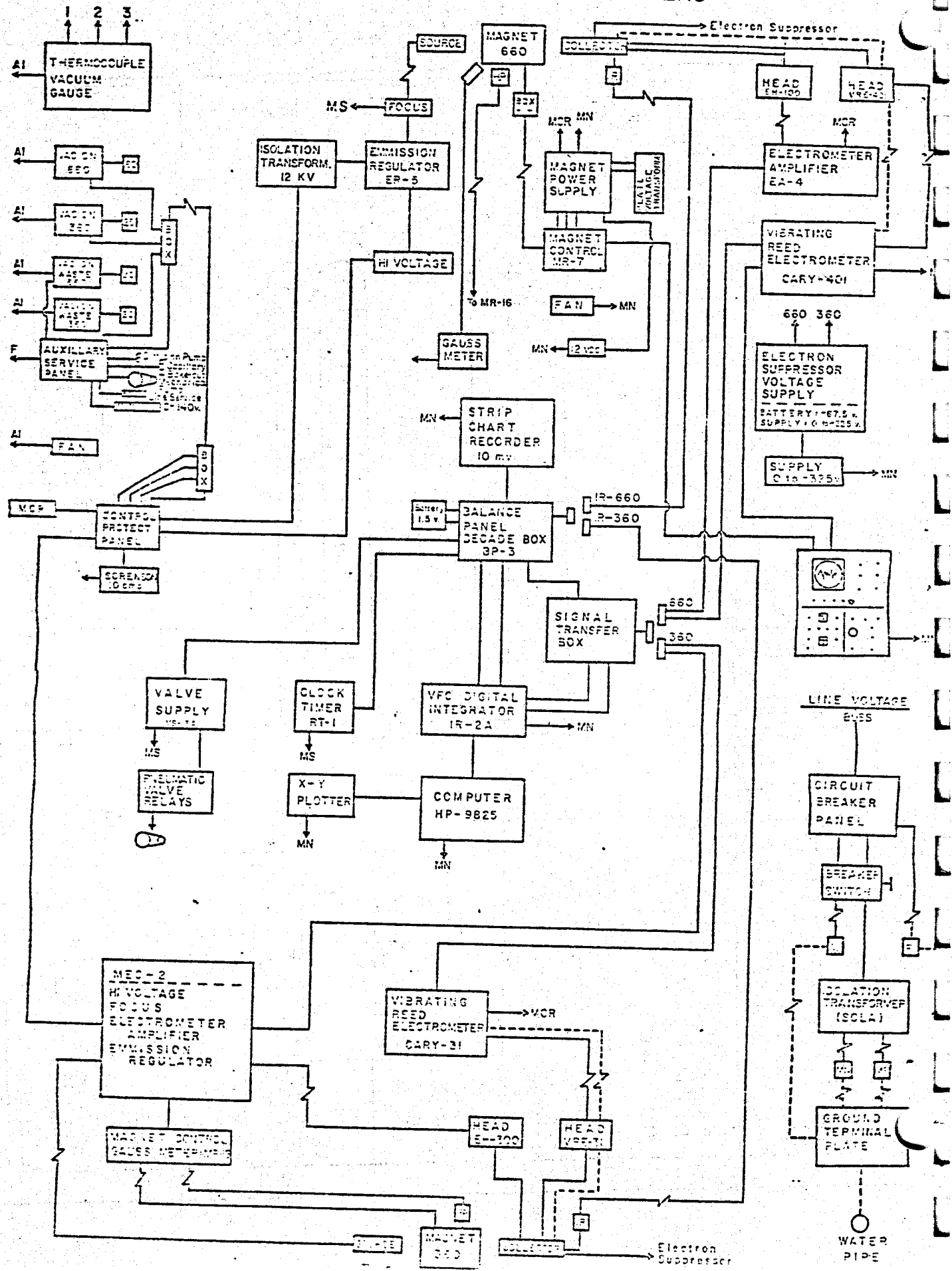

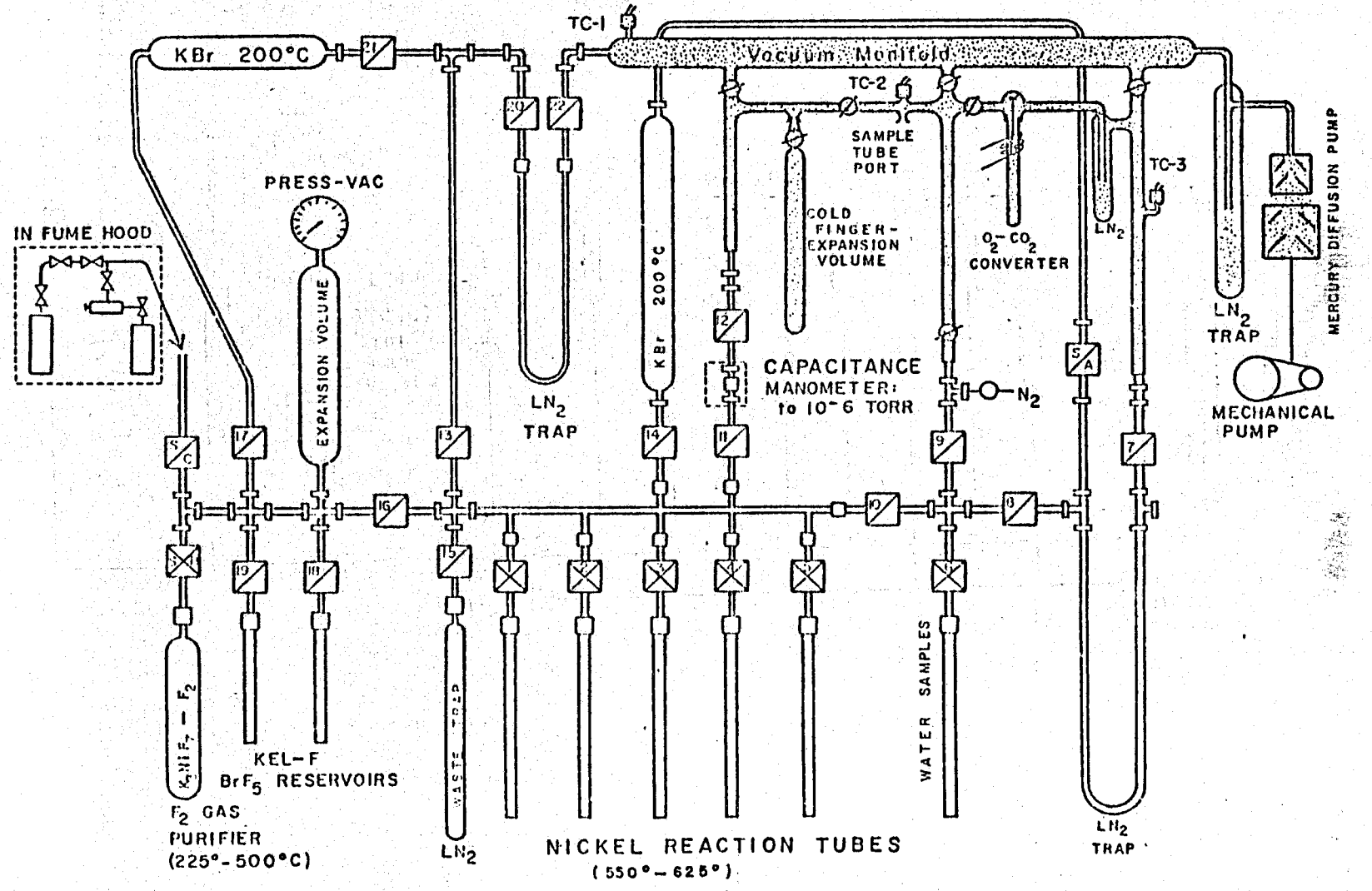

FLUORINATION LINE

(BROMINE PENTAFLUORIDE – FLUORINE GAS)

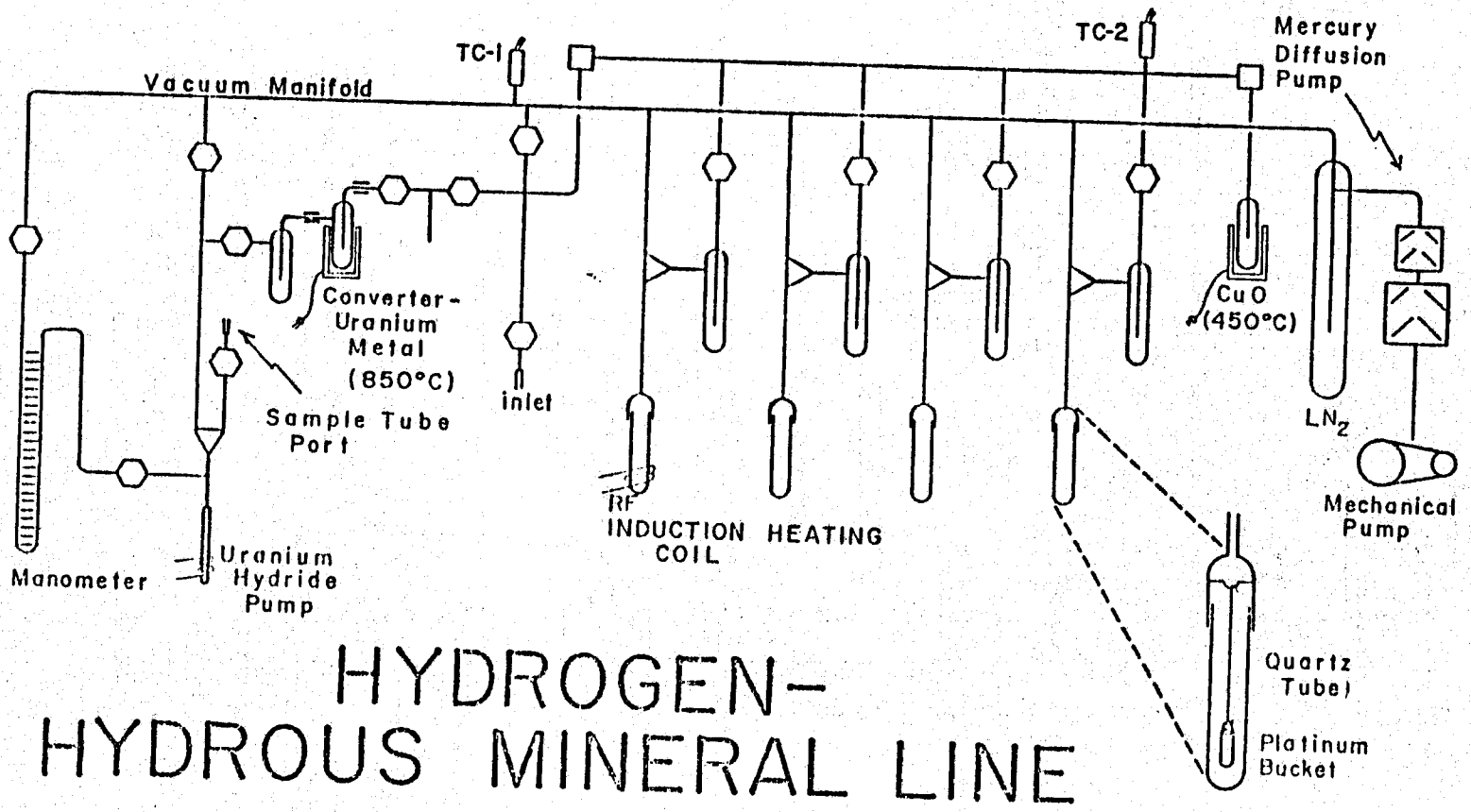

HYDROGEN-HYDROUS MINERAL LINE

MULTIPURPOSE LINE

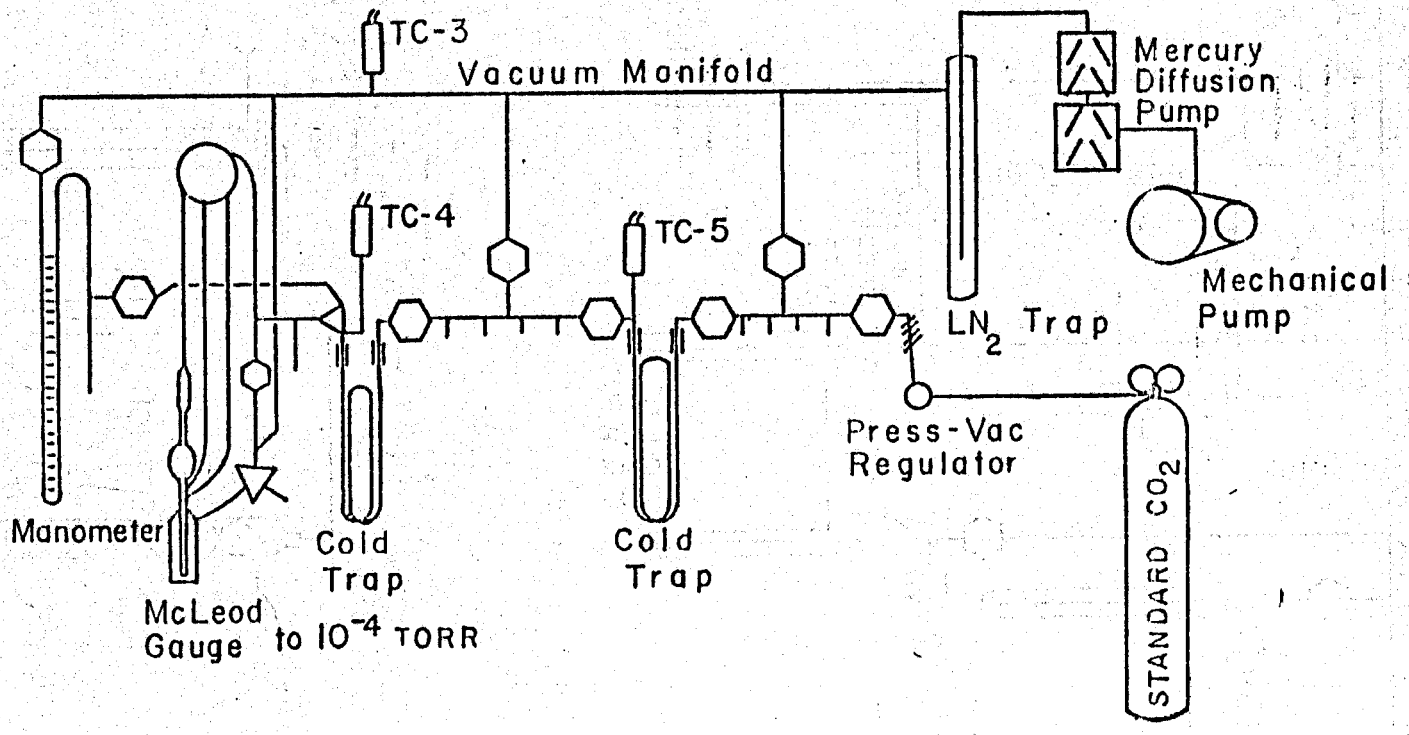

SULFIDE COMBUSTION

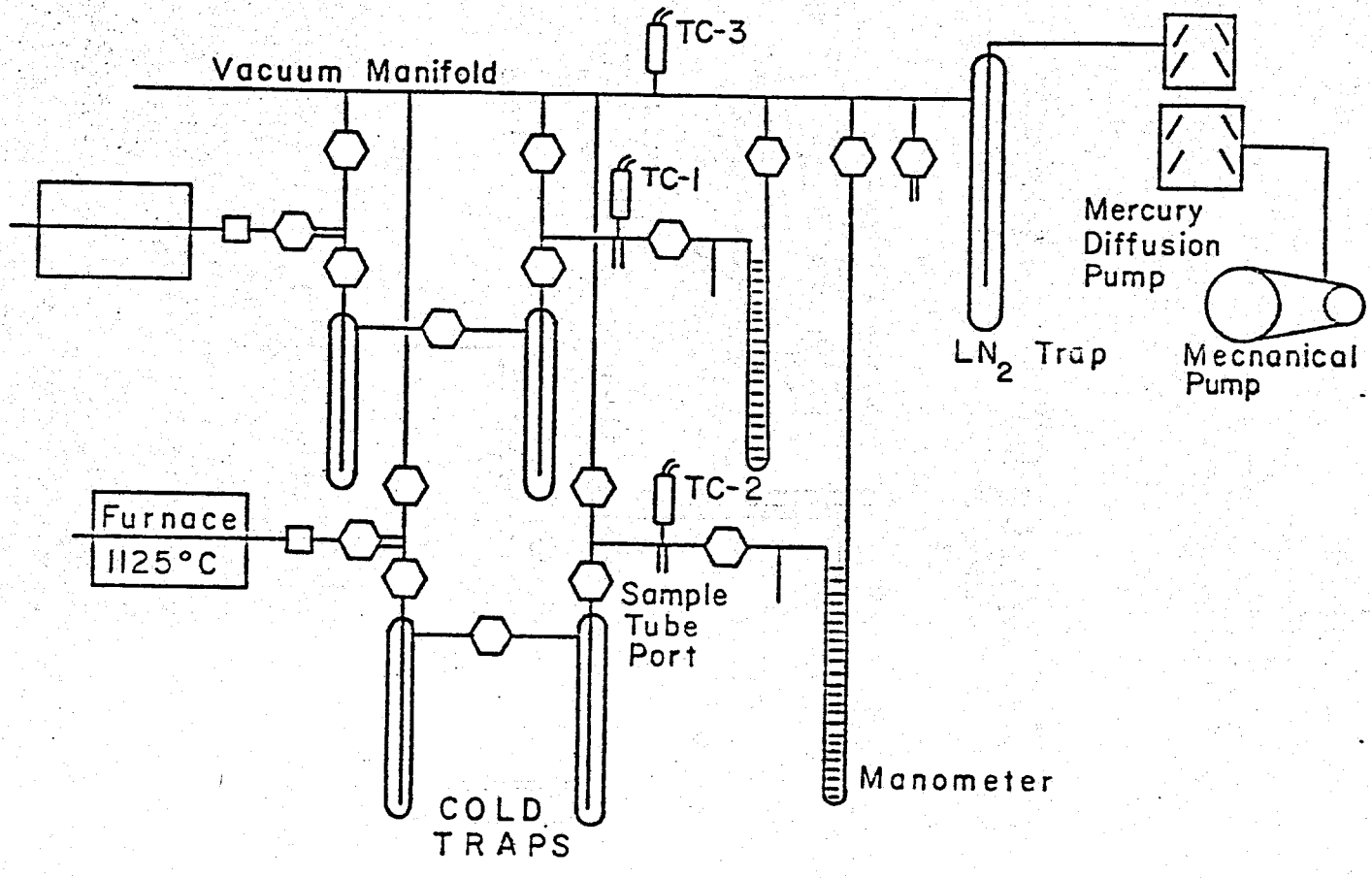

SULFATE REDUCTION

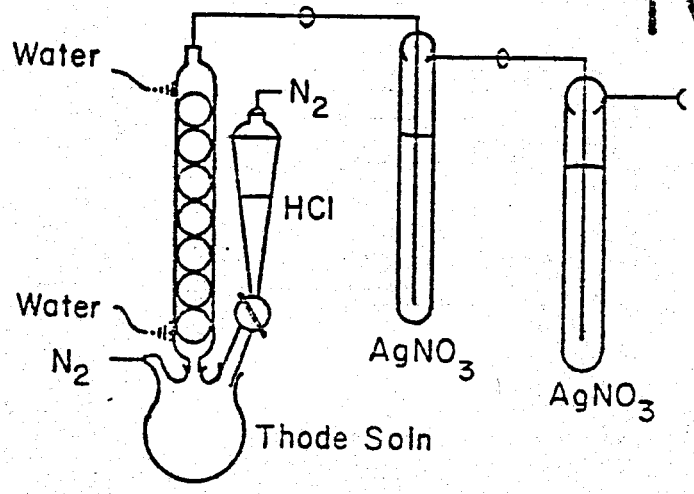

Work Completed on UNM Stable Isotope Laboratory Facility

Funding: U.S. Geological Survey Geothermal Energy: 14-08-0001-G-255
NMERDP: # 166 UNM 281-396-100
NMERDP: UNM 281-341-100/200
Sandia Laboratories - SURP : #51-9537, UNM 381-406-100
Los Alamos Scientific Laboratories: # LY5-70817-1
University of New Mexico

Amount: Equipment/Materials & Service = $80,000.

CODE: S = Surplus equipment, largely government sources
F = fabricated equipment, UNM, incl. design
$ = purchased equipment
# = repair and/or modification of equipment

I. Mass Spectrometer Electronics

CODE	No.	ITEM
F	2	30 amp power lines through main junction box
S	1	thermocouple vacuum gauge unit 3-station (TC-3A)
$#	4	VacIon Pump control units-power supplies-Varian and Ion Equipment
F	1	Auxilliary Services / protect panel
F	1	Control-Master Protect Vacuum Trip unit
F	1	Suppressor Voltage Power Supply + distribution box
S	2	Gauss meter magnetic field monitor
S#	1	Sorenson regulated line voltage supply
S	1	Clock timer switching unit (RT-1)
F	1	Solenoid/Air pneumatic switching system on inlet
S#	1	Balance Panel (BP-3)
$	1	VFC digital integrator-computer-printer output on-line data reduction system (IR-2A + HP/9825A)
F	1	Active/Passive BCD TTL positive true parallel interface circuitry
$	1	Strip chart recorder (Esterline)
F	1	Earth ground common junction strip
S#	2	Fans, electronic console
S#	1	High voltage supply (660 RMS)
F	1	Ion source hi voltage focus control (660 RMS)
S#	1	Emmission Regulator (ER-5) 660 RMS

CODE	No.	ITEM
$	1	Cary 401 M Vibrating reed electrometer (660 RMS)
S	1	Electrometer Amplifier EA-7 (660 RMS)
S#	1	MR-7/MS-6A, electromagnet current regulator power supply + 12 VDC filament supply (660 RMS)
F	1	Electrical system for capillary bakeout system
S#	1	High voltage power supply 6KV, spare
S#	3	Cary 31 vibrating reed electrometer (360 RMS)
$#	1	MEC-2: hi voltage supply, focus, emmission regulator, D.C. amplifier (360 RMS)
$	1	MR-16 electromagnet power supply-control (360 RMS)
F	1	Junction-signal transfer box
S#	1	Oscilloscope: trouble shooting, signal trace
F#	70	Multiconductor (some low leve l shielded) electronic cables and mated connectors

II. Mass Spectrometer Hardware

S	3	Electronic consoles, 19" relay racks
S#	1	6 inch-60 degree sector Nier type mass spectrometer for carbon, oxygen, sulfur isotopes
F	1	Vacuum pumping - roughing vacuum system (660-RMS)
F	1	Dual inlet system - vacuum transfer lines to 660 RMS and 360 RMS
F	1	Dual switching pneumatic gas inlet capillary leak
$	1	3 inch-60 degree sector Nier Type mass spectrometer for hydrogen isotopes (also C, O, S, N, Ar etc.)
F	1	Vacuum pumping/roughing system (360 RMS)

III. General Purpose - Sample Preparation - Extraction Lines.

F#	1	Lab room (333) with partition wall, lab benches hoods vented to roof
$	1	Analytical balance
S	1	fume hood
S	1	constant temperature water bath
$	1	Lepel RF induction unit
F	1	Lattice support racks, benches, with power, water and gas distribution
$	1	Vacuum oven

CODE	No.	ITEM
$	1	Misc. tools, lab glassware, consumable supplies, equipment
$	2	liquid nitrogen storage dewars (160 liters) plus miscellaneous small glass vacuum dewars
$	1	Capacitance manometer (MKS)
F	1	resistance furnaces (6 ea) proportional temperature controllers, w/digital readout of temperature for 12 general purpose station jacks on extraction support racks
F	1	Mineral separation, heavy liquids, sieving diamond saw, polishing etc.
F	1	glass blowing station and connecting gas lines to station hook-up near support racks
$		Misc. N_2 - CO_2 - F_2 - BrF_5 gas bottle cylinders
F	1	Multipurpose - Carbonate extraction line
F	1	H_2 - H_2O - Hydrous mineral extraction line
F	1	Sulfur extraction line
F	1	Thode process - sulfate reduction line
F	1	Fluorination line: bromine pentafluoride and fluorine gas; for oxides and silicates (CO_2) silicates (SiF_4), and SF_6)
F	2	microscope heating stage, proportional controller, digital temperature readout, and BCD digital printer
F	2	microscope freezing stage, digital temperature readout, "chilled" N_2 gas cooling medium
S#	1	Glove box, dry box
S#	1	Phillips cold cathode vacuum gauge
S	2	Liquid nitrogen dewar, 25 liter "genie" bottle
F	1	Rapid carbonate extraction system
F	1	solid source F_2 gas supply system
F	1	RF-Pt-Ni/NiO-C sulfate oxygen extraction system

APPENDIX E

RESIDUAL GRAVITY AND MAGNETIC PROFILES

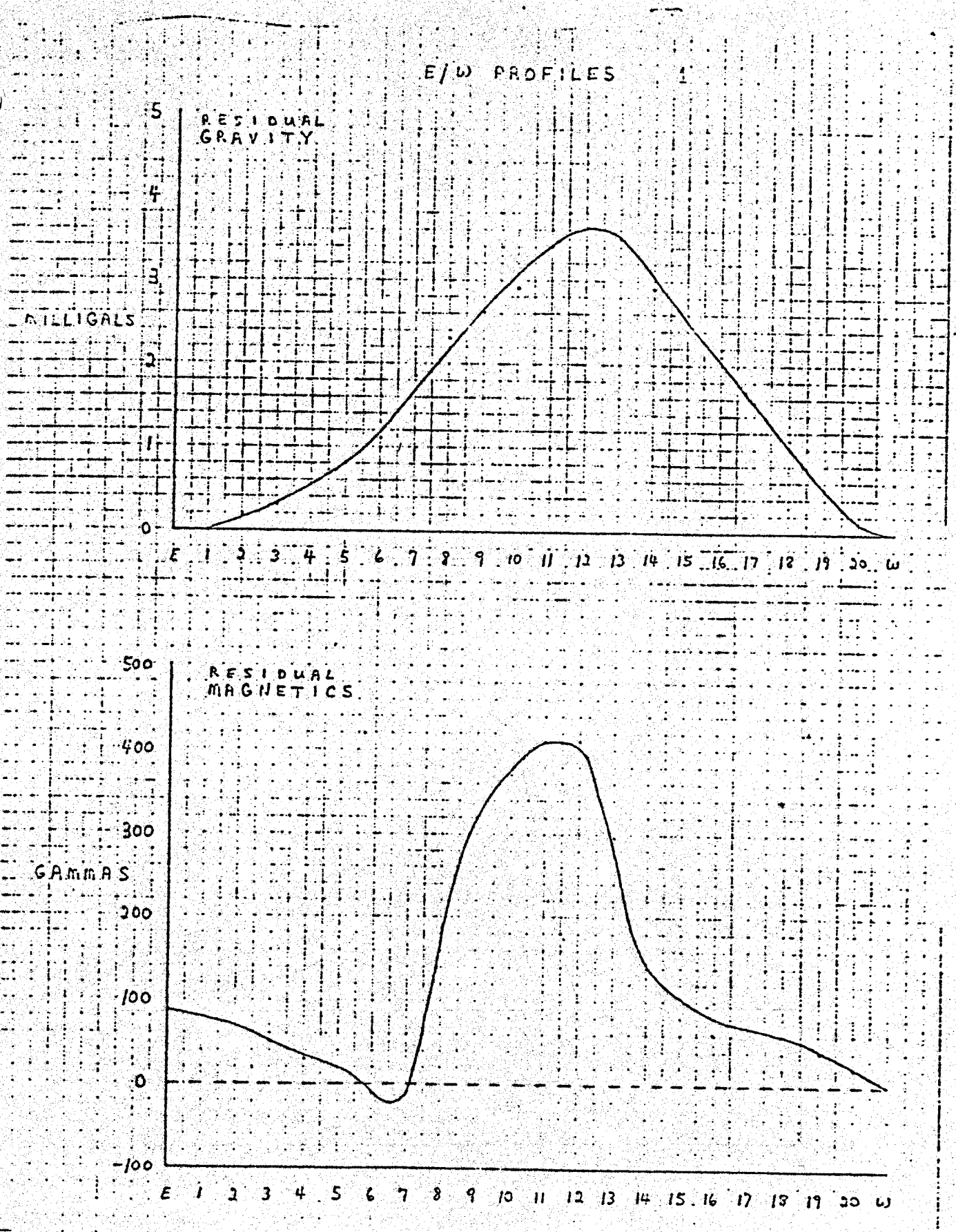
E/W PROFILES
RESIDUAL GRAVITY
MILLIGALS
5
4
3
2
1
0
E 1 2 3 4 5 6 7 8 9 10 11 12 13 14 15 16 17 18 19 20 W
RESIDUAL MAGNETICS
GAMMAS
500
400
300
200
100
0
-100
E 1 2 3 4 5 6 7 8 9 10 11 12 13 14 15 16 17 18 19 20 W

Figure 7

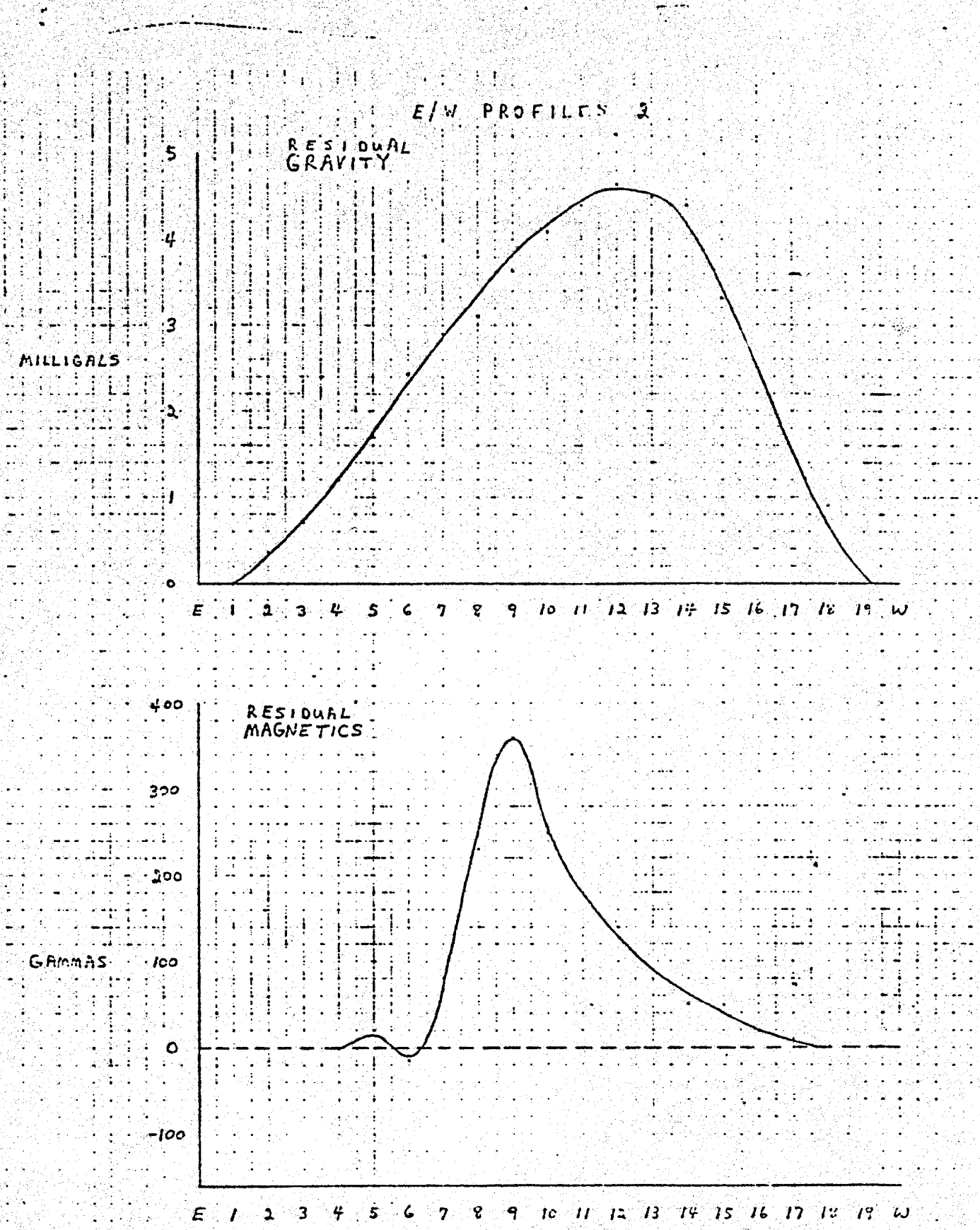
E/W PROFILES 2
RESIDUAL GRAVITY
MILLIGALS
5
4
3
2
1
0
E 1 2 3 4 5 6 7 8 9 10 11 12 13 14 15 16 17 18 19 W
RESIDUAL MAGNETICS
GAMMAS
400
300
200
100
0
-100
E 1 2 3 4 5 6 7 8 9 10 11 12 13 14 15 16 17 18 19 W

Figure 8

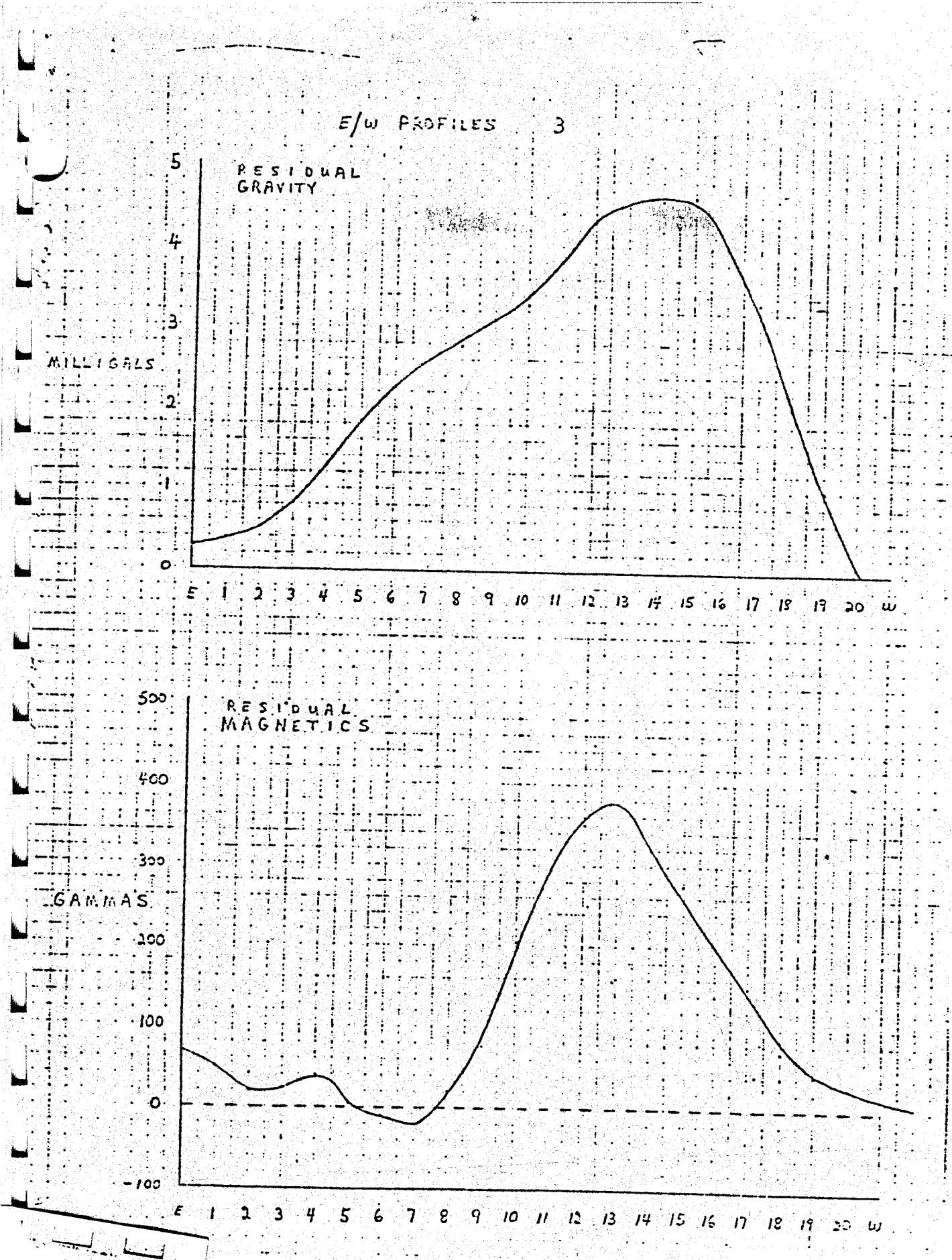
E/W PROFILES 3
RESIDUAL GRAVITY
MILLIGALS
5
4
3
2
1
0
E 1 2 3 4 5 6 7 8 9 10 11 12 13 14 15 16 17 18 19 20 W
RESIDUAL MAGNETICS
GAMMAS
500
400
300
200
100
0
-100
E 1 2 3 4 5 6 7 8 9 10 11 12 13 14 15 16 17 18 19 20 W

Figure 9

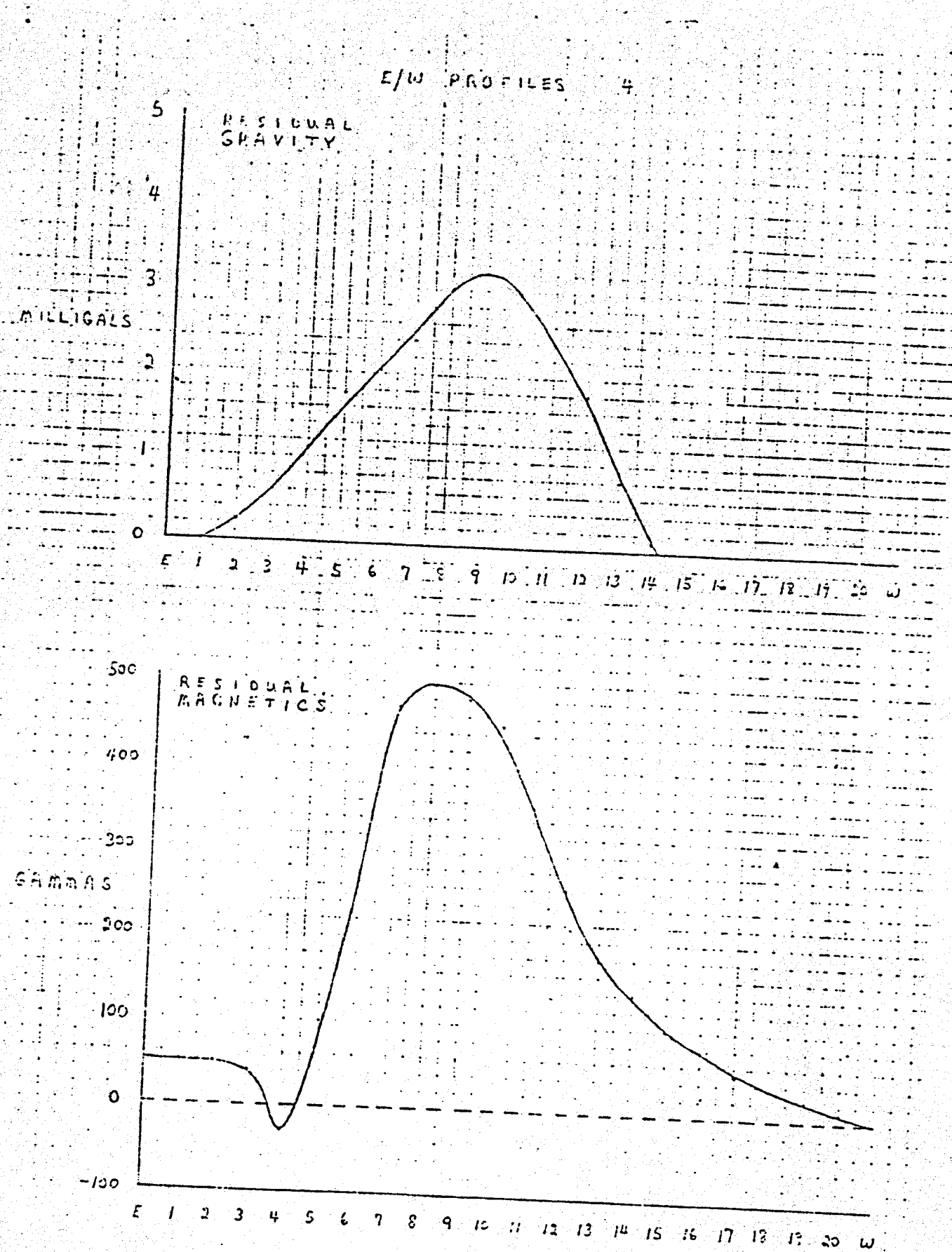
E/W PROFILES 4
RESIDUAL GRAVITY
MILLIGALS
5
4
3
2
1
0
E 1 2 3 4 5 6 7 8 9 10 11 12 13 14 15 16 17 18 19 20 W
RESIDUAL MAGNETICS
GAMMAS
500
400
300
200
100
0
-100
E 1 2 3 4 5 6 7 8 9 10 11 12 13 14 15 16 17 18 19 20 W

Figure 10

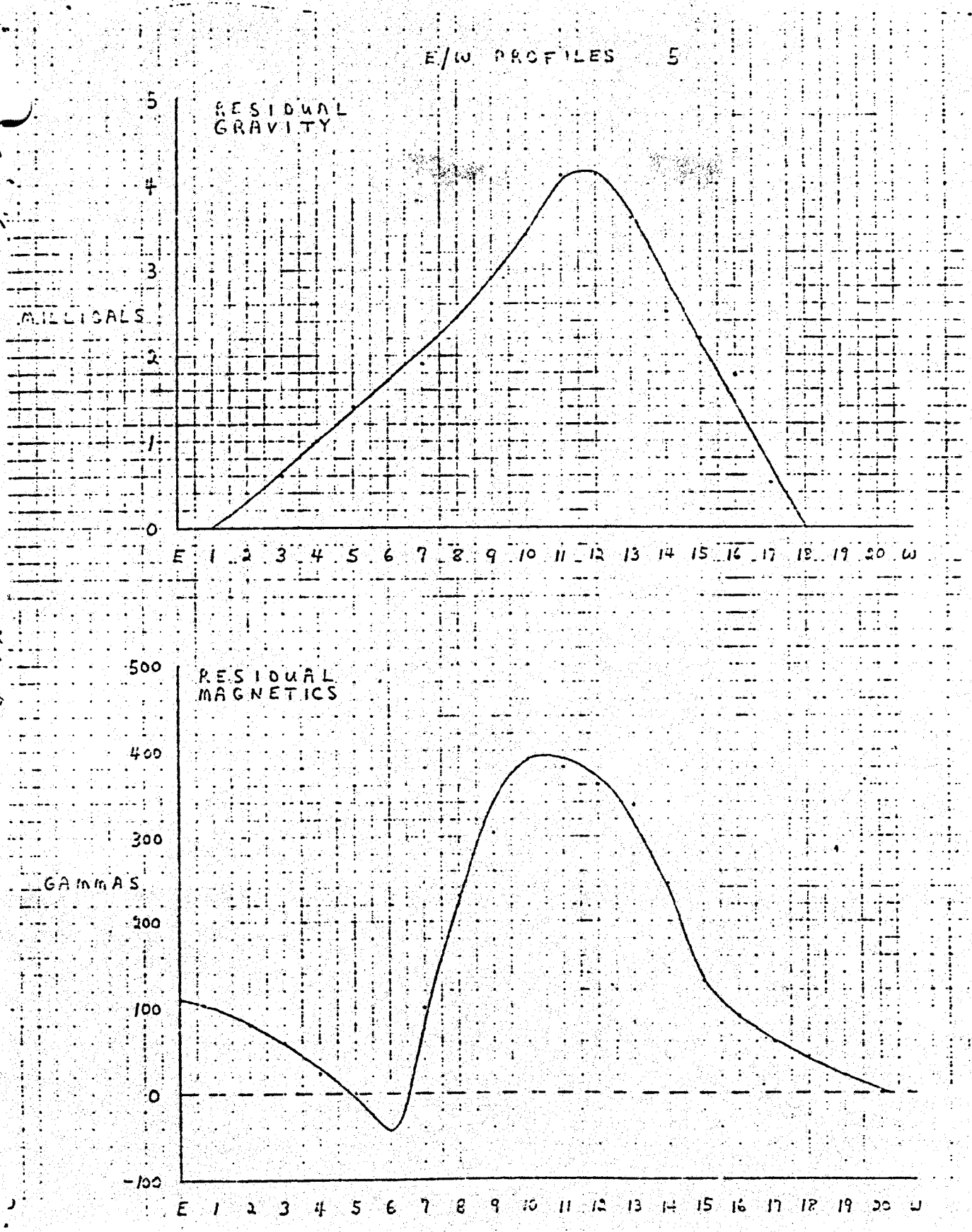
E/W PROFILES 5
RESIDUAL GRAVITY
MILLIGALS
5
4
3
2
1
0
E 1 2 3 4 5 6 7 8 9 10 11 12 13 14 15 16 17 18 19 20 W
RESIDUAL MAGNETICS
GAMMAS
500
400
300
200
100
0
-100
E 1 2 3 4 5 6 7 8 9 10 11 12 13 14 15 16 17 18 19 20 W

Figure 11